UNIVERSITY OF BELGRADE

SCHOOL OF ELECTRIC ENGINEERING

Asem Issa Al-Hasaeri

ADAPTIVE TECHNIQUES IN TARGET TRACKING SYSTEMS

Doctoral Dissertation

Belgrade, 2020

UNIVERZITET U BEOGRADU

ELEKTROTEHNIČKI FAKULTETA

Asem Issa Al-Hasaeri

ADAPTIVNE TEHNIKE U SISTEMIMA ZA PRAĆENJE POKRETNIH CILJEVA

doktorska disertacija

Beograd, 2020

Mentor of Doctoral Dissertation

Prof. dr Željko Đurović

University of Belgrade, School of Electrical Engineering

_____

Members of Committee:

Prof. dr Aleksandar Rakić

University of Belgrade, School of Electrical Engineering

_____

Prof. dr Milan Rapaić

Faculty of Technical Sciences in Novi Sad

_____

Prof. dr Marija Rašajski

University of Belgrade, School of Electrical Engineering

_____

Dr. Aleksandra Marjanović

University of Belgrade, School of Electrical Engineering

_____

date: _____

Acknowledgments

First of all, I would like to express sincere gratitude to my supervisor Prof. dr Željko Đurović for all the continuous support and encouragement, guiding me well throughout the research work from the title's selection to finding the results. His immense knowledge, motivation, and patience have given me more power and spirit to excel in research writing. Without his guidance and constant feedback, this PhD would not have been achievable.

I am also very grateful to dr Aleksandra Marjanović, dr Sanja Vujnović, and dr Predrag Tadić, who were always so helpful and provided me with their assistance throughout my study at University of Belgrade.

Finally, I would like to thank my mother, my wife, my daughter, and my sons for their continued support throughout these years.

Thank you from my heart.

Dissertation Title: Adaptive Technique in Target Tracking Systems

Abstract: The most critical and challenging task in the algorithms of multiple target tracking in the presence of false observations is the correct assignment of measurements to tracks the so-called *data association* task. That is the core component of all target tracking systems. Regardless of the particular method used, the efficiency of any target tracking system depends on the understanding of the background or clutters "certain parameters that describe the environment", and the parameters that describe the detection properties of the objects. The character of these parameters is statistical, and not only they are usually unknown in practice, and they are also time-invariant. Moreover, the statistics that describe the environment are spatially dependent.

The most important among these are the probability of target detection and the density of false alarm. These parameters are usually unknown as well as variable, and even though there are many algorithms for estimation of these parameters, the usefulness of these estimates is quite limited. Successful implementation of any target tracking system depends on the precise knowledge of the statistical quantities such as the probability of target detection and density of false alarm.

This thesis proposes one approach for estimating the time-varying probability of detection of each tracked object individually and the density of false alarm in the immediate vicinity of the current position of an object. The proposed approach is based on the generalized maximum likelihood (GML) approach, assuming the tracking of a single target. To reduce the numerical complexity, the proposed technique reduces the number of the formulated hypotheses based on the calculation of their likelihood.

The obtained estimators have a very simple form, but as shown, this simplicity comes with a significant bias, which is present in most similar techniques, and relatively large variance of the estimators. The research presented in the thesis coped with these two problems and resulted in an algorithm with significantly reduced bias and error variances.

This thesis also analyses the influences of the unknown measurement noise covariance on an estimation of the probability of target detection and density of false alarm and proposes an improvement in the case of noise covariance matrix uncertainty.

The thesis presents the applicability and constraints of the proposed solution. The results are illustrated by simulations and present a fair analysis of the proposed algorithm. Finally, the ideas for further improvement of the method are given.

Keywords: multi-target tracking system, probability of detection, density of false Alarms, gate size, bias, variance, covariance matrix, data association, generalized maximum likelihood, gate.

Scientific field: Electrical Engineering

Scientific discipline: Systems and Signals

Naslov teze: Adaptivne tehnike u sistemima za praćenje pokretnih ciljeva

Rezime: Vrlo izazovan i kritičan zadatak u algoritmima praćenja pokretnih ciljeva uz prisustvo lažnih alarma jeste pravilna asocijacija pristiglih opservacija takozvanim tragovima. To je osnovni i verovatno najvažniji deo svakog sistema za praćenje više pokretnih ciljeva. Bez obzira na to koja se metoda pridruživanja podataka koristi, efikasnost bilo kog takvog sistema itekako zavisi od poznavanja statističkih parametara koji karakterišu okruženje i parametara koji karakterišu ponašanje praćenih objekata, u smislu njihove detektibilnosti. Nažalost, u praksi, ovi podaci nikada nisu poznati, i gore od toga, vremenski su promenljivi, a parametri prisustva takozvanih lažnih alarma su i prostorno zavisni. Najvažniji od tih parametara su verovatnoća detekcije cilja i gustina lažnog alarma. Sama činjenica da postoje različiti pristupi za estimaciju ovih parametara govori, kako o njihovom značaju, tako i o kompleksnosti procedura za njihovu estimaciju. Lako se pokazuje da uspešna primena bilo kog algoritma za praćenje itekako zavisi od kvaliteta i nivoa neodređenosti u poznavanju ovih statističkih parametara kakvi su verovatnoća detekcije cilja i gustina lažnih alarma.

U ovoj doktorskoj disertaciji je predložen novi pristup za procenu vremenski promenljive verovatnoće detekcije ciljeva kao i gustine lažnog alarma ali u naposrednom okruženju objekta koji se prati. Predloženi pristup je zasnovan na dobro poznatom metodu maksimalne verodostojnosti, pri čemu je pretpostavljeno da se u prostoru od interesa nalazi samo jedan pokretni objekat. Kako bi se minimizovala numerička složenost predloženog algoritma, minimizovan je i broj hipoteza za koje se računaju odgovarajuće verodostojnosti.

Dobijeni estimatori imaju vrlo jednostavnu formu. Međutim, kao što se i očekivalo, statističke osobine dobijenih estimatora su vrlo slične onim estimatorima koji su dostupni u literature. Naime, pokazalo se da izvedeni estimatori imaju značajan pomeraj u proceni kao i nedopustivo veliku varijansu. Zato je posebna pažnja u disertaciji posvećena postupcima za eliminaciju pomeraja i smenjenje varijanse. Pokazano je da se uz minimalno povećanje numeričke složenosti algoritma značajno popravljaju njegove statističke performanse.

U ovoj doktorskoj disertaciji je takođe razmatran uticaj nepoznavanja statistika mernog šuma na kvalitet estimatora verovatnoće detekcije ciljeva i gustine lažnih alarma. Pokazano je da ova neodređenost može značajno da degradira kvalitet celokupnog postupka, tako da je predložena dodatna adaptacija koja u kontekstu primenjenog Kalmanovog filtra estimira kovarijacionu matricu mernog šuma.

Konačno, u tezi su ilustrovani primenjivost kao i ograničenja predloženog rešenja. Svi zaključci i pretpostavke su potkrepljeni iscrpnim simulacijama koje su kroz Monte Carlo simulacije sa više od 20.000 ponavljanja uspevale da potisnu uticaj nesavršenosti generatora slučajnih brojeva. Na kraju teze su date i ideje za dalje unapređenje predložene metode.

Кључне речи: Sistem za praćenje više pokretnih ciljeva, verovatnoća detekcije ciljeva, gustina lažnih alarma, veličina prozorske funkcije, pomerenost i konzistentnost estimatora, generalizovani pristup maksimalne verodostojnosti.

Content

vi

List of figures

ix

List of Tables

Chapter One

Introduction

Target tracking is a growing research field with various applications. During the previous decades, the scientific community has shown a great interest in the target tracking systems [1, 2, 3].

The beginning of researches in this field was mainly solely for military applications like detecting and estimating the positions, velocities, and directions of the incoming missiles or aircrafts. These systems utilize sensors like radar systems, sonar, or infrared sensors as input signals. However, later the focus has shifted to civilian applications, such as biological systems [4], traffic surveillance systems, autonomous vehicles, subway stops, pedestrian hubs [5], image processing, robotics, oceanography, and biomedicine [6]. The basis for tracking is estimating an unknown quantity recursively over time, maybe the share value on the market, the temperature inside the room, movement of some cells in the blood vessel, or positions of the aircraft flying around the airport. In the conventional setting, the interesting quantities are the position and the velocity of the object (called target), which named as states.

The first step in tracking is the prediction of the values of the next state. To predict the states, one needs a model to describe the quantities of interest in target tracking, referred to as the motion model. By the motion model, one can predict the value of the next state from the knowledge of the current state. Uncertainties in the prediction can also be expressed. The prediction is updated when the time made for prediction has been reached.

The traditional source of information in a target tracking system is radar, other popular sensors such as laser sensors and cameras. To take advantage of the data provided by the sensor, a relation must be modeled between the sensor output and a quantity of interest. i.e., one needs to define the measurement model.

The realistic measurement of any quantity is the actual value of the measured quantity plus noise. The noise element is added to express design errors as well as sensor inaccuracy. Beyond the precision and design uncertainties, it may also be that not all targets are always detectable, or they are so close to each other that they look like one object. Such considerations must also be regarded and considered in order to design the sensor measurements correctly.

Actually, in the literature, there are different proposed structures of moving target tracking systems with various solutions for target state estimation filters and different methods of data associations [2]. The main task of these systems was to gather the reflections (measurements) from the surrounded environment and analyze them to discriminate between the object of interest and the false alarms [3]. The reflections received from the object of interest would be used to form a so-called trace, and they would be processed accordingly. This task seems relatively simple, but in reality, it is a challenging, very complicated task and its complexity can be explained through the following points [3, 7, 8]:

- No object has a specific property of detection, which depends on several factors.
- Usually, environments are rich with clutter, which means that the number of reflections or observations which are gathered during the scan is significantly higher than the number of real objects in the scanned environment.
- The target reflections are samples of a stochastic process even when the detection occurs, and the measurements were influenced by noise.
- All the sensors have a certain resolution, which reduces the credibility of received observations.
- In one scan, usually, there is more than one object of interest. These objects are often very near to each other, intentionally and not a coincidence, which poses a challenge for the algorithm of the data association that connects the appropriate objects with a suitable track [3].

Successful implementation of the target tracking systems depends significantly on accurate knowledge of two critical parameters. These parameters are probability of target detection and density of false alarm [3]. Although the probability of detection depends on the scenarios and

accuracy of the sensors. Hence, the assumption of the complete knowledge of these two main parameters in advance may not be realistic for multi-target tracking. The way of overcoming the lack of knowledge of the probability of detection and density of false alarms is of significant importance in practice [9].

These statistical parameters have a disadvantage that they are hard to estimate because they were non-stationary in time and space [2]. The significance of this problem has been explained by Mahler [10] where it is stated that accurate knowledge of the probability of target detection and density of false alarms is essential for best performance of recent target tracking filters such as Probability Hypothesis Density (PHD) filter and Cardinalized Probability Hypothesis Density (CPHD) filter [2].

Therefore, many work and several solutions are illustrated in the literature for estimating the probability of target detection and density of false alarms, where most of these solutions suffer from shortcomings and drawbacks such as numerical complexity, sensitivity to the initial value of the filter and many other drawbacks.

This research proposes a new algorithm to estimate the probability of detection of a single target moving in a cluttered environment, along with the estimation of the density of false alarms in its immediate vicinity. The essential contribution of this research is that the estimation of the density of false alarm has relied on the measurements located around the predicted position within the target gate and not on measurements received from a wide region in which the target moves, as mentioned in many works available in the literature. Fundamentally, it is not necessary to assume that the observations in the wide surveillance region are uniformly distributed, which is commonly not a sustainable assumption. The new proposed method is based on Generalized Maximum Likelihood (GML) principles, and numerically is much simpler than previous methods since each scan contains a maximum of two specific hypotheses.

This procedure can be extended to include multiple targets where the two parameters are estimated in the immediate vicinity related to each track. Another advantage of the new proposed algorithm is that it is possible to be used in parallel with any target tracking algorithm, and it does not depend upon a specific data association algorithm.

1.1 Outline of the thesis

This thesis is organized as the following: In Chapter 2, the concepts of target tracking systems are introduced, the conventional approaches of filtering and predictions (fixed coefficient filters and Kalman filter) are explained, correlation and data association with commonly used methods are explained briefly, and the track management is explained with its subdivisions. Chapter 3 illustrates the influence of the probability of detection and density of false alarms on the quality of the target tracking system. This chapter starts with considering the previous literature in the field of estimation of these two parameters, the main motivation for this research, the contributions of the research, and at the end of the chapter, some simulation results are illustrated to show the effect of these two parameters on the efficiency of the target tracking system. Chapter 4 is represented as the most important part of this research, where starts by illustrating the steps of deriving the probabilistic expressions that will be used in the estimation of the probability of target detection and density of false alarms.

The proposed algorithm of estimating the two unknown parameters suffers from significant bias and a notable variance. Keep in mind that most of the results obtained from the previous literature suffer from these defects too. This thesis proposes two extensions of the derived algorithm for reducing the bias and variance of the errors, and the results of reduction were very satisfactory. The performance of the new proposed estimator was assessed in two ways. The first way was by comparing the *MSE* of a tracking system that utilizes the estimated probability of detection and density of false alarms with another tracking system that uses the known probability of detection and density of false alarms. The second assessment way was by comparing the computational

complexity of the new proposed algorithm and the PHD filter. The conclusion of the thesis is presented and summarized in chapter 5, containing the future work and the directions of research in the area of target tracking. Finally, a list of mentioned references is listed at the end of the thesis.

Chapter Two
Multiple target tracking systems

Multi-target tracking MTT is a fundamental requirement for all surveillance systems, utilizing at least one sensor, connected with a computer to represent the environment of interest [11, 12]. In the beginning, these systems were mainly military applications, using sensors such as infrared sensors, radar, and sonars [3]. The measurements reported from the sensors are originated from different sources, some of them from the real targets and the rest from the thermal noise or radar clutter.

The objective of the target tracking system was to gather the observations from the sensors and partition them into sets [3]. Each set of observations is received from the same source and forms a track for that source. After forming and confirming the tracks, the tracking system can estimate the number of real targets with their kinematic quantities for each track.

Wax [13] in 1955, was the first one who recognizes the fundamentals of the MTT system. At that time, the tracks in the radar systems were formed manually.

The next significant improvement in MTT theory is the publication of the Bayes formula in 1964 by Sittler [14], which is the base for the subsequent developments, and occurred before the wide publication of the Kalman filtering technique for recursive estimation of target states [11].

Thus, Bar-Shalom [15] and Singer [16] began to develop modern MTT technologies that merge correlation with Kalman filtering theory at the beginning of the 1970s.

The system Track while scan (TWS), is a particular case of MTT systems, receives data regularly, and classified as the simplest and probably the best type of multiple target tracking systems outlined by Hovanessian [17]. The radar TWS performs the functions of searching and track updating simultaneously.

With the expansion of computer capabilities, the applications based on MTT systems were increasing quickly and used in several applications such as satellite surveillance systems, image processing, oceanography, autonomous vehicles, robotics, biomedicine, and air traffic control systems [6, 11, 18].

2.1 Basic definitions in MTT system

Observation is a common terminology that is used to point to the measured quantities detected by the sensor (or detector). The observed data generally includes the kinematic quantities like target position or range rate with some target attributes, such as identification number, target type.

Commonly, observations are received regularly, like the TWS radar system [11]. Usually, the observations received during one scan, did not contain more than one observation from every real target, which may fall inside the target gate region.

MTT systems have two different processing schemes. The first scheme is a *batch processing scheme*, where all observations collected during some consecutive scans are processed together to form the target track, and the estimated states such as position and velocity are represented as the ideal (optimal) estimates. The second scheme of processing is *the recursive (sequential) method*, where the processing of estimating the states and updating the target track is done at every scan and uses only the data received during that scan [11].

2.2 Basic elements of MTT system

Many approaches were proposed in the literature along the previous years concerning MTT systems. The differences among these approaches are in the methods of solving the problems of *filtering* and *data associations* [18].

The main fundamental elements of a recursive MTT system are shown in Fig. 2-1 which is adopted from [11]. Functions of the MTT elements are overlapped considerably, but Fig. 2-1 represents the appropriate partitioning to provide the typical functions of the MTT system.

Assuming that the used tracking system is based on recursive processing, the tracks are formed from the previous scans, and the new received observations are considered for updating existing tracks. The task of determining which observation belongs to which track is not simple and can be summarized in two steps:

1) Gating which is a test for determining the candidates to track updates.

2) Data association algorithm, which is the second step to determine the final association.

Observation within the gate, not correlated to a target track, can initiate a new tentative track, and confirmed when satisfying the confirmation criteria. Low-quality target tracks are determined by update history and deleted. Lastly, after pairing, predict the tracks ahead, place the gates around the predicted points, and the cycle of processing is repeated [11].
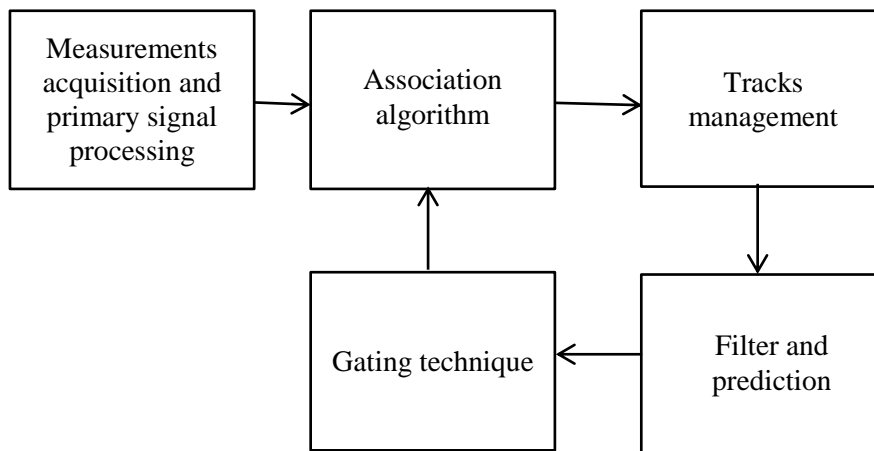
Fig. 2-1: Basic elements of the simple recursive MTT system

2.3 Measurement processing techniques

The measurement processing technique includes the filtering, the thresholding, the analysis, and interpretation of the data obtained from the sensors. Typically, measurements are collected in regular time intervals called scans and provide noisy information about the position, bearing, or distance of the objects within their range [19]. Some of these measurements are originated from the targets of interest, while the rest are classified as false alarms or clutter.

2.4 Gating techniques

Gating is a hard test to exclude unlikely observations to track updating. Gate is a region of interest surrounding the predicted position, and this region is called the validation region or gate. Any observations that satisfy the relationship of gating and fall inside the region of the gate, may be originated from a real target or originated from a false alarm, and considered as a candidate for track updates. The method of choosing an observation from several observations that exist inside the gate region to associate with a track is based on the so-called correlation or data association [20].

Let us consider Fig. 2-2 to illustrate the gating process, where the observed measurements are denoted as $z = (z_j, j = 1, 2, ..., 10)$, and a set of the existing tracks are denoted by $T = (T_1, T_2, T_3, T_4)$. The observations may be divided into three categories: the first category consists of the observations that belong to only one gate, like the observations (z_1, z_2, z_3) in

gate1, (z_4) in gate 2, (z_6, z_7) in gate 3, and (z_{10}) in gate 4. The second category consists of the observations within the gate of multiple tracks or overlapped gates like (z_5). The third category consists of the observations out of the gates such as (z_7, z_8).

      After applying the gating process, observations are classified as one of the next classifications:

•   *Candidate for updating a track,* represented by the observations which are inside the gates only (all observations in Fig. 2-2 except z_8, z_9). The observations inside the gates and not utilized to update the target tracks may be utilized to initiate new tentative track.

•   *Initiate a new tentative track*: Observation inside the track gate and did not correlate with any track or the observation did not inside any track gate such as $(z_8$ or $z_9)$. That observation is used as a candidate to initiate a new tentative track.
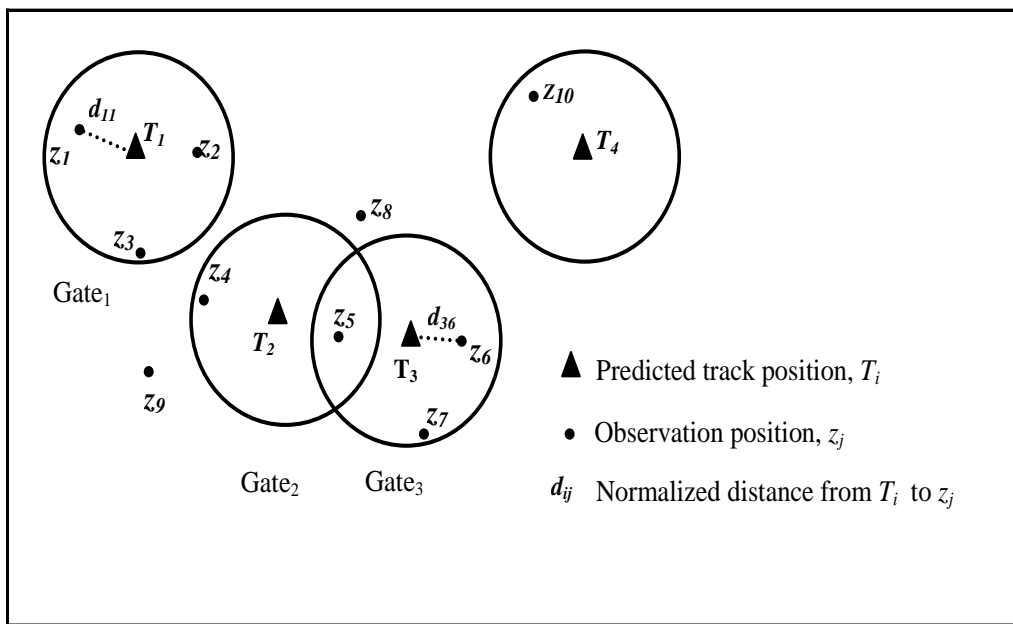
Fig. 2-2: The gating process

      The previous gating procedure illustrated in Fig. 2-2 is performed through the following: The gating procedure is started by predicting the position of the target in the next scan (T_1, T_2, T_3) obtained by applying the tracking filter, such as the Kalman filter, or fixed coefficient filter, or some other filters. Then, after that, one has to choose the data association approach to identify the true target. There are many approaches, that will be discussed later. The easiest and most intuitive approach is applied to this example. If only one observation exists within the gate region of a single track and that observation does not exist within other overlapped gates, the track is updated by that observation as (z_{10}) in gate 4. If a set of observations exists within the gate region of a single track as shown in gate 1, then the suitable observation to update that track is obtained from computing the distances (normalized distance) between each observation (z_1, z_2, z_3) and that track (T_1) after that chooses the observation with the shortest distance, and in this example it is (z_1). This method of association is known as the Global Nearest Neighboring (GNN) method and will explain it next. If a set of observations exist within the overlapped gates such as (z_5), then to correlate each observation with a suitable track, additional test logic is needed. The normalized distance (d_{ij}) is defined by (2.1).

$$d^2 = \frac{(R_p - R_o)^2}{\sigma_r^2} , \tag{2.1}$$

where R_o is the measured position, R_p is predicted position, σ_r^2 is the residual variance and defined as a function of predicted variance (σ_p^2), which is obtained from Kalman covariance matrix and measured variance (σ_o^2).

$$\sigma_r = \sqrt{\sigma_o^2 + \sigma_p^2} . \tag{2.2}$$

Normalized distance between observation and the predicted target track can be rewritten by the equation (2.3).

$$d^2 = \tilde{y}' S^{-1} \tilde{y} , \tag{2.3}$$

where $\tilde{y}$ is the *innovation* or *residual* vector, which is the difference between the received measurement vector y and predicted measurement vector $\hat{y}$, as given by (2.4), and S^{-1} is the inverse of the error covariance matrix S, which is given by (2.5).

$$\tilde{y} = y - \hat{y} , \tag{2.4}$$

$$S = HPH' + R , \tag{2.5}$$

where P is a prediction error covariance matrix, H is a measurement matrix, R is a covariance matrix of a zero-mean white Gaussian measurement noise. These relations will be precisely described later.

Maximum allowable error (*MAE*) is obtained utilizing the prediction and the measurement accuracy statistics, formed for all measured quantities and repeated for each observation and track pair. Then, the calculated normalized distances (d_{ij}) are compared with the calculated (*MAE*), and the observation, which is in the gate or satisfies the gate if d_{ij} does not exceed the computed *MAE* or satisfies the relationship (2.6).

$$\begin{aligned} d_{ij} &\leq MAE & \textit{Observation is within the gate}. \\ d_{ij} &> MAE & \textit{Observation is out of the gate}. \end{aligned} \tag{2.6}$$

The observation is said to satisfy the gate of a given track, and association is possible if the following relationship is satisfied by d^2 of the innovation.

$$d^2 = \tilde{y}' S^{-1} \tilde{y} \leq G , \tag{2.7}$$

where G represents the threshold constant of the gate.

The quantity d^2 is the total of squares of M Gaussian independent random variables, that is why d^2 will has Chi-square distribution χ_M^2 for associating observation with track correctly with M degree of freedom, and the allowable probability $P = 1 - P_d$ of the true observation falling out of the gate, P_d is known as the probability of detection. The table of Chi-square χ_M^2 distribution and the allowable probability of the true observation falling out of the gate can be used in defining the threshold G [20]. For optimum performance, the size of the gate should be infinite in cases where the detection probability is unity ($P_d = 1$), or there are no false alarms. In reality, the main objective

of gating is to minimize the number of observations that will be considered by the data association [11]. The gate has a specific shape and size, and these are considered in the following forms.

2.4.1 Rectangular gate

The rectangular gate is the simple gating technique, defined as a rectangular region surrounding the predicted target position. *MAE or G* is computed by (2.8).

$$G = K_g \sigma_r, \tag{2.8}$$

where K_g is the gating constant, and σ_r is a residual standard deviation and defined by (2.2).

With the uncertainty in the predicted position due to high density of false alarm or increases of measurement of noise, then the gate size should be decreased [11].

An example to illustrate the rectangular gate is shown in Fig. 2-3, where the predicted target position components are ($\hat{x}_i$ and $\hat{y}_i$), and the measured position components are (x_i and y_i).

$$| x_i - \hat{x}_i | \leq K_g \sigma_x .$$
$$| y_i - \hat{y}_i | \leq K_g \sigma_y . \tag{2.9}$$

The observation (z) should be fallen within the rectangular gate if it satisfies the following two conditions: The first condition belongs to the x-axis ($\hat{x}_i - K_g \sigma_x < z < \hat{x}_i + K_g \sigma_x$)), and the second condition belongs to the y-axis ($\hat{y}_i - K_g \sigma_y < z < \hat{y}_i + K_g \sigma_y$).
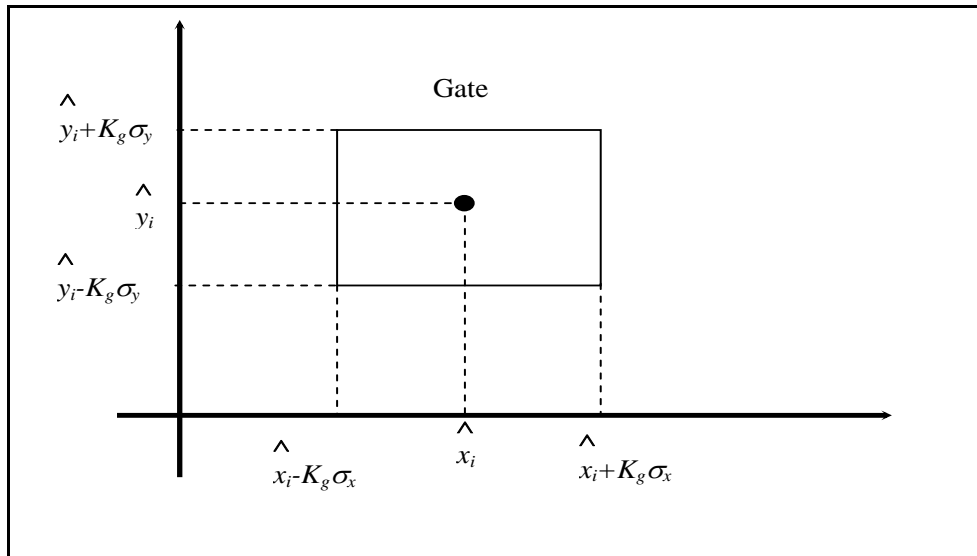
Fig. 2-3: Rectangular gate

The simulation result displayed in Fig. 2-4 illustrates the influence of K_g on the quality of the tracking system and the influence of the probability of detection and density of false alarm on obtaining the optimal gate size. The simulation program utilizes the following:

1.   Standard Kalman filter for filtering, and predicting the states.
2.   The algorithm used for correlating or associating the observation to track was the probabilistic data association (PDA) algorithm. Furthermore, whenever the track gate is free for several consecutive times, say (5), the nearest observation to the gate is set as the predicted position, the covariance matrix is reinitialized, and the gate is maximized because it is based on (σ_x and σ_y) which obtained from the covariance matrix.

10

3. Monte-Carlo simulation was used to minimize the influence of the generated random numbers and set by 5000.

4. Density of false alarm is kept constant $\lambda_{fa} = 4 \times 10^{-6}$, while probability of detection was took the values $P_d \in \{0.7, 0.9\}$.

The performance metric used to assess the tracking system is *Root-Mean-Square Error* (RMSE) and defined by the formula (2.10).

$$RMSE(j) = [\sum_{i=1}^{N}((x_i - \hat{x}_i)^2 + (y_i - \hat{y}_i)^2)/N]^{0.5}, \qquad (2.10)$$

where (x_i, y_i) is the actual target position, $(\hat{x}_i, \hat{y}_i)$ is the predicted target position, N is the number of Monte-Carlo simulations loops, and j is the scan number.

The figure shows that when K_g is small, the RMSE is high and decreases as K_g is increases, because the probability of the real target to fall inside the gate increases with increases of gate size K_g, up to some value of K_g which produces minimum RMSE. The size of that gate is called the optimal size or optimal K_g. After that point (optimal K_g), whenever K_g is increased, the RMSE also increases because as the gate size increases, the number of false alarms within the gate is increased, and miscorrelation has occurred, which produces an increase in MSE due to associating of wrong observation to a target track. Also, the figure shows the influence of the probability of detection on the performance of the tracking system and how the optimal K_g is changed by changing the probability of detection.
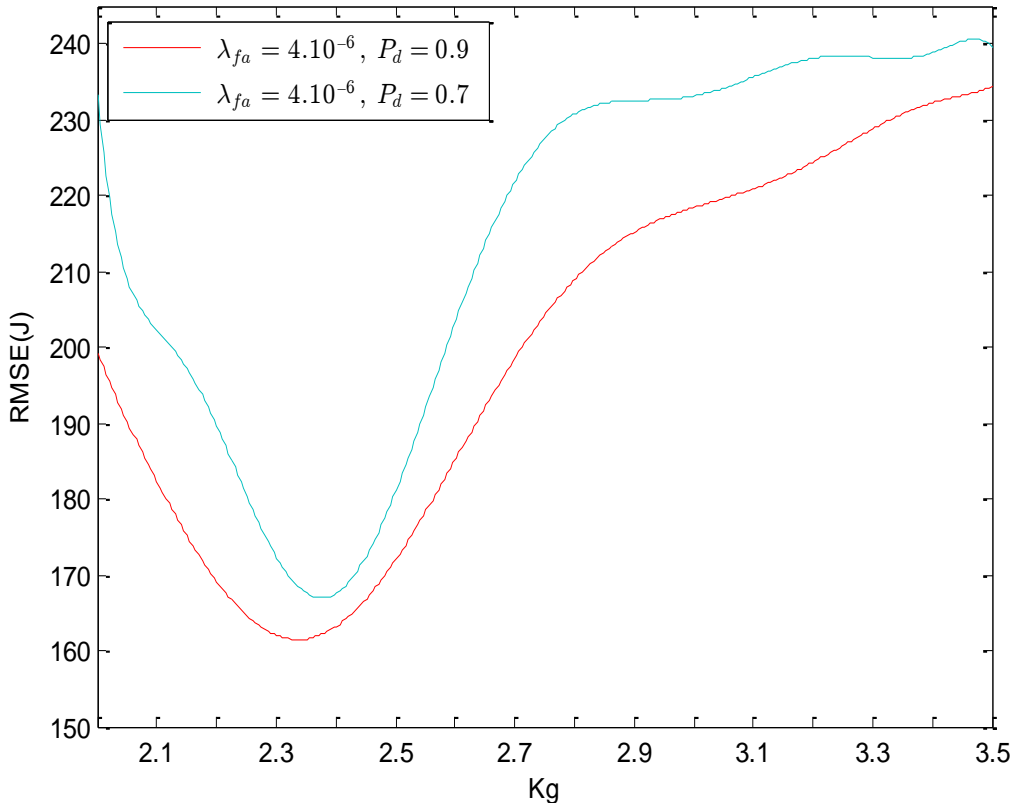
Fig. 2-4 Influence of gate size and the probability of detection on the accuracy of the target tracking algorithm

11

2.4.2 Ellipsoidal gate

Association based on using the ellipsoidal gate is allowed if the relationship (2.7) is satisfied by the normalized distance (d^2).

The maximum likelihood gate G can be defined in such a way that the observation fall inside the gate is more probable from track in question than from clutter or false alarm [11]. So optimized gate G is defined as a function of (P_d, β, M, S), P_d is the probability of detection, β is a new source density, M is a measurement dimension, and S is the error covariance matrix which represents the residual statistics.

$$G = 2\ln\left[\frac{P_d}{(1 - P_d)\beta(2\pi)^{(M/2)}\sqrt{|S|}}\right]. \qquad (2.11)$$

As the density of new source β approaches zero, or probability of detection P_d approaches unity, then, according to the formula in (2.11) G approaches infinity. While decreasing the probability of detection P_d, or increasing the residual error due to false alarms, then G is decreased. When G is approaching zero during the tracking, then attempting to further association becomes futile.

2.5 Filtering and prediction

Generally, the tracking algorithm comprises at least two components: filtering and correlation or data association. This section considers filtering and prediction, and the next section is devoted to the data association. The filtering process consists of two steps:

(1) *Prediction*. In this step, the next state of the quantity is predicted utilizing the knowledge of the current state.

(2) *Measurement update.* In this step, measurements are used to improve the prediction.

Target states are the unknown quantities in target tracking systems. Usually, these states are position and velocity of a specific moving object. The objective of the Filtering and prediction is to estimate the states of the tracked object using the data corrupted by measurement noise, extracted from the received observations [18]. The sequence of the *estimated states* of one object forms a *track* [19].

Filtering and predictions are essential elements of any target tracking system. Usually, the first problem facing the specialists of any MTT system is the choice of filtering and prediction method [11].

Filtering methods are utilized to estimate the present and the future target states such as the position, velocity, and some filters estimate the acceleration.

There are many methods of filtering and predictions, and the commonly used methods for MTT systems are fixed coefficient filter and the Kalman filter.

Fig. 2-5 is adopted from [11], and illustrates the filtering and the prediction flow diagram, valid for both approaches, where: x represents the vector of target states such as the position, velocity and maybe acceleration of a moving target, y is the observed target states influenced by additional measurement noise (v), $\hat{x}(k|k)$ is the estimated states at scan (k), x_p or $\hat{x}(k+1|k)$ is the predicted states at the scan (k).

Gains are utilized to obtain the filtered state estimates and used to get the predicted estimates of a next scan. The gains of the fixed coefficients filter are fixed and predetermined in advance, while for the Kalman filter are computed dynamically[11]. The residual ($\tilde{y}$) is utilized to

update the filtered estimates and also used as maneuver detection by checking the consistency of the adopted model.
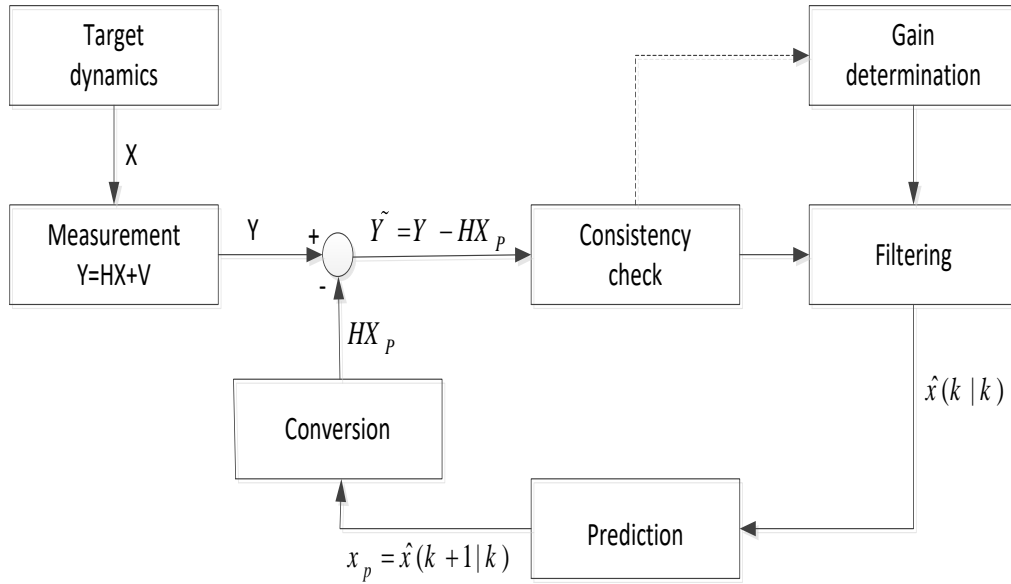
Fig. 2-5: Flow diagram of the filtering and the prediction process

2.5.1 Fixed coefficient filter

The fixed coefficient filter is the simplest in implementation and used for systems with dense targets.

There are two types of fixed coefficient filters, α-β filter and α-β-γ filter. The α-β filter is probably the widely used fixed-coefficient filter because it requires a low computational load and low resources. This filter is utilized only when the position measurements are available, the vector of states contains position and velocity only, and defined by (2.12).

$$x_s(k) = \hat{x}(k \mid k) = x_p(k) + \alpha[x_o(k) - x_p(k)],$$

$$v_s(k) = \hat{\dot{x}}(k \mid k) = v_s(k-1) + \frac{\beta}{qT}[x_o(k) - x_p(k)], \tag{2.12}$$

$$x_p(k+1) = \hat{x}(k+1 \mid k) = x_s(k) + Tv_S(k),$$

where: $x_s(k)$ is the smoothed position or the estimated position, $x_p(k+1)$ is the predicted position, $x_o(k)$ is the received observation, $v_s(k)$ is estimated velocity, T is the sampling time, (α, β) are the filter gain coefficients.

When a set of observations are received on a scan (k), q is set to one in a typical case, when there is no miss-detection $(i.e.\ P_d = 1)$, estimation of the states (x_s, v_s), and the predicted position (x_p) are defined by (2.12). However, when the observations are not received (miss-detection occurred) on scan (k) due to the probability of detection is less than one $(i.e.\ P_d < 1)$, then $x_s(k) = x_p(k)$, $x_o(k) = x_p(k)$, q is identified as the number of scans from the last measurement, and $x_p(k+1)$, $v_s(k)$ are calculated as usual by (2.12).

The second filter is α-β-γ filter, which is an extension of the α-β filter, where includes the estimation of acceleration into the state vector, and the equations are defined by (2.13).

13

$$x_s(k) = x_p(k) + \alpha[x_o(k) - x_p(k)],$$

$$v_s(k) = v_s(k-1) + Ta_s(k-1) + \frac{\beta}{qT}[x_o(k) - x_p(k)],$$

$$a_s(k) = a_s(k-1) + \frac{\gamma}{(qT)^2}[x_o(k) - x_p(k)],$$

$$x_p(k+1) = x_s(k) + Tv_s(k) + \frac{T^2}{2}a_s(k),$$

(2.13)

where: α, β, and γ are the filter gain coefficients and predetermined in advance.

When the values of the filter gain coefficients are decreased the filter will be less responsive, while increasing these coefficients leads to improve the performance versus complex inputs. Relationships among the coefficients of fixed coefficient filters are derived in [21, 22, 23]. These relationships define the gain coefficients, which makes a compromise between steady-state maneuvering and noise reduction.

Kalata [23] derives the relationship between the coefficients for both trackers as in (2.14) and (2.15), while Benedict [21] derives a relationship which is mostly agreed with Kalata, as in (2.16) and (2.17).

$$\beta = 2(2 - \alpha) - 4\sqrt{1 - \alpha}.$$ (2.14)

$$\gamma = \frac{\beta^2}{2\alpha}.$$ (2.15)

$$\beta = \frac{\alpha^2}{2 - \alpha}.$$ (2.16)

$$\gamma = 2(\alpha + \beta) - \frac{4\beta}{\alpha}.$$ (2.17)

The selection of the gain coefficients for these types of filters must reflect the compromise between dynamic (maneuver) performance and the noise [11]. One widely suggested solution to this issue is to choose the filter gains depending on the target behavior, as defined by the maneuver detector.

There are two problems associated with the utilization of the fixed coefficients filters. The first situation is that, when the probability of target detection is less than unity $(P_d < 1)$, then the filter gains must be adjusted to improve the performance of the tracking algorithm to follow the target [24]. The second situation occurs when maneuver is detected, and then the filter gain coefficients should be increased to follow the maneuvered target. Thus due to these drawbacks, the fixed coefficient filter is not convenient for many areas, which makes the option of the Kalman filter is more appealing, and the preferable one for the applications that require high accuracy [11].

Simulation results for estimating the position and the velocity of a moving target using the α-β filter are shown in Fig. 2-6 and Fig. 2-7, respectively. The gain α has different values, and for each value of the coefficient α, the corresponding gain β is calculated by (2.16). From the shown figures, it is evident that the gains in the fixed coefficient filter have a notable influence on the overall performance of the filter. Hence, at low values of the gain coefficients, the estimated trajectories are deteriorated, and the filter produces a very low performance, while the performance is improved by increasing the gains.
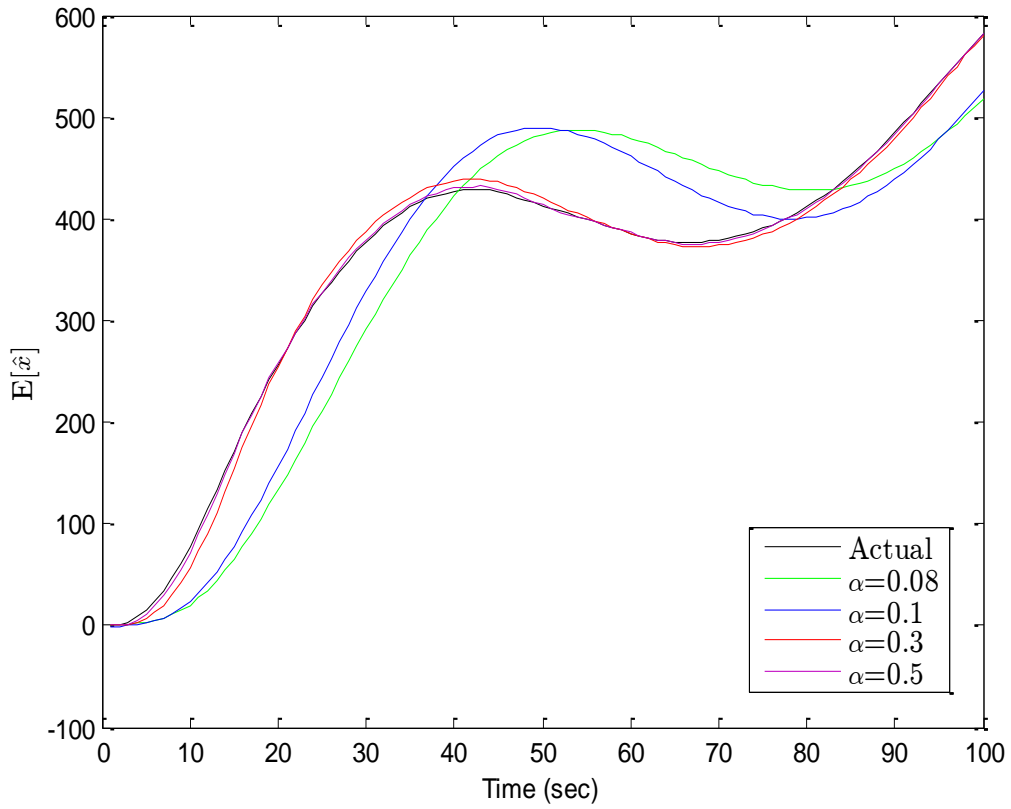
Fig. 2-6: Estimation of position (α-β filter)
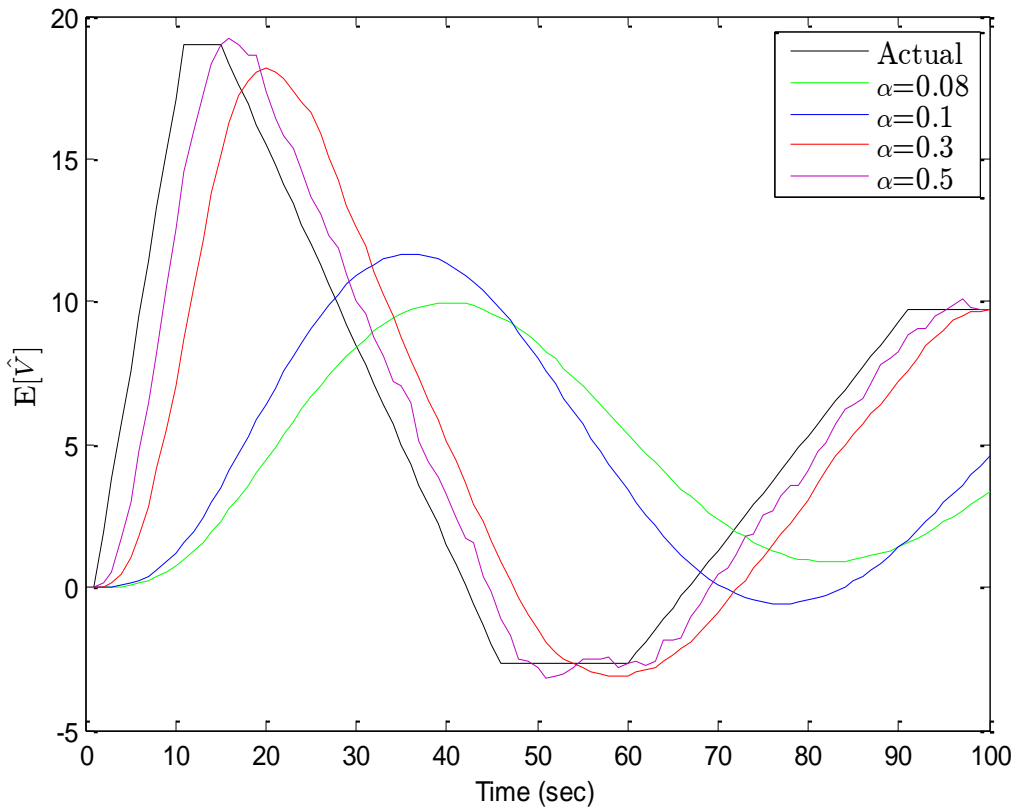
Fig. 2-7: Estimation of velocity (α-β filter)

Another simulation results are shown in the next figures to illustrate the estimated vector states (position, velocity, and acceleration) of a moving target in space using the fixed coefficient filter α-β-γ. The estimated states are shown in the figures (Fig. 2-8, Fig. 2-9, and Fig. 2-10) with different values of gain coefficient $\alpha \in \{0.08, 0.1, 0.3, 0.5\}$. The gain coefficients β and γ are computed by (2.16) and (2.17) respectively.

Again the coefficients of α-β-γ filter have a considerable influence on the performance of the filter. At a low value of the gain coefficients, the estimated states are not accurate, suffer from considerable deterioration, and have an obvious error. With increasing the gain coefficients of the filter, the performance of the filter is improved considerably.

Comparison in the estimation of target position using both filters the α-β-γ filter and α-β filter is shown in Fig. 2-11. It is evident from the results that the performance of the α-β-γ filter in the estimation of position is better than that of the $\alpha\beta$ filter. The prediction of target position using the α-β-γ filter is more accurate than that of $\alpha\beta$ filter due to additional term regarding acceleration.
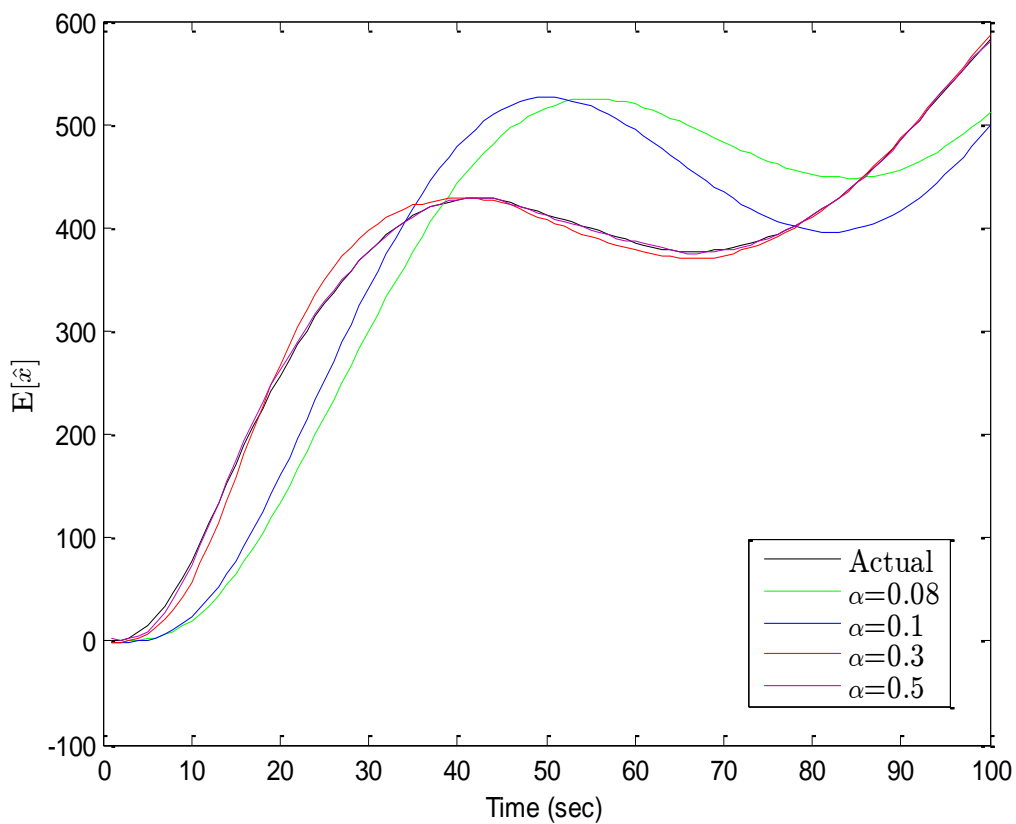
Fig. 2-8: Estimation of position (α-β-γ filter)
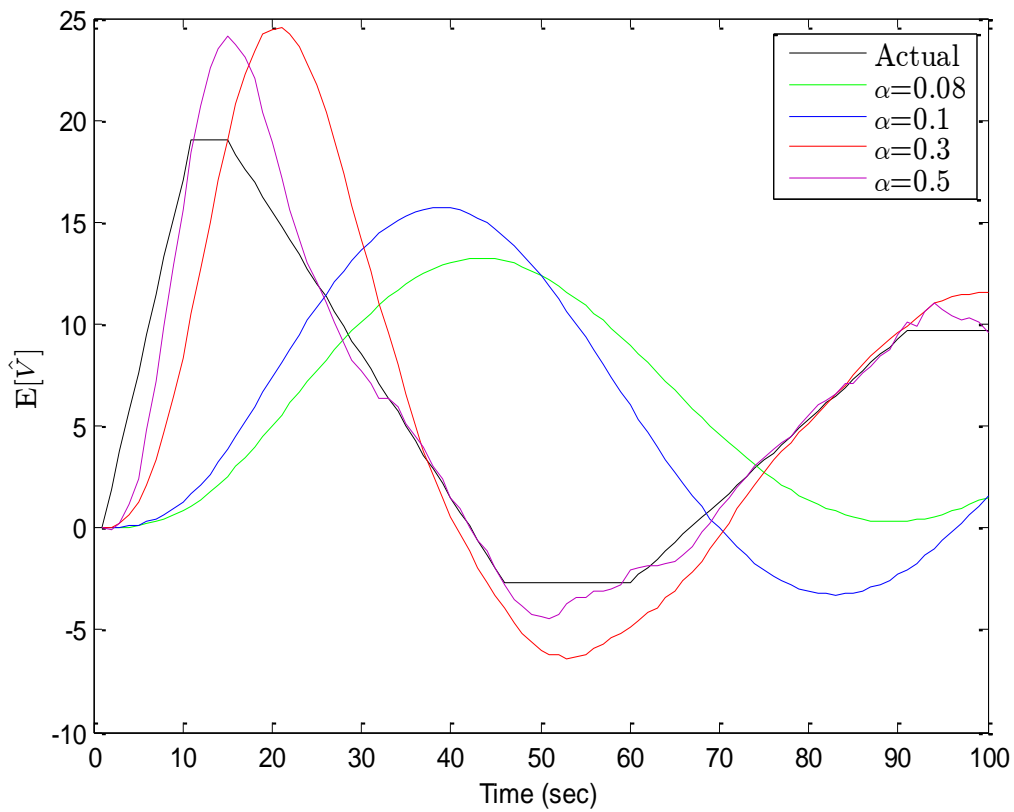
Fig. 2-9: Estimation of velocity (α-β-γ filter)
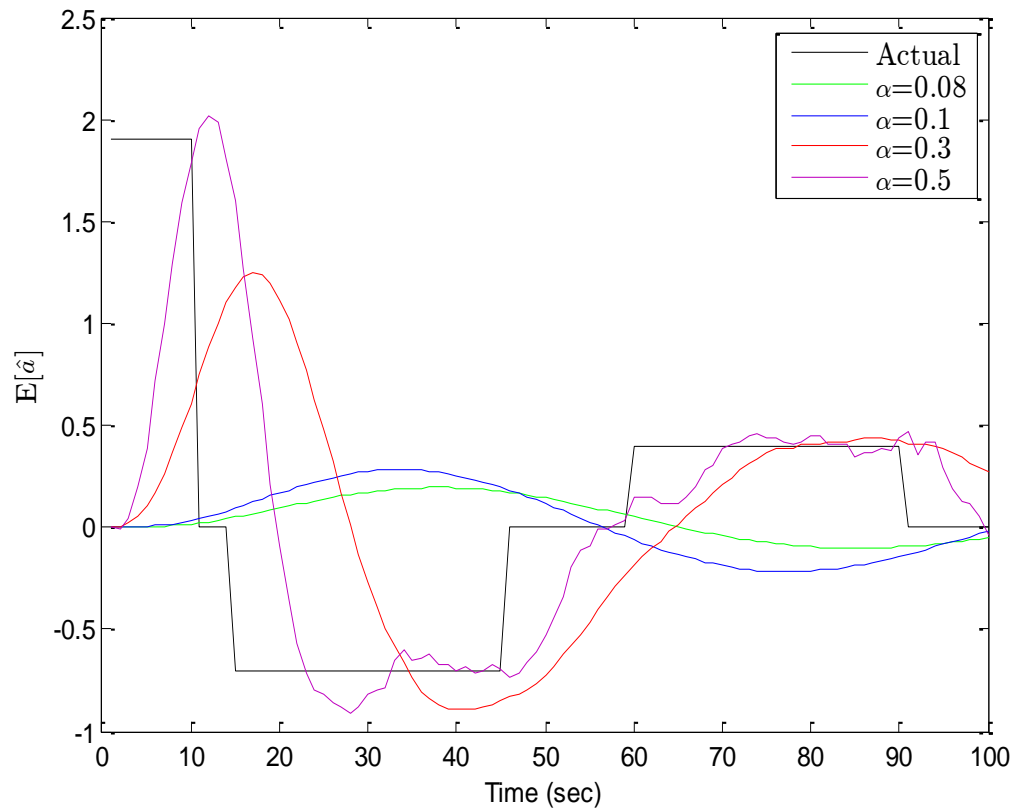
Fig. 2-10: Estimation of acceleration (α-β-γ filter)

17
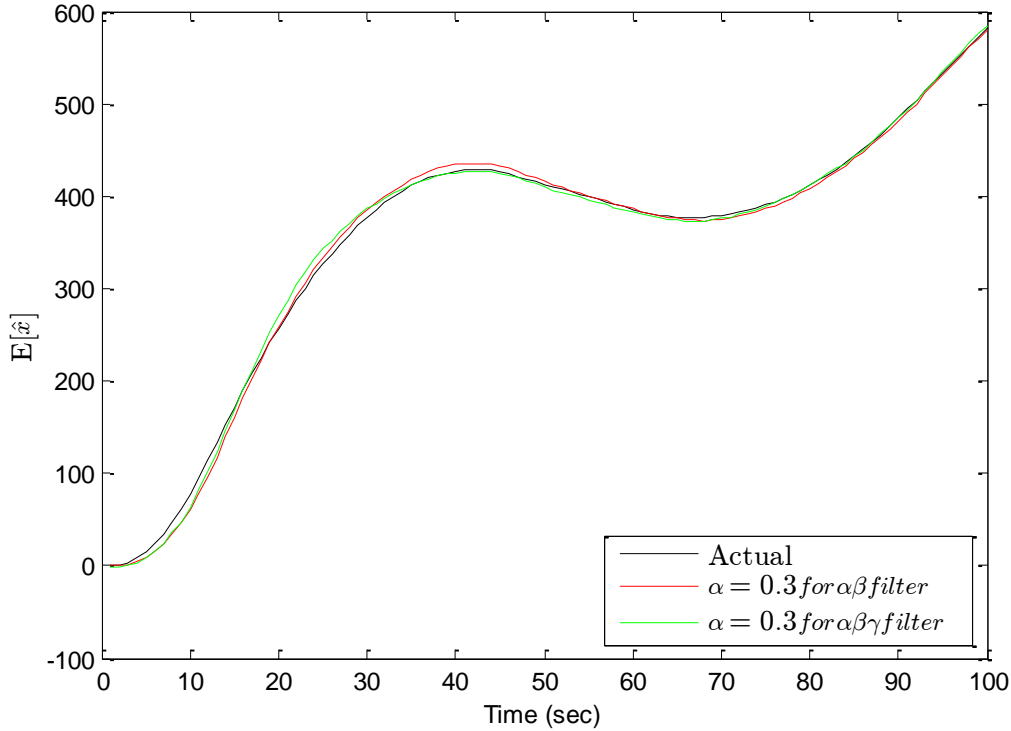
Fig. 2-11: Comparison in the estimation of the position
between (α-β and α-β-γ) filters

2.5.2 Kalman filtering

Kalman filter is pervasive in the aviation and navigation fields due to its accurate estimation characteristic [25], and commonly utilized and more reliable filter for most of the system designers.

Kalman filter is a series of equations to provide an effective (*recursive*) means of estimating a process's state. Accuracy of the Kalman filter algorithm is based on minimizing the mean error of the chosen criteria, such as mean square error, and also depends on the accurate modeling of the measurement noise and the target dynamics. This linear filter is only appropriate for linear systems with the Gaussian process [11]. If the mapping from the states to measurements or target dynamics is described by nonlinear function, other techniques should be employed [3, 18], these techniques are, such as the particle filter, extended Kalman filter, or unscented Kalman filter [18, 6]. Kalman filter is characterized by the property of recursive and does not need to keep all the previous data in the storage.

The filter is effective in many fields and applications such as aviation, guidance, sonar, radar, computer vision systems, signal processing, and navigation systems.

Many derivations of the Kalman filter are given in the literature [26]. Thus, this research will only use the derived equations. Two assumptions are assumed as follows: The target dynamics are modeled in discrete Markov process form, as in (2.18), and the measurements are represented in a linear system state variables combined with uncorrelated noise. So, the measurement vector with dimension M is modeled as in the equation (2.19).

$$x(k+1) = Ax(k) + q(k), \tag{2.18}$$

$$y(k) = Cx(k) + v(k), \tag{2.19}$$

where x is the target state vector, A is the transition matrix, $q(k)$ is the process noise with zero-mean and known covariance matrix Q, C is the measurement matrix, and $v(k)$ is a measurement noise with zero-mean with known covariance matrix R.

18

Markov process is defined as that process in which it is statistical representations of a process in the next scan time is determined entirely by the current state, and Kalman filter equations are concluded as:

$$\hat{x}(k|k) = \hat{x}(k|k-1) + K(k)[y(k) - C\hat{x}(k|k-1)],$$
$$K(k) = P(k|k-1)C^T [CP(k|k-1)C^T + R]^{-1},$$
$$P(k|k) = [I - K(k)C]P(k|k-1), \tag{2.20}$$
$$P(k+1|k) = AP(k|k)A^T + Q,$$
$$\hat{x}(k+1|k) = A\hat{x}(k|k),$$

where: $\hat{x}(k|k)$ is the estimated state vector, $\hat{x}(k|k-1)$ is the predicted state vector, $K(k)$ is the Kalman gain, $P(k|k)$ is the error covariance matrix, $P(k+1|k)$ is the predicted error covariance matrix.

These equations have been partitioned into two groups for simplicity and organization [27]:

(1) *Time update equations* are the equations that responsible for projecting the current state with the error covariance estimates forward to obtain the prior estimates of the next step and considered as predictor equations.

(2) *Measurement update equations* are the equations that are responsible for obtaining the improved posterior estimates by incorporating the new received measurement with the prior estimate and considered as corrector equations.

The estimation algorithm is similar to the prediction-corrector algorithms for resolving the numerical problems [27] and shown in Fig. 2-12.
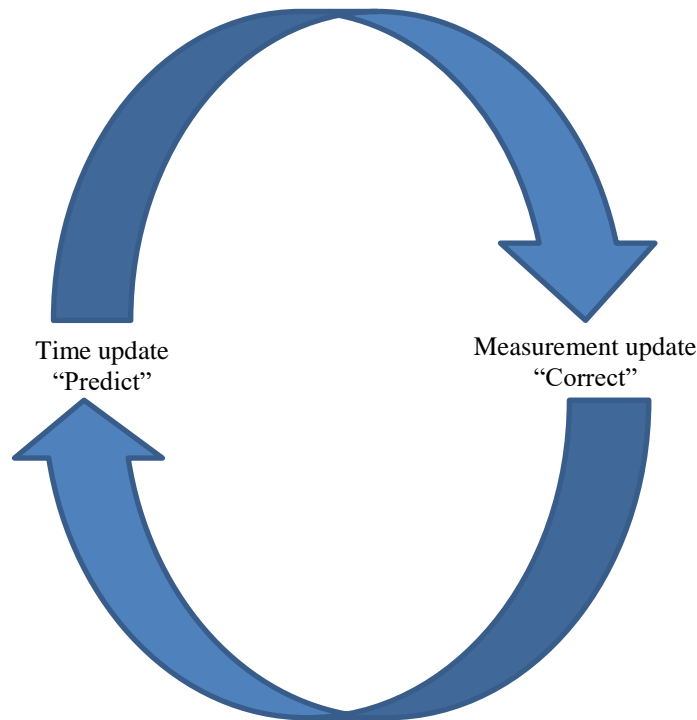
Fig. 2-12: Discrete Kalman filter cycle

The objective of time update equations, as illustrated previously, is to project both the covariance and the state estimates from time step (*k-1*) to a next time step (*k*).

$$\hat{x}(k+1|k) = A\hat{x}(k|k) + Bu(k|k). \tag{2.21}$$

$$P(k+1|k) = AP(k|k)A^T + Q. \tag{2.22}$$

The main functions during measurement update are to calculate the Kalman gain K_k as in (2.23), generate the posterior state estimate $\hat{x}_k$ as in (2.24), and obtain a posterior covariance estimate $P(k|k)$ as in (2.25).

$$K(k) = P(k|k-1)C^T [CP(k|k-1)C^T + R]^{-1}. \tag{2.23}$$

$$\hat{x}(k|k) = \hat{x}(k|k-1) + K(k)[y(k) - C\hat{x}(k|k-1)] . \tag{2.24}$$

$$P(k|k) = [I - K(k)C]P(k|k-1). \tag{2.25}$$

After the update of both time and measurement, the processes are repeated each time between the two phases, and the previous posterior estimates are utilized to predict the new prior estimates. Repeating of the predicting and the correcting phases is called recursive, which is the main attractive feature of the Kalman filter [27].

The following figures, Fig. 2-13 and Fig. 2-14, show a single object moving in two-dimensional space. The tracking system produces an excellent performance under good circumstances, where the density of false alarms $\lambda_{fa} = 10^{-7}$, gate constant $K_g = 2.0$, and the probability of detection $P_d = 0.9$. The question is what will happen when the density of false alarms is increasing for example, up to $\lambda_{fa} = 5 \times 10^{-5}$. As expected, miscorrelation has happened, and the trajectory which based on the Kalman filter is deteriorated due to a high number of false observations inside the gate. The real target is out of the gate as the covariance matrix is permanently decreasing, and the tracking system chooses a false target as if it was a real target. Several approaches have been proposed to minimize the possibility of miscorrelation [11, 18].
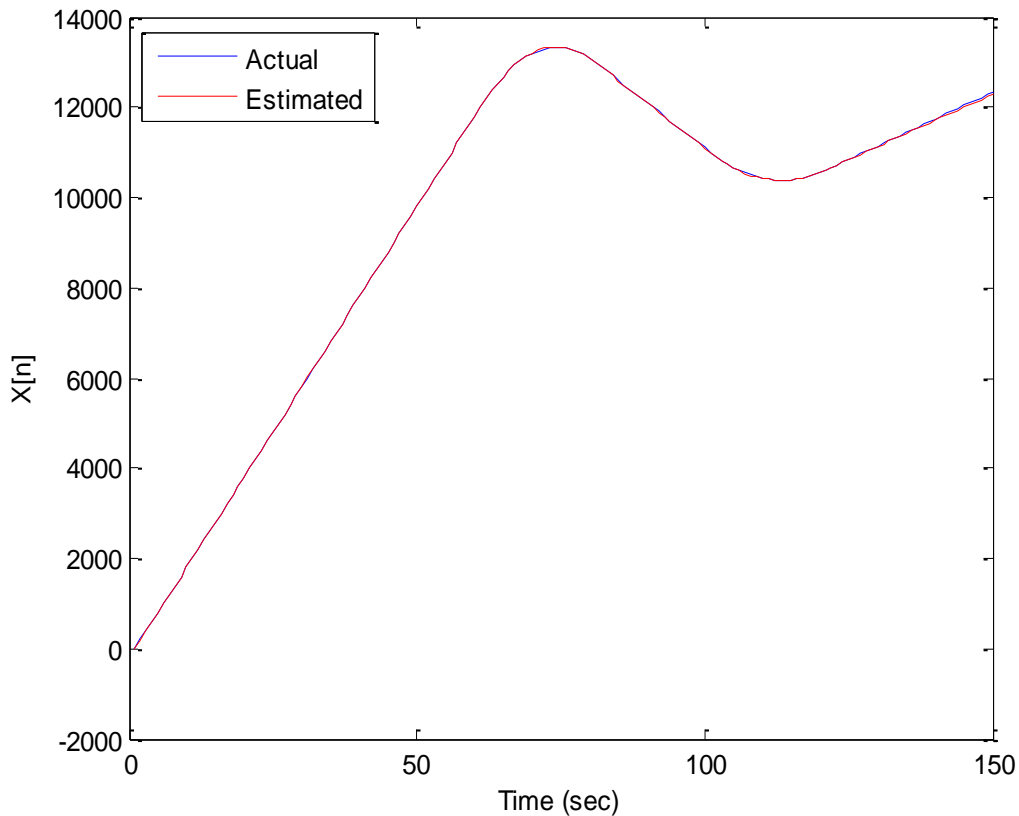
Fig. 2-13: Kalman filter performance in x plane

20
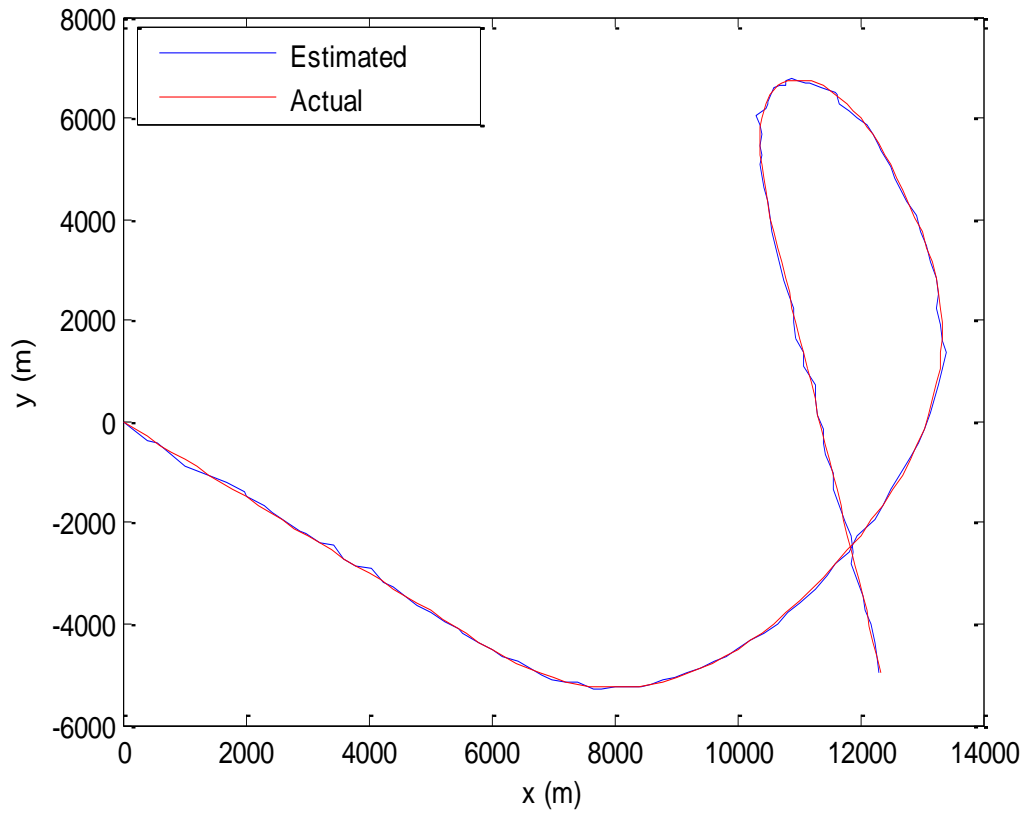
Fig. 2-14: Kalman filter performance in two planes
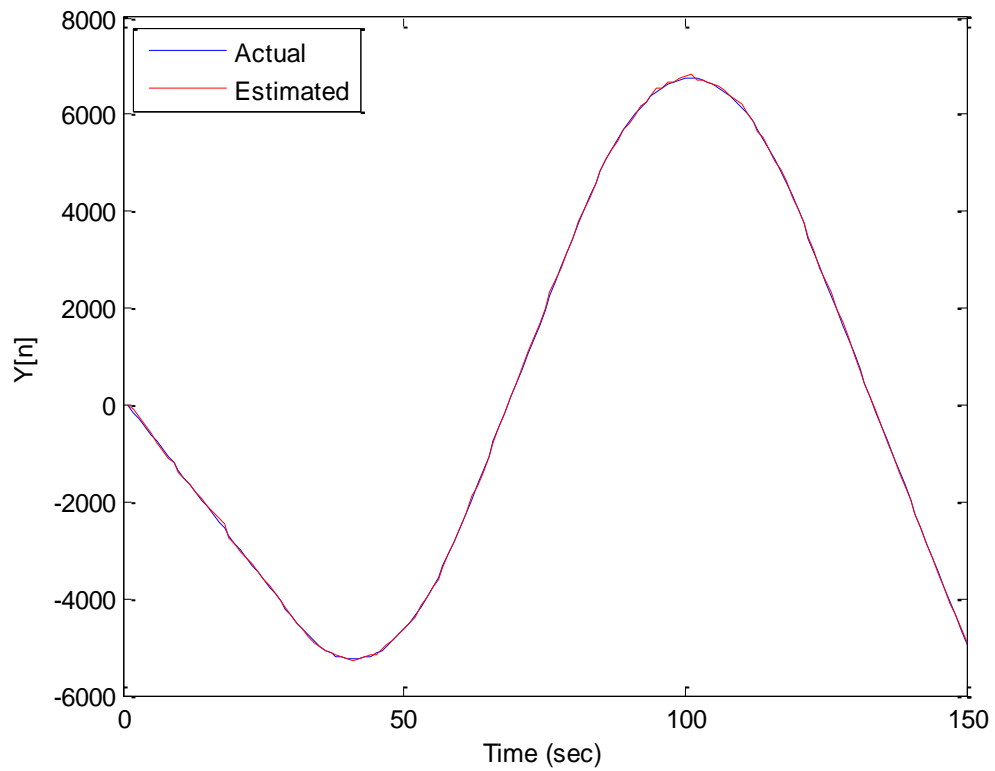
Fig. 2-15: Kalman filter performance in Y plane

21
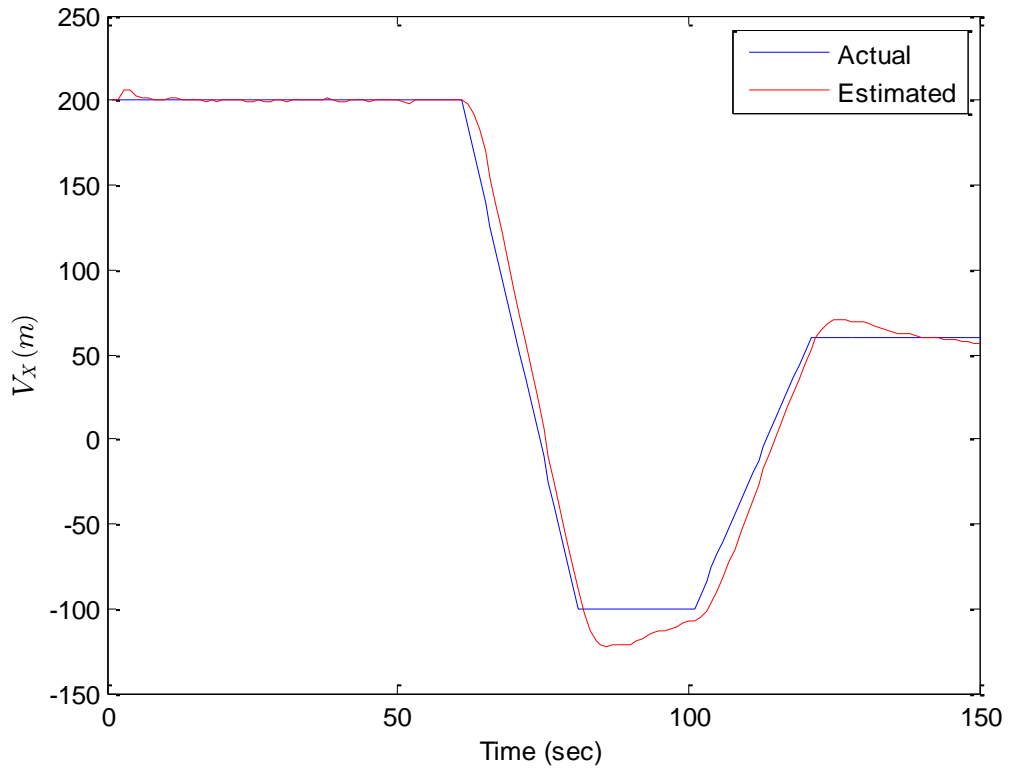
Fig. 2-16: Estimation of velocity along x-axis
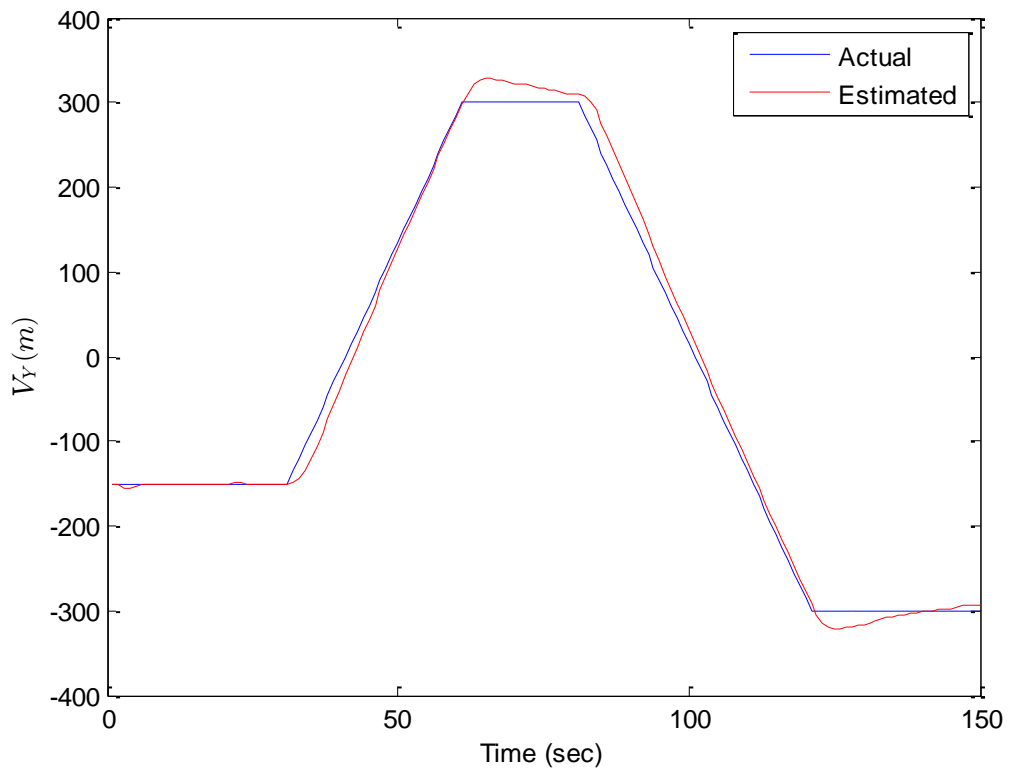
Fig. 2-17:Estimation of velocity along the y-axis

When the gate of the target track contains more than one observation, then, the main objective of the used data association is to determine which of these observations should be associated with the current target track. There are several data association methods, and the easiest method is the sequential nearest neighboring (SNN). This method is based on computing the distance between the predicted position of target track and the position of each observation in that gate of the target track. The SNN method chooses the assignment, which minimizes the overall distance. This method is simple and straightforward, which makes it appealing from a practical viewpoint. However, this method considers only the observations received in the current scan, which makes it prone to *miscorrelation*.

Miscorrelation is an assignment of erroneous observation to a target track and represented as an additional source of errors. False track updates lead to problems in gating, track maintenance, and filtering and prediction, which produce a poor performance [18]. Several methods have been proposed to reduce the possibility of this problem in the sequential nearest neighboring method. One can reduce the probability of miscorrelation by deferring the assignment decision until receive data from several scans, which is the basis of the known multiple hypotheses testing (MHT) method [11, 18]. Another method to overcome this problem is based on modifying the state and error covariance matrix estimates [28]. This method is based on defining a variable γ to indicate the origins of the observation, which is correlated with the track, such that $\gamma=1$ when the observation belongs to true target, $\gamma=0$ when the observation belongs to false alarm, and the Kalman filter equations were modified to be as following [28]:

$$\hat{x}(k\mid k,\gamma) = \hat{x}(k\mid k+1) + \gamma K(\kappa)[y(k) - C\hat{x}(k\mid k-1)],$$
$$P(k\mid k,\gamma) = [I - \gamma K(k)C]P(k\mid k-1), \tag{2.26}$$

where $p(\gamma=1)$ is the probability of correct correlation (P_{cc}), $p(\gamma=0)$ is a probability of wrong correlation $(1-P_{cc})$.

The formed composite estimator of $\hat{x}(k\mid k)$ is (2.27), and the new covariance equation is (2.28).

$$\hat{x}(k\mid k) = P_{cc}\hat{x}(k\mid k,\gamma=1) + (1-P_{cc})\hat{x}(k\mid k,\gamma=0). \tag{2.27}$$

$$P(k\mid k) = \sum_{\gamma=0}^{1} p(\gamma)\left[P(k\mid k,\gamma) + \hat{x}(k\mid k,\gamma)\hat{x}^T(k\mid k,\gamma)\right]$$
$$-\hat{x}(k\mid k)\hat{x}^T(k\mid k). \tag{2.28}$$

In a target tracking system, the performance of the Kalman filter in the presence of missed detection $(P_d < 1)$ and the presence of false observations that originated from clutter or noise is degraded and can be improved by applying the modified Kalman filter. However, improving the performance is based on modifying equations of the filter, which depends strongly on the proper choice of the probability of correct correlation P_{cc}.

Throughout this simulation, the original Kalman filter is denoted by algorithm A1, and the modified Kalman filter given by (2.27) and (2.28) is denoted by Algorithm A2. The tested case is for a single object moving in a plane, as shown in Fig. 2-18. The duration of the experiment was 150 seconds, and the sampling period was 1 second. The target dynamics is corresponding to military aircraft, with a velocity of 300 m/s and the acceleration up to 2G. At every scan, a response is received from the real target with the probability of detection $P_d < 1$ and the density of false alarms is λ_{fa}.
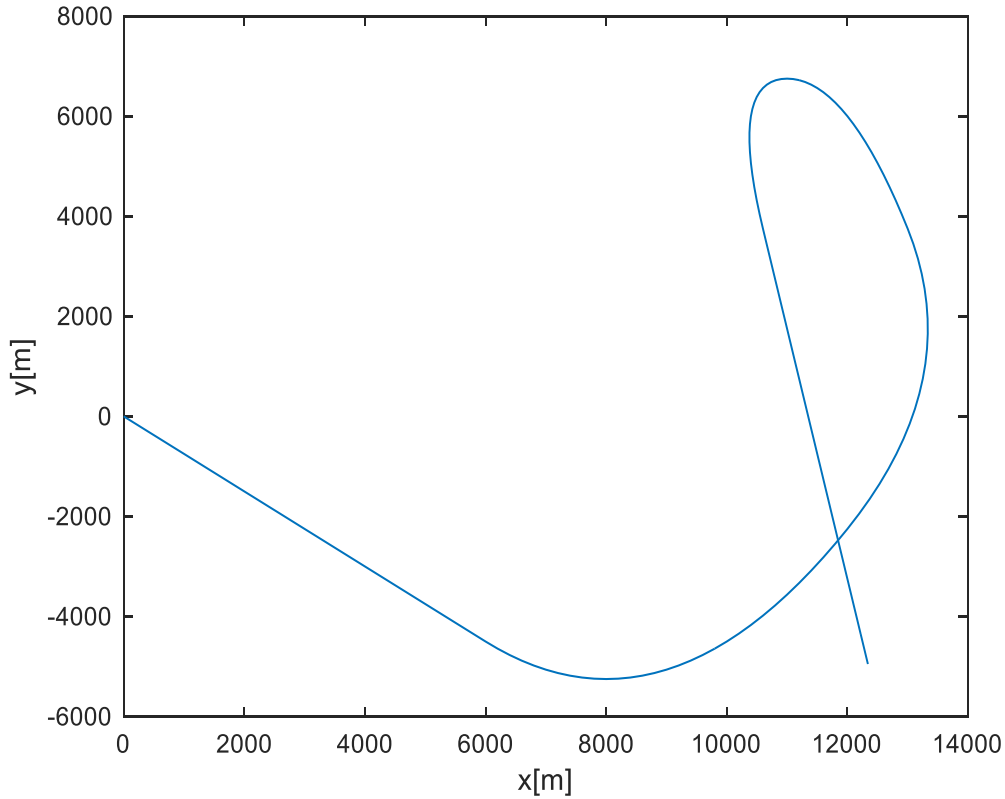
Fig. 2-18: The true trajectory of the tracked target

In this simulation, there is only one real target, and the possibility of false observations is ranging from zero to several observations are received in the gate at every scan. The data association used was sequential nearest-neighboring SNN. The value of the parameters, such as the density of false alarm is $\lambda_{fa} = 1.3 \times 10^{-4}$ and the probability of detection is $P_d = 0.8$. Rather than estimating the probability of correct correlation P_{cc} on-line adopted to a fixed value of $P_{cc} = 0.43$ for modified Kalman filter or algorithm A2.

The next figures (Fig. 2-19 and Fig. 2-20) show the true and the estimated values for the x coordinate for each of the two algorithms.

As shown in the figures Fig. 2-21 and Fig. 2-22, the mean square error of the algorithms A1 and A2 are given by.

$$J = \frac{1}{N} \sum_{i=1}^{N} ((x[i] - \hat{x}[i])^2 + (y[i] - \hat{y}[i])^2) \qquad (2.29)$$

Mean square error is measured and expressed in normalized units, actually in meter square. In order to make this and other paragraphs easy, these units are omitted.

From the two figures (Fig. 2-21 and Fig. 2-22), it is evident that the mean square error (J), which is based on the Kalman filter (algorithm A1), is independent of P_{cc} and seems similar to a flat curve. While in the case of modified Kalman filter the mean square error (J) is based on the value of probability of correct correlation P_{cc}.

In the next two simulations the probability of detection is constant $P_d = 0.8$, and the density of false alarms has two different values. The first value of density of false alarms was $\lambda_{fa} = 1.3 \times 10^{-4}$, and the estimated probability of correct correlation is $P_{cc} = 0.43$ as in Fig. 2-21,

24

while in the second simulation, the value of density of false alarms was decreased to $\lambda_{fa} = 2 \times 10^{-5}$, and the estimated probability of correct correlation is $P_{cc} > 0.62$ as in Fig. 2-22. When the density of false alarms is high, the performance of the Kalman filter or algorithm A1 is deteriorated, as in Fig. 2-21. The interesting point that the performance of the modified Kalman filter or algorithm A2 is worse than the performance of Kalman filter or algorithm A1 when $P_{cc} < 0.33$, but for $P_{cc} > 0.33$ the performance of algorithm A2 is better than A1. Fig. 2-22 shows that the performance of the modified Kalman filter or algorithm A2 is improved when the probability of correct correlation $P_{cc} > 0.62$, but worse than that of A1. This is because the density of false alarm, in this case, is relatively low, and the possibility of miscorrelation is rare.

One concludes from the previous simulations that the correct choice of the probability of correct correlation P_{cc} is essential and suggests that special care should be taken to construct an effective way of estimating this parameter on-line.
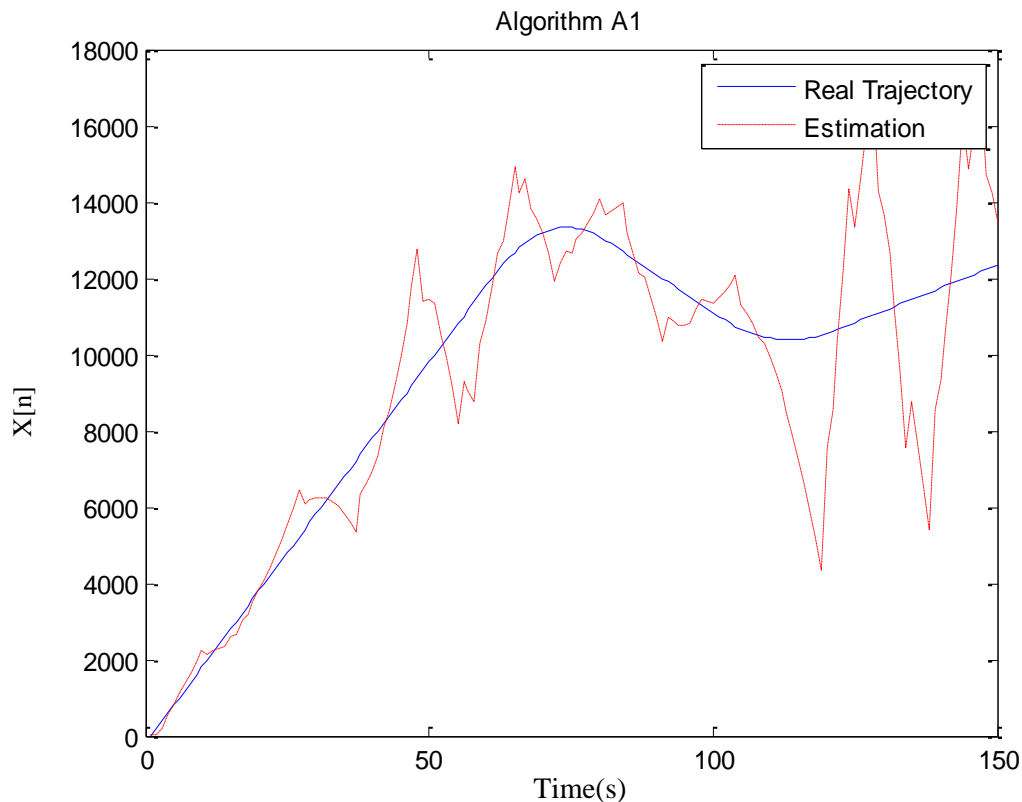
Fig. 2-19: Performance of the standard Kalman filter
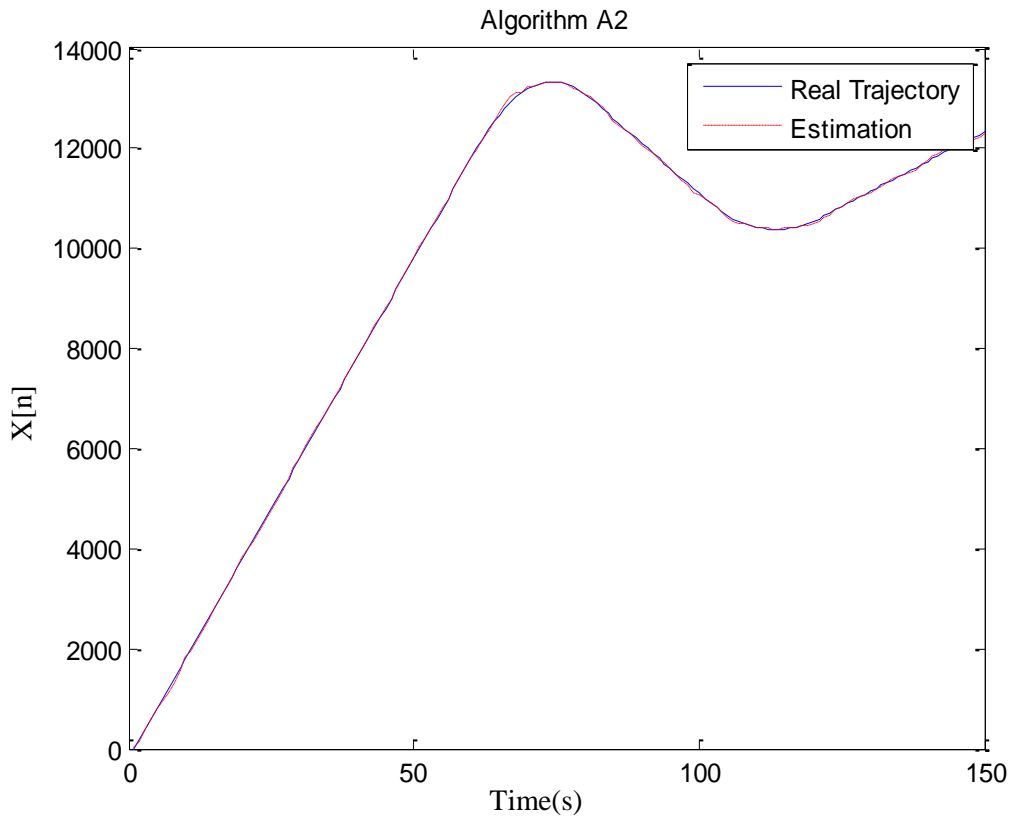
Fig. 2-20: Performance of the modified Kalman filter
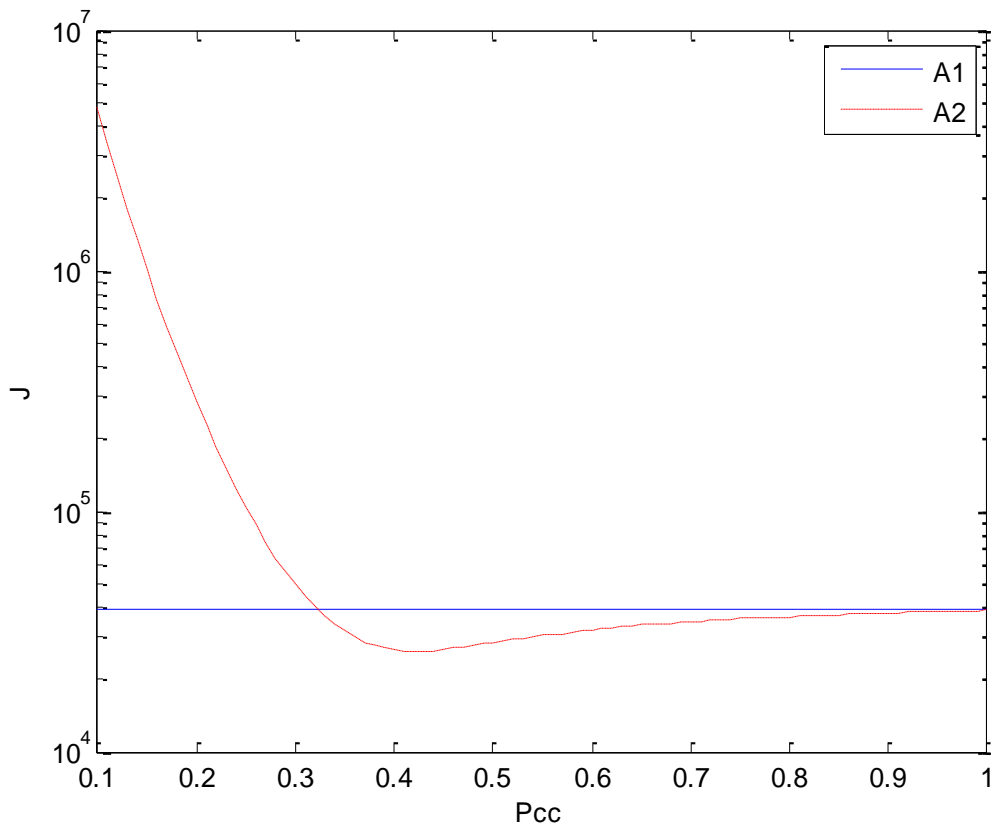
Fig. 2-21: Mean squared errors for $\lambda_{fa} = 1.3 \times 10^{-4}$

26
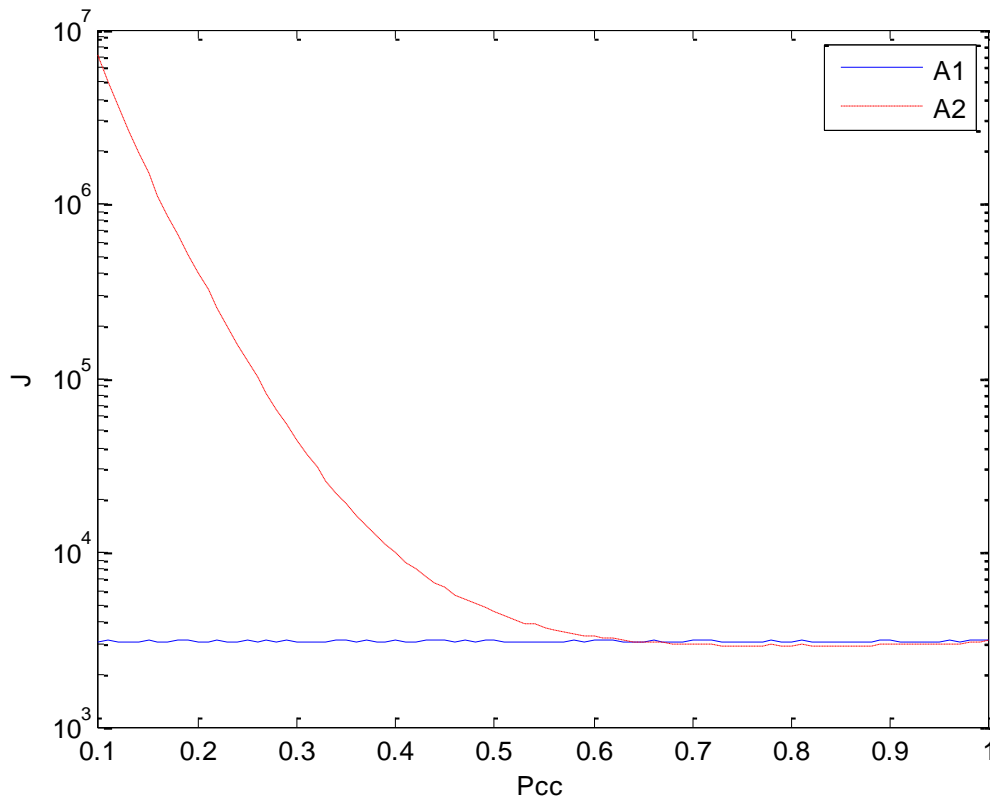
Fig. 2-22: Mean squared errors for $\lambda_{fa} = 2 \times 10^{-5}$

Kalman filter is an optimal estimator, requires full knowledge of the noise covariance matrix that excites the dynamic system. The measurement noise covariance matrix R is usually known from the error statistics of the sensor.

Another simulation result is shown in Fig. 2-23 to illustrate the influence of the process noise and measurement noise on the performance of the target tracking system, which uses the Kalman filter for filtering and prediction.

The process noise covariance matrix Q statistics is usually unknown. It is an essential parameter, requires to be included in the model. Finding process noise variances is not so straightforward as finding measurement noise variances. Wrong estimation or computation of the Q matrix, lead to deterioration of estimation quality or failure of underlying algorithm. There is no standard way of calculating the Q matrix [29]. It is constructed intuitively, usually done by adjusting the weight coefficient of matrix Q.

From Fig. 2-23, the process noise is supposed to be changeable from 10^{-6} to 10^{3} and the measurement noise is supposed of three different values (10, 20, 25). It is evident that the process noise has a considerable influence on the efficiency of the target tracking system. When the user or programmer did not guess the probable value of process noise, then the performance of the target tracking system will be not good. However, if the model is not appropriate, for example, for the model with constant velocity, if the user expects often maneuver movement, then the model will not be suitable and consequently matrix Q must be high enough. Actually matrix Q is the measure of model uncertainty. On contrary, if the model is reliable, that means the target is moving with constant velocity or constant acceleration, the matrix Q should be small enough. In that way, small values of matrix Q will decrease the values of the Kalman gain and consequently, the estimator will believe in the prediction more than the measurement.

There have been several attempts in the literature to estimate the process noise covariance matrix. One can divide these methods into several categories: correlation method [30], maximum likelihood estimation [31], and covariance matching methods [32].
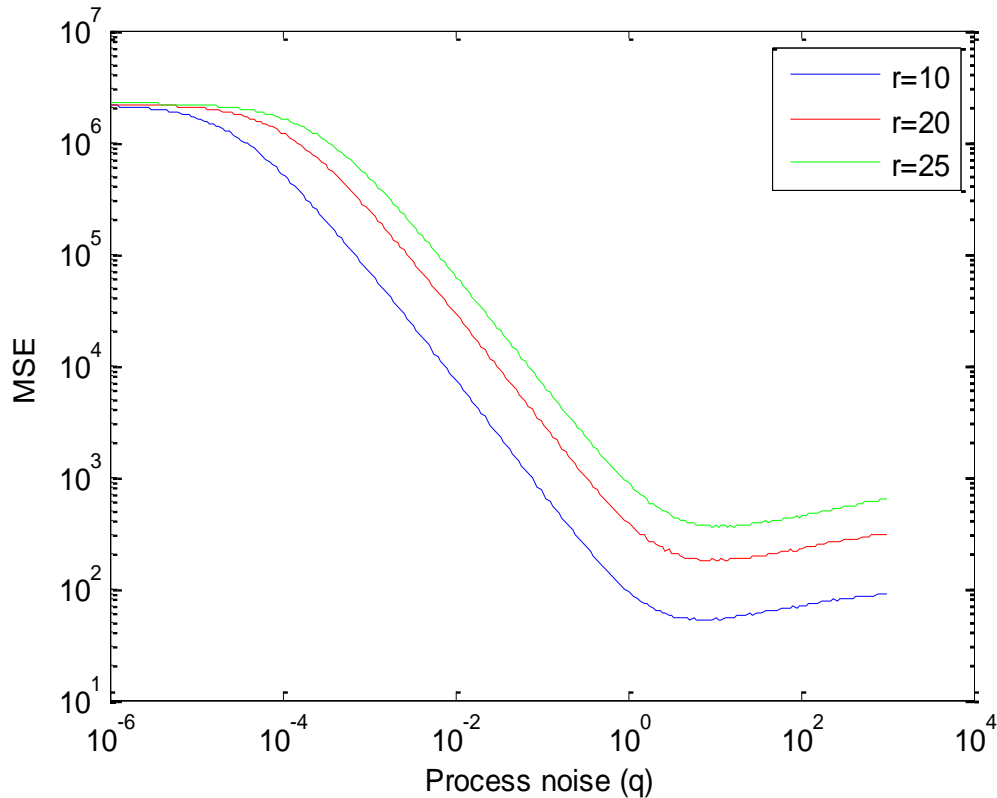
Fig. 2-23: Influence of process noise on the performance of the tracking system.

2.6 Correlation and data associations

The objective of the multiple target tracking system is to collect the data (observations) by the sensor from the surrounded environment. Usually, the collected data contains one or more targets of interest and several false alarms. The most challenging task in the target tracking system is partitioning the received data into sets of observations, where each set forms a track [33]. Each track is composed of a set of observations received from the same source (target).

The method of choosing which observation will be utilized for updating the track is called a *data association or the correlation process*. Over the previous years, several data association methods were proposed. The main difference between these methods is in the way of making the decision to assign the observation to track. Some methods are making a decision on each scan while other methods defer the decision for several scans until collect enough data to make the decision. Some methods make a hard decision while other algorithms make a soft decision, due to the previous classifications. Each of the methods has some advantages and some disadvantages. Some methods suffer from the problem of miscorrelation when the environment is condensed by false alarms, while other methods suffer from a delay in deciding the decision, and so on.

The track updating process usually starts with the gating procedure, which is utilized to eliminate the unlikely observations to be associated with that track.

The main objective of the data association is to determine and associate each real target with its true track. This task is not simple, uncertain, and hard to make an ideal association (associate real target with its true target track) due to many reasons that can be summarized as follows:

(1)   The existence of random false alarms and clutter in the scanned environment and their number is much higher than the number of real targets, and the targets are closely spaced [12].

(2)   Detection of real targets is not possible always (miss-detection), due to many factors such as the low probability of target detection $(P_d < 1)$, terrain obscuration, and power limitations.

(3)   The resolution of the sensor to observe the observations (sensor efficiency), where not all the real targets are always detected, this problem leads to the number of real target detections are fewer than the actual real targets.

There are many approaches related to the multiple target tracking systems in the literature were proposed. These approaches especially consider the issues of the data association as the most considerable difficulty in this field, and can be summarized to the following methods:

- *Nearest Neighbor method* (NN), this method is based on choosing the nearest object to the predicted target position as the correct target and associates that object with that track and considered as the simplest approach [34].

- *Multiple Hypothesis Tracking method* (MHT), the mechanism of this method is based on generating all the possible hypotheses for all received objects within the track gate and considered as the most sophisticated approach. This method uses the measurement oriented approach [12].

- *Joint Probabilistic Data Association method* (JPDA), this method of track updating or data association uses the all nearest neighboring (ANN) approach, which based on sharing all the observations received on that scan and fall in the gate [35]. This method uses an approach known as a target-oriented approach.

2.6.1   The assignment problem

In reality, there are several observations available inside the gate region of a single target track, as usually in the dense environment. Or sometimes these observations are distributed inside the multiple gates of multi-tracks. The target tracking system needs an extra logic for correlating these observations to their true target tracks. Commonly, the available approaches to solve these problems are categorized into two ways:

The first approach is called the nearest-neighbor (NN), where only one observation is chosen from all the received observations that have been fallen in the gate to update the target track. This approach can be modified to be more efficient, but more complicated and named as multiple hypotheses testing techniques, where the final decision is delayed until extra data are received.

The second approach is called all nearest-neighbors (ANN). This approach is named a soft decision approach, where it shares all the observations inside the gate to update the target track. Updating the target track using the ANN approach utilizes the probability theory [11].

The issue of correlating observations to tracks using the sequential nearest neighboring (SNN) approach is one of the examples of a classic assignment issue [36]. The statistical distance function or normalized distance is defined as the measured distance from the observation j to the predicted point of the track i [20]. The optimal assignment is the assignment that associates a maximum number of observations-tracks with minimum total distance function [11, 37].

2.6.2   Normalized distance function

Assume that the residual described by (2.4) is Gaussian, then the likelihood function that relates to assigning the observation j to the target track i with the measurement dimension M can be described by (2.30).

$$g_{ij} = \frac{e^{\frac{-d_{ij}^2}{2}}}{(2\pi)^{\frac{M}{2}} \sqrt{|S_i|}}, \tag{2.30}$$

$$d_{ij}^2 = \tilde{y}_{ij}^T S_i^{-1} \tilde{y}_{ij}, \tag{2.31}$$

where S_i is the error covariance matrix of a track i, and $\tilde{y}_{ij}$ is a residual or error vector between the observation j and the track i.

The assignment that maximizes the g_{ij} term is chosen as the best assignment. Maximizing of the g_{ij} by taking its logarithm is equivalent to the minimizing of (2.32)

$$d_{Gij}^2 = d_{ij}^2 + \ln|S_i|. \tag{2.32}$$

With the assumption of measurement dimension is the same for all observations, a convenient and more appropriate way of defining the distance function is the quantity d_{Gij}^2 given by (2.32), to be used for the problem of associating observations to tracks [11].

2.6.3 Assignment matrix

Assume that there are n tracks that exist when a set of new observations are received. The received observations may be used to update the tracks or used to initiate new tentative tracks. One assumes that, in a dense environment of observations, at time k, m observations are received by the sensor, and it is challenging to make a distinction between the observations originated from real targets, and the observations originated from false alarms. A validated observation is an observation that is inside the gate or on the border of the gate and defined by (2.7). The threshold G must be selected to guarantee that the real measurements with the defined probability are inside the gate. The inequality defined in (2.7) is the validation test. For the problem of assignment, the cost matrix is defined as:

$$\left[C_{ij}\right] = \overbrace{\begin{bmatrix} c_{11} & c_{2n} & : & c_{1n} \\ c_{21} & c_{22} & : & c_{2n} \\ : & : & : & : \\ c_{n1} & c_{n2} & : & c_{nm} \end{bmatrix}}^{j} \Biggr\} i. \tag{2.33}$$

The elements of the cost matrix c_{ij} have the values.

$$c_{ij} = \begin{cases} 1000 & \textit{if the measurement is out of gate of track } i \\ d_{ij}^2 & \textit{if the measurement is in the gate of track } i \end{cases}.$$

This means that if the measurement j is in the gate of target track i, then c_{ij} is defined by (2.32). The purpose of using a cost matrix is to get a number of possible assignments between observations that exist within the track gates and the existing tracks. The optimal assignment is the assignment that produces a maximum number of assignments with the minimum summed total distance. The optimal solution is defined by enumeration. However, this method "enumeration" is too much time-consuming in complicated cases. One chooses to solve the problem of assignment by realizing the Munkres algorithm extension, given in [38]. As a result, one yields the optimal association of measurements to tracks. But, due to the possibility of missed detection (the probability of detection less than unity), which causes some tracks to be updated by false

measurements. That is why it is essential to check each measurement, is it inside the gate by the condition $c_{ij} < G$.

These solutions are the simplest compared with the branching algorithm [11, 20]. These solutions and algorithms cannot be graded as the optimal solutions for all conditions, mainly when missed detection occurs ($P_d < 1$).

2.6.4 Data association approaches

Data association is known as a challenging problem in MTT. The dense environment represents a considerable challenge for the data association, where the problem of the correct data association is not simple to be solved.

Usually, all the observations received from the cluttered environment may not originate from the actual targets, and most of these observations are originated from false alarms or clutter. As a consequence, the assignment between the earlier known targets and the new measurements are always uncertain, and the ambiguities always exist [20]. Assigning incorrect measurements always leads to lost tracks, which lead to track breaks. Also, clutter can create false tracks, and when the density of the false alarms is sufficiently high, probably the produced false tracks can crush the computing resources available for MTT systems. For these rationales, MTT researchers have given much consideration to the data association techniques.

There are several data association techniques utilized by the MTT systems starting from the nearest-neighbor methods to the complicated method as multiple hypotheses trackers (MHT) [20].

2.6.5 Global Nearest Neighboring approach (GNN)

Target tracking is the primary function of every radar surveillance system. The fundamental part of this issue is the data association processing. Mostly all data association algorithms need a measure of the probability to evaluate the alternative hypotheses. The approach Global Nearest Neighbor (GNN) tries to find the most likely hypothesis in every scan.

In a dense environment, the measurements received by the sensor may not all originate from the true targets. Some of these measurements may originate from false alarm or clutter. As a result, ambiguities always exist in the association of the measurements and the previously known target tracks.

The global nearest-neighboring approach (GNN) is the simplest and the easiest compared to the other approaches, but in a dense environment, the performance is degraded. Improved performance is provided by the MHT approach, but it is more complex and challenging to implement. Moreover in cluttered environments may need to maintain a considerable number of hypotheses, which need more computational resources. Due to these problems, other algorithms having less computational requirements are developed [39]. With this approach, the processing of data is done at every scan and uses only the received data on that scan for updating the target track.

In brief, the GNN method is assigning the nearest measurement within the gate to the target track, and during one scan, at most associates, only one observation to the target track [20]. The conventional GNN data association approach works well when targets are widely spaced, the measurements are accurate, a few false alarms are in the gate (not dense environment), and the probability of detection is high, otherwise, miscorrelation will occur [33]. By experience, often, a single miscorrelation leads to loss of the track, and usually, two consecutive miscorrelations will leads inevitably to loss of the track [33]. In order to account miscorrelation, increase the covariance matrix of the Kalman filter, while this worsens the problem by allowing more false alarms to be in the gate [11, 16, 18].

Assume that n target tracks already exist, when the sensors receive a set of m observations at a time index k. These observations are a combination of observations that originated from false alarms, and observations originated from real targets. Commonly, observations originated from the

actual targets are less than that of false alarm. Apply the equations (2.3), (2.4), and (2.7) to all observations in the gate to identify the observations that can be the candidates to correlate with the existing tracks. The observations which satisfy the gating criteria are used to fill the assignment matrix, and the assignments with summed minimum total distance function are chosen as the optimal assignment. The observations which are within the gate and not used to update the track are utilized to initiate the new track.

2.6.6 Multiple Hypotheses Tracking approach (MHT)

One of the first successful and most popular algorithms is multiple hypotheses tracking (MHT)[40] and proposed in [1, 12]. Given the high power of computing, MHT is referred to as a powerful algorithm for addressing the uncertainty of measurement.

The basic principle of the multiple hypotheses tracking algorithm is that difficult decisions of data association are deferred until sufficient data are received [33].

Multiple hypothesis tracking is popular in the community of radar target tracking and classified as the successful and the most efficient algorithm in modern tracking systems to solve the problems of data association [33, 40].

The basic fundamental and the origin of multiple hypotheses tracking in false alarms background for single target is introduced and published by Sea, Singer, and Housewright [41]. Donald Reid was the first who developed the complete algorithmic approach in 1979, and he defines in his algorithm a systematic way of forming and evaluating the multi-data association hypotheses for the multiple targets problem in the presence of a false alarm [12]. The idea of this approach is to form all possible hypotheses concerning target to track associations and to assess each before selecting the best hypothesis.

Using the approach of Reid's algorithm, hypotheses are being transferred from the earlier scan, then, upon receiving new observations, each hypothesis in the previous scan is extended into a number of new hypotheses. Assessing the alternative hypotheses of track formation needs the probabilistic expression that covers all sides of the problem of data association [33]. The considered aspects are, such as a prior probability of the detected target, the density of false alarms, the dynamic consistency, and the sequences of detection of the observations present in the track [12, 33]. This probabilistic expression was presented by Reid. Another equivalent mathematical expression, which is the preferable computational form, and it is the logarithm of the likelihood ratio (LLR), first proposed by Sittler [14] and after that detailed by Blackman and Samuel in [11].

The likelihood ratio (LR) for forming a given data (a prior probability data is included) into the track is defined utilizing a recursive relationship which follows the Bayes rule as given in (2.34) [11, 33].

$$LR = \frac{P(D \mid H_1)P_0(H_1)}{P(D \mid H_0)P_0(H_0)} \triangleq \frac{P_T}{P_F}, \tag{2.34}$$

where H_1 is the true target hypothesis with probability P_T, H_0 is false alarm hypothesis with probability P_F, $P(D \mid H_i)$ is a probability density function of the received data D given H_i is correct, $P_0(H_i)$ is a prior probability of H_i.

It is appropriate and preferable to use the logarithm of a likelihood ratio (LLR) that is known as *track score*, utilized to determine the quality of the track and the track score utilized for track confirmation, defined by (2.35), and the probability of true target is defined by (2.36) [33].

$$LLR = \ln[P_T / P_F]. \tag{2.35}$$

$$P_T = \frac{e^{LLR}}{\left[1 + e^{LLR}\right]}. \tag{2.36}$$

At scan k, the track score $L(k)$ in the recursive form can be placed as (2.37) [11, 32].

$$L(k) = L(k-1) + \Delta L(k). \tag{2.37}$$

$$\Delta L(k) = \begin{cases} \ln(1 - \hat{P}_d) & \text{no update on scan } k \\ \Delta L_u(k) & \text{track update on scan } k \end{cases}. \tag{2.38}$$

Loss in a track score is caused by miss-detection, which is a function in the estimated probability of detection $(\hat{P}_d)$, while upon update, ΔL_u in a track score is a function in many parameters, such as covariance matrix (S) obtained by (2.5), residual error $(\tilde{y})$ obtained by (2.4), estimated false alarm density $(\hat{\lambda}_{fa})$, and the estimated probability of detection $(\hat{P}_d)$ [1, 33].

The score of the hypothesis is that the total of all the track scores found in the hypothesis, and the hypothesis probabilities are computed from the hypothesis score [1, 11]. Many hypotheses maybe exist in one track. Hence track probability is computed as the total of all the hypotheses probabilities contained in that track.

In order to compute the track probabilities and hypothesis from a track score as in the previous equations, the developers of MHT systems assume some assumptions to improve the performance of the approach, to obtain better results, and these assumptions are as follows [33]:

(1) The measurement error statistics and the target dynamics may be approximated by Gaussian models.

(2) False alarms are uniformly distributed.

The MHT system generates potential hypotheses after each scan, the number of hypotheses is increasing, and to keep the hypotheses growth limited, several techniques are developed. These techniques include track merging, track and hypothesis pruning, and clustering [33].

The clustering operation has many features, such as reducing the generated and evaluated hypotheses and partitioning the significant hypotheses tree into a number of small hypotheses. Then the efficiency of processing is improved due to processing within every cluster is done independent from other clusters. Hypotheses are evaluated within each cluster, and tracks and hypotheses with low probabilities are deleted [33].

2.6.7 Probabilistic Data Association (PDA & JPDA)

This approach of data association considers how multiple hypotheses are successfully formed after every scan of observations. This approach is based on combining and performing the hypotheses created during the current scan before processing the observations of the next scan. The obtained updated estimate is a contribution of all the neighboring observations that lie within the valid region of the target track gate.

Associating a target in a dense environment with a single track, using an all-neighbors approach was first proposed by Edison and Bar-shalom [15] and denoted as a probabilistic data association (PDA).

Performance of the PDA is very low in the existence of multiple targets. To solve this problem and improve the performance, the approach (PDA) is modified and denoted as Joint Probabilistic Data Association (JPDA) approach [42].

Commonly these two approaches PDA and JPDA are a particular case of MHT, and have several points that must be mentioned, such as:

(1)   This approach never makes any hard decision on correlating measurements to tracks, because all the observations in the gate are shared to produce a soft data association decision [43].

(2)   This approach has no explicit provision for track initiation and necessary to define distinct track initiation functions, like the method mentioned by Fortman [42] and denoted as the operator-interactive process.

The PDA approach is a suboptimal Bayesian algorithm, assumes that at the $k-th$ scan, there are N observations $z_j(k), j = 1,2,3,....N$ in the gate of the track i, and only one observation from these observations is a real target with a probability of detection P_d. Assume the density of false observations is Poisson distribution, with density β, where β includes both of the false alarms and the new targets $(\beta = \beta_{FT} + \beta_{NT})$.

The approach forms $(N+1)$ hypothesis, where the first generated hypothesis assumes all the observations inside the gate are false alarms and dented as H_0, and the probability of the hypothesis H_0 is proportional to (2.39), while the rest of N hypotheses are $H_j (j = 1,2,..N)$ and their probabilities are proportional to (2.40). The probabilities (p_{ij}) are computed by the normalization (2.41) and simplified to (2.42).

$$p'_{i0} = \beta^N (1 - P_d), \tag{2.39}$$

$$p'_{ij} = \frac{\beta^{N-1} P_d e^{-\frac{d_{ij}^2}{2}}}{(2\pi)^{M/2}\sqrt{|S_i|}} , j = 1,2,..N , \tag{2.40}$$

$$(p_{ij}) = \frac{p'_{ij}}{\sum\limits_{i=0}^{N} p'_{ij}}, \tag{2.41}$$

$$p_{ij} = \begin{cases} \dfrac{b}{b + \sum\limits_{l=0}^{N} \alpha_{il}} & , \; j = 0 \text{ (no target exist)} \\[4ex] \dfrac{\alpha_{ij}}{b + \sum\limits_{l=0}^{N} \alpha_{il}} & , \qquad 1 \le j \le N \end{cases}, \tag{2.42}$$

$$b = (1 - P_d)\beta(2\pi)^{M/2}\sqrt{|S_i|}, \tag{2.43}$$

$$\alpha_{ij} = P_d e^{-\frac{d_{ij}^2}{2}} . \tag{2.44}$$

The residual of the track i in the $k-th$ scan is calculated as a weighted sum of N residuals by (2.45) after calculating the probabilities P_{ij} by the equations (2.39),(2.40), and (2.42).

$$\tilde{y}_i(k) = \sum_{j=1}^{N} p_{ij} \tilde{y}_{ij}(k). \tag{2.45}$$

Subsequently, the Kalman filter update and covariance equations at scan k are modified as in (2.46) and (2.47) respectively.

$$\hat{x}(k \mid k) = \hat{x}(k \mid k-1) + K(k)\tilde{y}(k),$$ (2.46)

$$P(k \mid k) = P^o(k \mid k) + dP(k),$$ (2.47)

$$P^o(k \mid k) = p_{i0}P(k \mid k-1) + (1 - p_{i0})P^*(k \mid k),$$ (2.48)

$$dP(k \mid k) = K(k)\left[\sum_{j=1}^{N} p_{ij}\tilde{y}_{ij}\tilde{y}_{ij}^T - \tilde{y}_i\tilde{y}_i^T\right]K^T(k),$$ (2.49)

$$p_{i0} = \frac{b}{b + \sum_{l=0}^{N}\alpha_{il}},$$ (2.50)

where $P^o(k \mid k)$ is the computed covariance matrix, $dP(k)$ is a term added to account miscorrelation, $K(k)$ is the Kalman gain, and $P^*(k \mid k)$ is the covariance matrix. Both parameters $K(k)$ and $P^*(k \mid k)$ are defined by (2.20).

The association probabilities (p_{ij}) for JPDA are computed utilizing all tracks, and all observations (the probability equation (2.42) must be modified to be valid for multiple tracks) [11]. With the JPDA approach, hypotheses probabilities $P'(H_i)$ are defined as a function in (β, g_{ij}, P_d).

Let observations within the track gate are denoted as N_o, and the number of tracks is denoted as N_T. The factor that commonly appears in all hypothesis probabilities $P'(H_l)$ can be calculated as follow.

$$C_f = \begin{cases} \beta^{(N_o - N_T)} & N_o > N_T \\ (1 - P_d)^{(N_o - N_T)} & otherwise \end{cases}.$$ (2.51)

With the assumption of a unique P_d for all tracks, and the normalized probabilities $P(H_i)$ are calculated using the equation (2.52), and the overall number of hypotheses is denoted as N_h.

$$P(H_i) = \frac{P'(H_i)}{\sum_{i=1}^{N_h} P'(H_i)}.$$ (2.52)

2.7 Track management

Track status is commonly composed of three stages (tentative, confirmed, and deleted). Usually, a new tentative track is formed from any observation that satisfies the gating conditions and not assigned to any track.

In radar systems, if the tentative track did not correlate with any observation for a set of consecutive scans, say 4, then the tentative track dismissed as a false alarm. The simplest track deletion is based on missed detections for N consecutive scans.

There is a set of approaches to track initiation and track confirmation for both recursive and batch techniques, and other approaches to track deletion.

2.7.1 Track initiation

Track initiation is an integral part of the target tracking algorithm [44, 45]. In the dense environment, there are some challenges to track initiation [44], such as the long-distance from targets to sensors, inaccuracy of the measurement received, and the lower detection of sensors. The efficiency of the target tracking algorithm depends heavily on the target track initiation [45].

Track initiation in conventional radar systems is considered in two techniques [45, 46]: *sequential processing technique, batch processing technique.*

The *sequential processing technique*: is usually appropriate in the existence of a comparatively uncluttered environment, requires low computational cost, and commonly used in radar, sonar tracking, and has two approaches (*the heuristic rule method* and *the logic-based method*).

The second technique is the *batch processing technique*, which is the preferred technique, based on processing of the measurements collected during the previous N scans to declare a target trajectory, often used in dense clutter environment, but has a heavy burden of computation and slower process, and has two approaches (*the Hough transform method, the modified Hough transform method*) [46]. However, still, there is a severe lack of assessment of the practical application of these two types of track initiation approaches [11, 46].

2.7.1.1 Heuristic rule method

The heuristic method utilizes two basic rules to minimize the potential initiation of false tracks. These are named as speed and acceleration constraints.

Suppose that, the positions of the measurements from N previous scans are r_i, $i = 1, 2, ..N$. The track is initiated by this method if a set of M measurements observed from N scans complies with the following requirements [46]:

1) The estimated or measured velocity is lower than the maximum velocity and higher than the minimum velocity, and expressed as follow:

$$v_{min} \leq \left| \frac{r_i - r_{i-1}}{t_i - t_{i-1}} \right| \leq v_{max}. \tag{2.53}$$

2) The estimated or measured acceleration is lower than a maximum acceleration (a_{max}), if the number of returns occurs more than one, then choose the return with the lowest acceleration to form a new track and expressed as follow:

$$\left| \frac{r_{i+1} - r_i}{t_{i+1} - t_i} - \frac{r_i - r_{i-1}}{t_i - t_{i-1}} \right| \leq a_{max}(t_{i-1} - t_i). \tag{2.54}$$

3) Angle limiting rule is implemented to reduce the chances of creating false tracks. Let the angle ϕ is between the vectors ($r_{i+1} - r_i$ and $r_i - r_{i-1}$), and computed as follows.

$$\phi = \cos^{-1}\left[\frac{(r_{i+1} - r_i).(r_i - r_{i-1})}{|r_{i+1} - r_i| |r_i - r_{i-1}|} \right]. \tag{2.55}$$

The angle limit is expressed as $|\phi| \leq \phi_0$, where $0 < \phi_0 \leq \pi$, and if $\phi_0 = \pi$ then, the angle ϕ is not limited.

2.7.1.2 Logic-based (LB) method

In sequential processing techniques, the approach logic-based is the common track initiation [1], where the hypotheses are produced during a number of sequential scans, and these hypotheses are confirmed through associating measurements with the predicted target position. The track is initiated if m success associations have occurred from n scans. In the literature, there are several improvements and extensions to the approach logic-based [47].

This technique utilizes the gating and the prediction to identify the possible tracks in the multiple hypothesis fashion [11, 45, 46].

This method starts with measuring the distance between the two measurements $z_i(t)$ and $z_j(t+1)$, as in the equation (2.56).

$$d_{ij}^k = \max[0, z_j^k(t+1) - z_i^k(t) - v_{\max}^k \cdot t_s]$$
$$+ \max[0, z_j^k(t+1) - z_i^k(t) - v_{\min}^k \cdot t_s], \tag{2.56}$$

where t_s is the time between two consecutive scans, with the assumption of measurement error is normal, independent with zero mean and covariance $R_i(t)$, and the square normalized distance is defined as:

$$D_{ij}(t) = d_{ij}^T(t)\left[R_i(t) + R_j(t+1)\right]^{-1} d_{ij}(t), \tag{2.57}$$

where $D_{ij}(t)$ is utilized as the test statistics to be compared with the threshold γ.

The procedure is summarized in the following steps [46]:

(1) Surround the received measurement in the first scan $z_i^1(t)$ by a region, and any measurement fall within that region is a potential track.

(2) Straight-line extrapolation is made for each potential track composed of two measurements, utilized for the third scan. The nearest observation to the prediction in a third scan is utilized to update the potential track.

(3) For each potential track, composed of more than two observations, prediction to the next scan is made by a polynomial of a second-order and updated by the nearest observation to the prediction.

(4) Repeat step (3) several times (scans) and use the least square method to compute the residual.

If the potential track validation region is empty during the process, the track will be deleted. Uncorrelated observations to the tracks in each scan are utilized to start new potential tracks as in step (1).

2.7.1.3 Hough transform (HT) technique

Hough transform is a traditional track initiation approach. Feature extraction techniques are used in digital image processing plus computer vision [48].

The HT transforms a measurement (x_i, y_i) in a Cartesian coordinate to a curve in a parameter space (ρ, θ) using the equation (2.58).

$$\rho = x \cos\theta + y \sin\theta, \tag{2.58}$$

where ρ is the perpendicular distance between the line and the origin, θ is x-axis angle made by this perpendicular [45, 46].

Each measurement in the Cartesian plane (x_i, y_i) describes a curve in the (ρ, θ) plane, and a collection of measurements produces a set of curves that intersect at a point (ρ_0, θ_0).

The (ρ, θ) parameter space is discretized to $N_p \times N_\theta$ cells with distance spacing Δ_ρ and angle intervals Δ_θ. The center of the interval is computed as:

$$\theta_m = (m - \frac{1}{2})\Delta_\theta \quad , m = 1, 2, ... N_\theta. \tag{2.59}$$

$$\rho_n = (n - \frac{1}{2})\Delta_\rho \quad , n = 1, 2, ... N_\rho. \tag{2.60}$$

In a case there are many collinear points in the (x, y) plane, then, these points will accumulate in the respective cell. After several scans, points will accumulate in a particular cell from objects moving along the straight line. If the points in a particular cell exceed a predetermined limit or threshold, a straight-line target trajectory will be detected [46].

2.7.1.4 Modified Hough transform (modified *HT*) technique

A modified HT method is suggested to fix the HT issues. The modified HT method initiates the track by detecting the intersection in the (ρ, θ) plane, due to that the controlling parameter is reduced to one, and the use of histogram is canceled [46].

Suppose there are N returns from N scans $\{(x_i, y_i), i = 1, .., N\}$, these measurements are transformed by HT to a set of curves $\rho_i(\theta)$, where $\theta \in [0, \pi]$ *and* $i = 1, ..N$. The difference is formed as:

$$\Delta\rho_i(\theta) = \rho_{i+1}(\theta) - \rho_i(\theta). \tag{2.61}$$

Some pieces of information are obtained from zero-crossing of $\Delta\rho_i(\theta)$ like:

(1) the coordinate θ is indicated from the crossing point ρ_i and ρ_{i+1} and denoted as θ_i^0.

(2) At the crossing, the slope sign is based on the vector direction.

Two criteria for track initiation are defined based on these pieces of information.

- The points of zero-crossing θ_i^0 and θ_{i+1}^0 have to be at similar proximity.

$$|\theta_i^0 - \theta_{i+1}^0| \leq \sigma_\theta, \tag{2.62}$$

where $\Delta\theta \leq \sigma_\theta \leq m\Delta\theta$ is a value of tolerance, and this criterion is for collinear testing.

- The sign of both slopes at points (θ_i^0 and θ_{i+1}^0) must be the same, and this criterion is used to define the target movement direction.

2.7.2 Track confirtion

Rules of simple track confirmation are often defined based on some number of associations between the observations and the tentative track. The conditions of confirming a tentative track depend on the used system, where radar system requires only one observation is sufficient to confirm the tentative track, while with other systems, it requires more restrictive rules, such as correlating *M* observations from *N* consecutive scans [11].

2.7.2.1 Track confirmation using sequential analysis

Sequential probability ratio test ($SPRT$) is the simplest type of the sequential analysis techniques, which chooses one hypothesis from two hypotheses (H_0, H_1), where: H_0 is defined as the hypothesis when all observations are false alarms, H_1 is defined as the hypothesis which indicates existence of a real target within the gate of the target track [11].

The SPRT method assumes three alternatives whenever new data are received. These alternatives are $(H_0, H_1,$ delaying a decision until enough data are obtained). Suppose the first observation has been detected and must determine as originated from a real target or a false alarm. Assume after that, the receiver detects m observations during k consecutive scans. Then, for the hypothesis H_1, the likelihood function is defined by (2.63), and that for H_0 is defined by (2.64).

$$P_{ik} = P_d^m (1 - P_d)^{k-m}, \tag{2.63}$$

$$P_{0k} = P_f^m (1 - P_f)^{k-m}, \tag{2.64}$$

where P_d is the probability of detecting a real target, P_f is the probability of detecting a false alarm.

Some statistic definitions should be defined, to be used in obtaining the final decision logic given by (2.65). These definitions include both of the upper limit $T_u(k)$ and the lower limit $T_L(k)$ is given by (2.66), and the test statistics $ST(k)$ given by (2.67) [11].

$$ST(k) \leq T_L(k), accept\ H_0\ (not\ target\ is\ present),$$
$$ST(k) \geq T_U(k), accept\ H_1\ (true\ target\ present), \tag{2.65}$$
$$T_L(k) < ST(k) < T_U(k), continue\ testing,$$

$$T_U(k) = \ln C_2 + ka_2,$$
$$T_L(k) = \ln C_1 + ka_2, \tag{2.66}$$

$$ST(k) \triangleq m\, a_1, \tag{2.67}$$

where the thresholds C_1 and C_2 are given by(2.68), and constants a_1 and a_2 are defined by(2.69).

$$C_1 = \frac{\beta}{1-\alpha}, \qquad C_2 = \frac{1-\beta}{\alpha}, \tag{2.68}$$

$$a_1 \triangleq \ln\left[\frac{P_d / (1-P_d)}{P_f / (1-P_f)}\right], \qquad a_2 \triangleq \ln\left[\frac{1-P_f}{1-P_d}\right], \tag{2.69}$$

where $T_u(k)$is the upper threshold, $T_L(k)$is the lower threshold, α is the probability to accept the hypothesis H_1 when the true hypothesis is H_0, β is the probability to accept the hypothesis H_0 when the true hypothesis is H_1.

The upper and lower thresholds ($T_L(k)$ and $T_u(k)$) are two parallel lines and increase by a_2 on every scan. Whenever the tracking system receives a new detection, the test statistic $ST(k)$ will increase by a_1. Make a decision whenever either of the thresholds $T_L(k)$ and $T_u(k)$ is penetrated by test statistic $ST(k)$ [11].

2.7.2.2 Baysian track confirmation

Bayes rule [49] is applied to develop a comparatively simple sequential method for track confirmation [11]. The probability of the true track given a measurement data D using the Bayes rule is given by (2.70).

$$P(T \mid D) = \frac{P(D \mid T)P_0(T)}{P(D)}, \tag{2.70}$$

$$P(D) = P(D \mid T)P_o(T) + P(D \mid F)P_o(F), \tag{2.71}$$

$$P_o(F) = 1 - P_o(T), \tag{2.72}$$

where $P(D|F)$ is a probability of accepting data D given a presence of a false alarm, $P(D|T)$ is a probability of accepting data D given presence of the true target, $P_0(T)$ is a *prior* probability of the true target, $P(D)$ is a probability of receiving a measurement data D, $P_0(F)$ is a *prior* probability of the false alarm.

After substitute in (2.70), one gets (2.73).

$$P(T \mid D) = \frac{L(D)P_0(T)}{L(D)P_0(T) + 1 - P_0(T)}. \tag{2.73}$$

Equation (2.70) can be represented in two different forms. The first form is defined by defining L_k, which is the likelihood ratio of the data received in the $k - th$ scan, the probability of the true target given measurement data in scan k is denoted as $P(T|D_k)$, and defined by (2.74). The second form is represented by defining the likelihood of data received in all k scans. Then, the likelihood function of data in all k scans $L(D)$ is defined as the product of all individual likelihoods (L_k) as in (2.75):

$$P(T|D_k) = \frac{L_k P(T \mid D_k)}{L_k P(T|D_k) + 1 - P(T \mid D_k)}. \tag{2.74}$$

$$L(D) = \prod_{k=1}^{K} L_k. \tag{2.75}$$

Then, whenever new data is received equation (2.73) is updated utilizing the equation (2.75), and the hypothesis H_1 will be accepted whenever it reaches the acceptance threshold probability P_A [11].

$$P(T \mid D) \geq P_A. \tag{2.76}$$

So, combining the equations (2.73) and (2.76) gives $L(D)$ in (2.77).

$$L(D) \geq \frac{P_A(1 - P_0)}{(1 - P_A)P_0}. \tag{2.77}$$

The likelihood (L_k) is computed as follows: The data set D_k is determined by defining both probabilities $P(D_k|T)$ and $P(D_k|F)$. After dropping the subscript k, then $P(D|T)$ is computed as probability of detection (P_d) multiplied with Gaussian likelihood function, that is defined by (2.30), and for false targets $P(D|F)$ is computed as probability of detecting a false target (P_f) multiplied

with a likelihood function $(1/V_G)$ and with the assumption of false alarms are uniformly distributed within the gate region. Thus,

$$L_k = \frac{\dfrac{P_d e^{\frac{-d^2}{2}}}{[(2\pi)^{M/2}\sqrt{|S|}]}}{P_f\left(\dfrac{1}{V_G}\right)} = \frac{P_d e^{\frac{-d^2}{2}} V_G}{P_f (2\pi)^{M/2}\sqrt{|S|}}, \qquad (2.78)$$

$$P_f = \beta_{FT} V_G, \qquad (2.79)$$

where d^2 is obtained by (2.3), $|S|$ is obtained by (2.5), β_{FT} is the density of false alarms.

$$L_k = \frac{P_d e^{\frac{-d^2}{2}}}{\beta_{FT}(2\pi)^{\frac{M}{2}}\sqrt{|S|}}. \qquad (2.80)$$

A prior probability of the true target $P_0(T)$ is defined by (2.81) .

$$P_0(T) \triangleq P_0 = \frac{\beta_{NT}}{\beta_{NT} + \beta_{FT}}. \qquad (2.81)$$

When the probability of detection is less than unity $P_d < 1$, the likelihood is given by (2.82).

$$L_k = \frac{1 - P_d}{1 - P_f}. \qquad (2.82)$$

The equations (2.73) to (2.82) give a suitable sequential confirmation outline that can be adapted with the environment and the length of test can be controlled by selecting suitable P_A. By taking the logarithm of the likelihood defined by (2.77), the test statistics mostly becomes constant.

2.7.3   Track deletion

Degraded tracks always must be deleted. The prevalent type of degradation occurs due to missed data ($P_d < 1$). The simplest criterion for track deletion utilizes the number of successive missed detection attempts. There is an additional more complex method that considers the history of the track update and uses the sequential methods for track deletion. Based on the sequential analysis, the deletion of the track occurs whenever the test statistic $ST(k)$ falls under the lower threshold $T_L(k)$, or whenever the test statistic $ST(k)$ outstrips the upper threshold $T_U(k)$, the track is reconfirmed.

The gate given by (2.11) can be utilized for obtaining the track termination criteria. As the normalized distance function d^2 between the received observation and the predicted target position satisfies the condition given by (2.7), the association is more probable than declaring the observation originates from a false target or new target. So while $G > 0$ there is a possibility that the track will be updated but, if $G \leq 0$ then, any received observation is mostly from a false alarm or new target. Maged [50] recognizes a principle similar to this approach.

For the elliptical gate, the target track is deleted if the computed gate G by (2.11) for that track is lower than the minimum value G_{min}. The value of G_{min} can be obtained from the chi-square

χ_m^2 table, to guarantee that the tracks are not removed as long as the predetermined probability of the track update exists.

The Baysian approach can be utilized in track deletion by utilizing the likelihood function of all data received during the scans, and obtained by (2.75). For individual scan, the likelihood functions are obtained by (2.80) or from (2.82), in case of missed detection $(P_d < 1)$ has occurred. Then the criteria for deletion becomes like (2.83).

$$P(T/D) \leq P_{DEL},$$
$$or \hspace{4cm} (2.83)$$
$$L(D) \leq \frac{P_{DEL}(1-P_0)}{(1-P_{DEL})P_0},$$

where P_{DEL} is defined as the probability of track terminated.

Two tests are performed simultaneously, such as a test for deletion and test for confirmation. After confirming the track, the test starts again with suitable high value for P_0.

Chapter Three

On the influence of the probability of detection and density of false alarms to the quality of tracking.

The objective of MTT systems is estimation of the number of real targets in the scanned environment and the individual states of each target. Also, the MTT system is expected to provide the target tracks or the trajectories, from a set of measurements obtained from the sensing devices in complex scenarios [51]. Target tracking systems became a subject of particular interest in the 1970s when the pioneering papers reported initial results of upgrades of moving tracking filters and the development of techniques for the data association of observations during tracking in a dense environment [12, 15, 41, 52, 53]. The performance of the target tracking system is highly dependent on the accuracy of detection and severely degrades when the detection includes false alarms and errors due to missing- targets, especially in closely-spaced trajectories or dense clutter [54].

The interest in target tracking systems has been growing during the past decades. There seem to be two reasons for the increased output of scientific results. The first reason is that the applicability of the algorithms developed has expanded considerably. The focus has switched from military to civilian systems [5]. The second significant reason for the increasing interest is the novel theoretical framework in which such systems are developed. Previously, the tracking algorithms were based on conventional Bayesian probabilistic approaches like multiple hypothesis tracking (MHT) and All Neighbors Data Associations, including their versions: Probabilistic Data Association (PDA) and Joint Probabilistic Data Association (JPDA) [1, 9, 55]. However, over the previous ten years, the random finite sets (RFS) theory has provided a basis for the development of new tracking filters, such as Probability Hypothesis Density (PHD) and Cardinalized Probability Hypothesis Density (CPHD) filters [4, 10, 56].

Literature sources describe a considerable number of structures of target tracking systems, various solutions for target state estimation filters, and several different algorithms of data association for associating measurements with tracks. However, the efficacy of these concepts largely depended on the knowledge of the probability of target detection P_d and the density of false alarms λ_{fa}. Except in rare cases, these parameters are unknown, and many attempts are made to estimate them.

3.1 Overview of the literature in the field of research

A lot of literature has been read carefully to explore the existing algorithms and solutions in the area of adaptive techniques for moving targets tracking. Much more focus was placed on their contributions in this field to identify the deficiencies and shortcomings suffered by these contributions and work to avoid and address them accurately.

In this field, a lot of researchers and authors devoted their effort to the methods that enable simultaneous observations association and estimation of the unknown parameters [3]. Commonly, the object is characterized by the probability of detection P_d, and the process of generating false alarms is usually described as the Poisson process with mean value λ_{fa} [3].

Significant results in the field of estimation of these two unknown parameters are reported by the next authors [57].

- Mahler at al. (2011) [10], claims that the probability of detection and density of false alarms are critical parameters for improving the efficiency of the PHD and CPHD filter. Two versions of filters were developed, which can adaptively estimate these two unknown parameters. Beta and Gaussian mixtures were utilized to obtain a closed-form solution. The contributions of the estimators by Mahler et al. were demonstrated by an increase in the Optimal Sub Pattern Assignment (OSPA) miss distance, clutter rate estimation, and cardinal statistics. There are many drawbacks to this approach, such as, very high numerical complexity, the density of false alarm is estimated from a wide region, significant sensitivity to the initial values of the filter, the dynamics

44

of the unknown parameter estimation is related to the dynamics of the filter itself, and the computed probability of detection is not specified for a particular target.

- Yildrim et al. (2014) [58] reported a valuable result, where they have used the Expectation-Maximization (EM) algorithm for estimating the parameters in Gaussian MTT models, which include both of the probability of detection and the density of false alarms. The research developed both batch and on-line procedures based on experimental experience and concludes that the Sequential Monte-Carlo (SMC) online EM procedure is suitable for MTT applications that require data processing in real-time, even if the estimated parameters have a bias. On the other side, when the available data sets are long, the Markov Chain Monte Carlo Expectation Maximization (MCMC-EM) procedure can provide better results, albeit this strategy is not acceptable for many online users. This approach has some disadvantages, such as numerical complexity, and the density of false alarms is estimated in a large area, which implies the assumption that the clutter rate is homogeneous in a wide observation area.

- An application described by Schlangen et al. (2017) [4] is very interesting because the clutter rate of a PHD filter is estimated as part of image analysis in single-molecule localization microscopy. The results were very satisfactory, keeping in mind that the molecule detection probability is not estimated and that a wide surveillance region for estimating the unknown density of false alarms parameter λ_{fa} is observed simultaneously.

- New results obtained by He Shaoming et al. (2018) [9] should be mentioned due to JPDA filter for data association is used to estimate the density of false alarm λ_{fa} and probability of detection P_d. The results have been shown that the new proposed algorithm has many advantages when compared with traditional JPDA filter, demonstrated by a smaller mean Optimal Sub-Pattern Assignment (OSPA) distance. The disadvantages of the approach are such as the probability of detection was not calculated for certain targets, and the density of false alarms is estimated for a wide surveillance region as in [4, 10].

- Remarkable research by Chen et al. (2012) [59], and assumes a non-homogenous clutter background. They develop two techniques. The first technique is the Generalized Maximum Likelihood (GML) estimator based on predictive measurement set likelihood function. The second technique utilizes a combination of the PHD filter with the normal-Wishart mixture function. The simulation result shows that the PHD filter performance is improved by the developed clutter rate estimators. The authors demonstrate how this type of estimation considerably improves the accuracy of the number of tracks relative to the actual number of targets, but their probability of detection is not calculated.

A careful review of the available literature leaves an impression that the estimation of these parameters is extremely complex [57]. Many authors reported progress, originating from the fact that the number of measurements in a certain local volume of the monitored space is a function of both the unknown density of false alarms and the unknown number of targets, along with their unknown probability of detection. This is why many researchers are trying to decouple the estimation of these two parameters by estimating the clutter rate in a much wider region, assuming that it is homogeneous. As a consequence, the number of included false targets increases, relative to the number of actual targets, such that the relative effect of the actual targets are reduced. On the other side, keeping in mind the increasingly demanding and complex environments in which MTT systems are used, it is clear that the clutter-rate homogeneity assumption is often not sustainable. Also, given the relations of the Kalman filter that needs to be adapted to the fact that a certain measurement is associated to a track with only a certain probability, there is a definite need to associate a probability of detection P_d with each target.

Finally, available estimators are highly demanding, either because of the number of needed mathematical operations in real-time or the complexity of expressions that have to be computed.

3.2   Motivations for this research

If the requirements in designing the estimators, the limitations arising from their practical implementation, and the motives underlying the main driving force of research in this field were to be summarized, the list would be too long. Therefore, I was inclined to highlight the motives representing the main driving force of this research [57]:

- The method for estimating the probability of target detection and density of false alarm must be simple enough to be implemented in real-time.

- This method must be applicable when the time window, within which the observations are obtained, is short because real applications often involve tracking targets that remain in the observational area for a short time.

- This method should provide a good compromise between the quality of the probability of moving target detection and the density of false alarm estimates because it is known in the literature that the quality of the second estimate undermines the quality of the first one.

- This method should be functional even when the probability of target detection is much less than one, and the density of false alarms is as large as possible.

- The new method should enable the local estimation of false alarm density, i.e. in the vicinity of the moving target.

- It would be practical if the new method could assign the probability of detection to each target being monitored.

- The new method should offer a good compromise between the ability of tracking non-stationary parameters P_d and λ_{fa}, and the estimation quality.

- The new method should not be too sensitive to initial values of the estimator thereby not requiring too much a priori knowledge. Also, it should not require precise adjustment of a large number of parameters affecting the quality of the whole algorithm.

- The new method should have a general form and its applicability should not depend on the reference system in which the observation is carried out, its dimensionality, the structure of the filter used for tracking kinematic characteristics of the target, and the structure of measurement association algorithm. In other words, the new method should be a system capable of supporting different multi-target filtering and tracking systems.

3.3   Main contributions of the new proposed algorithm

The new proposed algorithm for estimating both unknown parameters ((P_d, λ_{fa}), has the following distinctive qualities that can be considered as contributions to the field [57]:

(1) The new proposed method is numerically simple and can be implemented easily in real-time operation.

(2) The method simultaneously estimates the probability of detection for each target and density of false alarms in the immediate vicinity of each of the target's position.

(3) A compromise between estimator variance and the ability to track non-stationary parameters P_d and λ_{fa} is easily achieved.

(4) It shows good results even in the case when the probability of target detection is significantly smaller than unity, and the density of false alarms is large.

(5) Its implementation requires a minimum of a priori knowledge about the nature of the object being monitored as well as its surroundings. The literature shows that the comparison of various systemic solutions of this type is very unappreciative, because different techniques have been developed under different assumptions, implying that their numerical complexity differs, and

perhaps most importantly, they involve diverse a priori knowledge about environmental and target statistics.

(6) The new proposed technique does not require a specific form of data association. The proposed estimation algorithm cannot replace either the data association algorithm or the filtering procedure. A complete system for moving target tracking should include all of these three elements, regardless of their implementation form. The idea was to propose an estimation algorithm which can be used in combination with the different association and filtration solutions. The final result and the tracking performance of the moving target tracking system, both depend on the quality of each of these individual subsystems.

3.4   Density of false alarm

In data processing of the multiple target tracking MTT systems, the clutter measurements are classified as false alarms/detections that do not originate from actual targets[56]. Methods or algorithms for the target tracking in the clutter environment receive a number of measurements in every scan without any prior indication of their origins. Moreover, there is not any prior information about the existence of the targets and their trajectories in the space [1].

In many MTT systems, observations collected by the sensor in the wide measurement space are non-uniform with unknown distribution. In order to obtain a precise result for track association and new track initialization, the MTT system requires data about the distribution of these observations [55]. Usually, in measurement space, the clutter rate is a non-homogenous Poisson point process (NHPP) [60] and requires the spatial density to characterize the distribution of the NHPP process [61]. Thus, the clutter rate density is required as a priori data for the MTT system [55]. Also, the observations in a measurement space are real targets mixed with false alarms, and cannot distinguish between them before processing by the MTT system [12,62], and the MTT system should be used after estimation of the spatial density of clutter rate. The density of false alarm has no prior information and should be estimated adaptively to enhance the tracking accuracy [56].

Generally, there are two methods for estimating the clutter rate density spatially. The first method is based on the assumption that the distribution of false alarms inside the validation region of the gate is uniform. This method is heavily depending on the size of the validation gate, which is based on the covariance matrix and gate constant K_g. However, the estimation of density of false alarms by this method depends on the size of gate, if the gate size is too small, then there are a few measurements inside the gate, and the estimation of density of false alarms will suffer from considerable variance, while if the gate size is large, then the assumption of a uniform distribution of the false alarms may not hold. This method also suffers from bias because the data association cannot distinguish between the origins of the measurements within the validation gate.

The second method is used on the wide measurement space on the estimation of the density of false alarms. This method is based on dividing the measurement space into small bins, and there are two approaches based on this method, which are the classic clutter map [63] and the nearest neighbor-based estimator [64]. These two methods assume some assumptions, such as, for the first assumes that the clutter density inside each bin is constant, while for the other approach assumes that that distribution of false alarms inside each bin is Poisson.

3.5   Probability of detection

Effect of the probability of detection on MTT systems has been considered by many authors, such as Wang et al. [51], and they conclude that the performance is degraded significantly under the low probability of detection in practice, mainly when miss detection occurs continuously.

Probability of detection is a time-varying individual descriptor of each object and depends on the scenarios and sensors. Many factors are affecting the value of this parameter, such as the following:

- The distance between the object and the sensor,
- The reflective surface of the object,
- Specific attributes of the material it is comprised of,
- Radiation power of the transmitting antenna,
- Receptive properties and wavelength properties of the medium through which the wave is transmitted.

3.6 Influence of probability of detection and density of false alarms on the performance of the target tracking system

Most target tracking systems need knowledge of the density of false alarms and the probability of detection. These two parameters have a significant effect on the efficiency of the target tracking system [9]. When these parameters are not known or not estimated precisely, the tracking system produces erroneous information.

To illustrate this influence, a simulation program for a single target moving in a plane with constant speed is performed. The criterion utilized in measuring the performance of the target tracking system was the mean square error (MSE). Performance is measured for different combinations of the probability of detection P_d and density of false alarms λ_{fa}, and the simulation results are plotted in the figures (Fig. 3-1 and Fig. 3-2).

These results are obtained from a simulation program that utilizes the Kalman filter for filtering and prediction, probabilistic data association PDA method for data association, probability of detection $P_d \in \{0.5, 0.6,..., 1.0\}$, and density of false alarm $\lambda_{fa} \in \{10^{-9}, 10^{-8}, 10^{-7}, 10^{-6}\}$ with 500 Monte-Carlo loops to minimize the influence of random number generator.

It is clear from the first glance to the figures (Fig. 3-1 and Fig. 3-2), that increasing the probability of detection P_d or decreasing the density of false alarm λ_{fa} improves the performance of the target tracking system. Also, one can conclude from Fig. 3-1, that the influence of the probability of detection significantly depends on the value of the density of false alarm. To illustrate this, let us consider the influence of the probability of detection with two different values of the density of false alarm were $\lambda_{fa} \in \{10^{-9}, 10^{-6}\}$. In the first case assume the density of false alarm is $\lambda_{fa} = 10^{-6}$ and the probability of detection is $P_d = 1$, the measured mean square error was about 422 with a standard deviation was about 21, and when the probability of detection is $P_d = 0.5$ the measured mean square error is about 1.8275×10^5 with a huge standard deviation about 427. In the second case when the assumed density of false alarm is $\lambda_{fa} = 10^{-9}$, the probability of detection $P_d = 1$, the measured mean square error was about 250 with a standard deviation about 15, and when the probability of detection is $P_d = 0.5$ mean square error is 6430 with a standard deviation about 80. It is clear from the previous two cases how the influence of the probability of detection P_d on the performance of the target tracking system is affected by the value of density of false alarm λ_{fa}.

Also, one can conclude from Fig. 3-2, that influence of density of false alarm considerably depends on the value of the probability of detection. The influence of the density of false alarm λ_{fa}

on the performance of the target tracking system is significant at low probability of detection P_d, and this influence is decreasing with increasing probability of detection P_d.
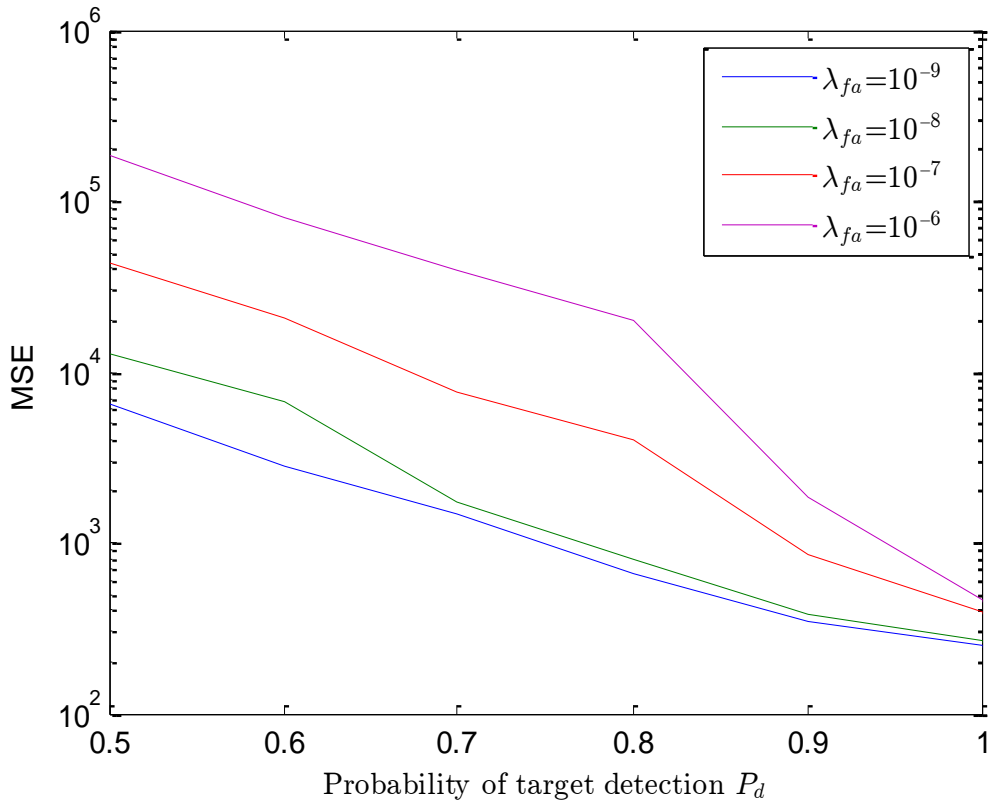

Fig. 3-1: Influence of the probability of detection on
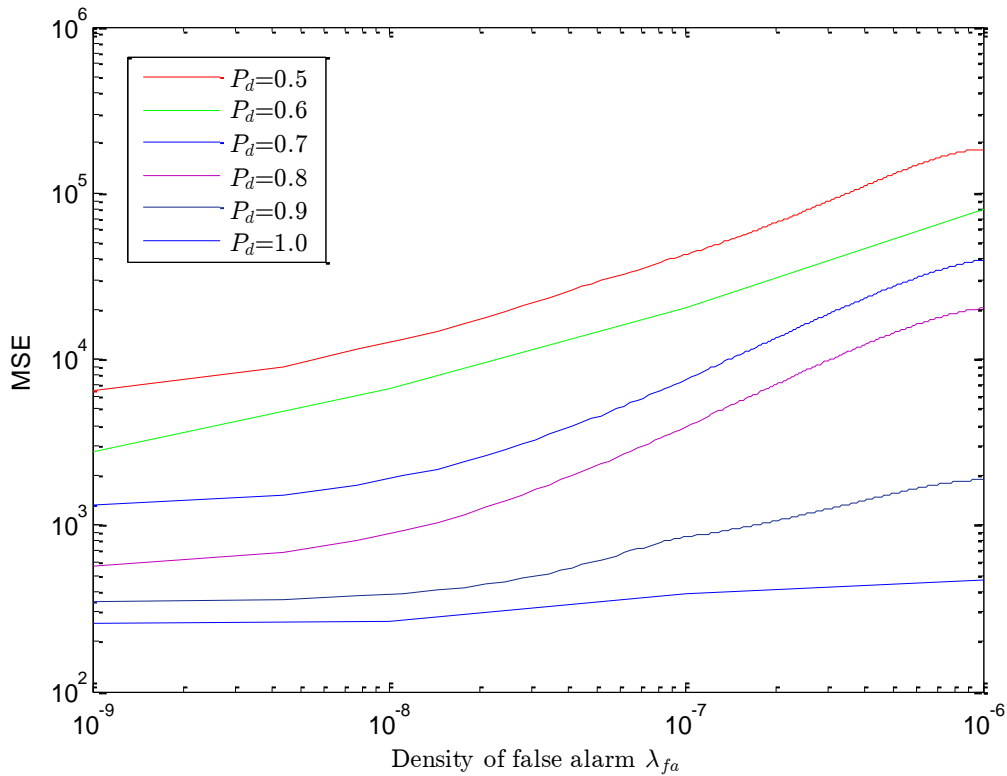the performance of the target tracking system

Fig. 3-2: Influence of the density of false alarm on
the performance of the target tracking system

49

Another simulation results were obtained to illustrate the effect of applying inaccurate values of the probability of detection P_d and density of false alarms λ_{fa} on the performance of the target tracking algorithm. In this simulation, the true values of the probability of detection $P_d = 0.8$ and density of false alarms $\lambda_{fa} = 10^{-7}$ were constants and used only in generating false alarms, while there was no prior knowledge of these parameters while designing the target tracking system. The target tracking system uses other different values of $(\hat{P}_d, \hat{\lambda}_{fa})$, $\hat{P}_d \in \{0.6, 0.65, 0.70, ..., 1.0\}$ and $\hat{\lambda}_{fa} \in \{10^{-9}, 10^{-8}, 10^{-7}, 10^{-6}\}$.

Two different simulations were applied to illustrate this influence. In the first simulation, after generating the false alarms and running the target tracking algorithm with a constant probability of detection $(\hat{P}_d = 0.8)$, and different values of density of false alarm $\hat{\lambda}_{fa} \in \{10^{-9}, 10^{-8}, 10^{-7}, 10^{-6}\}$. The results are interesting and as expected. The minimum mean square error is obtained when $(\hat{\lambda}_{fa} = \lambda_{fa})$ and increases as $\hat{\lambda}_{fa}$ moves away from λ_{fa} as shown in Fig. 3-3.

In the second simulation, the density of false alarm is kept constant $(\hat{\lambda}_{fa} = 10^{-7})$ with different values of probability of detection $\hat{P}_d \in \{0.6, 0.65, 0.70, ..., 1.0\}$. The results are as expected, and the minimum mean square error is obtained when $(\hat{P}_d = P_d)$ and the mean square error increases as the probability of detection $\hat{P}_d$ moves away from P_d as shown in Fig. 3-4.

From the two figures (Fig. 3-3 and Fig. 3-4), one can notice, that the influence of inaccurate density of false alarm on the performance of a target tracking system is more than the effect of inaccurate probability of detection. To illustrate this, let us consider the mean square error when the accurate density of false alarm was $\hat{\lambda}_{fa} = 10^{-7}$ and the mean square error when inaccurate density of false alarm were $(\hat{\lambda}_{fa} = 10^{-9}$ and $\hat{\lambda}_{fa} = 10^{-6})$. The difference in the mean square error is significant and the difference in standard deviation is significant too. While in a case of the inaccurate probability of detection, the difference between the mean square error obtained from the accurate probability of detection and the mean square error obtained from the inaccurate probability of detection was not significant like that caused by the inaccurate density of false alarm.

One concludes from the previous experiment, that precise knowledge of the two critical parameters of the measurement process and the environment is important for accurate target tracking algorithm.

The most critical parameters are the probability of detection P_d and density of false alarms λ_{fa}. This example was to illustrate the robustness of the data association algorithm utilized by the target tracking system with respect to the errors in the probability of detection and density of false alarms. Also, one concludes that the performance of the target tracking system (*MSE*) is considerably deteriorated when the target tracking system works with erroneous in the density of false alarms and necessary to determine it in advance. Also, take into account that the density of false alarm is non-stationery in time and place and hardly affected by the environment.

It is necessary to design a reliable method for estimating these two parameters for successful target tracking systems, which is the primary goal of this research.
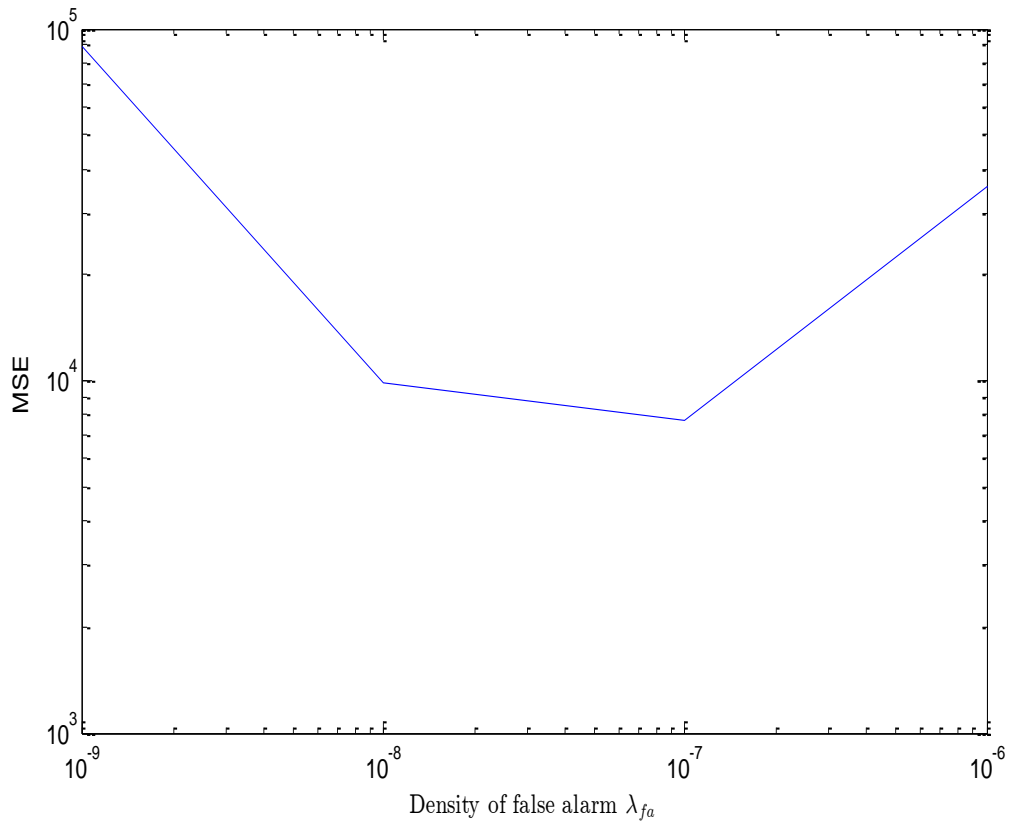
Fig. 3-3: Influence of applying inaccurate values of density of false alarm
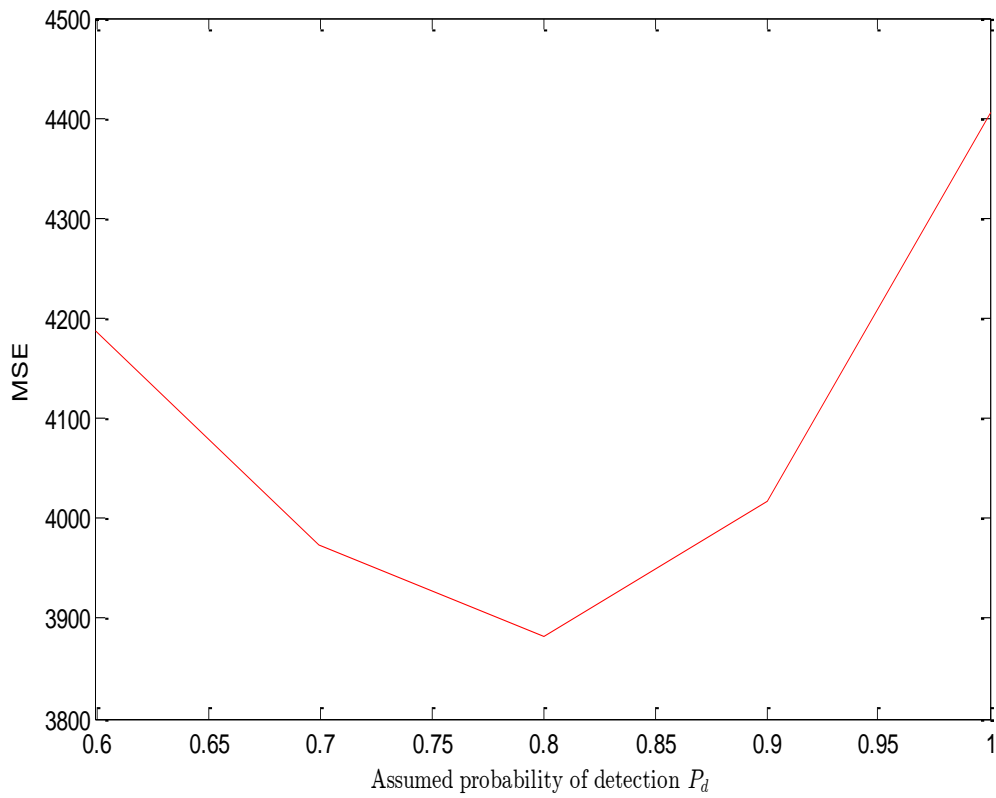on the performance of the target tracking system

Fig. 3-4: Influence of applying inaccurate values of probability of detection
on the performance of the target tracking system

52

Chapter Four

Estimation of the probability of detection and density of false alarms based on a maximum likelihood approach

This chapter proposes a novel method to estimate the probability of detection (P_d) of a single target moving in a cluttered environment along with an estimation of the density of false alarm (λ_{fa}) in the region of the predicted target position. The significant contribution of the proposed method is reflected from the fact that the estimation of the density of false alarms is not based on the measurements collected from a wide region in which the target moves, but only on measurements collected from a region located around the predicted target position, and the distribution of the false alarms in a wide surveillance region is not uniform (unknown distribution), because it is not a sustainable assumption. The new method proposed in this thesis is based on GML (Generalized Maximum Likelihood) principles and numerically must be much simpler than the previous methods described in the literature because each scan contains no more than two particular hypotheses [57]. The procedure can be generalized for multiple targets, whereby a probability of detection and density of false alarm in the immediate vicinity are associated with each track. Another advantage of the proposed technique is that it does not require a specific form of data association so that it can be used in parallel with any moving target tracing algorithm or a general estimator of the detection profile and clutter environment.

4.1   Structure of the proposed algorithm

The following assumptions are made in order to apply a two-step GML approach to the estimation of the probability of target detection (P_d) and density of false alarm (λ_{fa}), which are essential statistical parameters of an MTT system. Let the Kalman filter be based on the moving target model

$$x(k+1) = Ax(k) + Bw(k), \tag{4.1}$$

where: A is the state matrix, $\mathrm{x}(k)$ is a track state vector, B is the input matrix, $w[k]$ is the stochastic process of the model error, and $(A\ \&\ B)$ are time-dependent in general case. Let us assume the adopted observation relation is

$$y(k) = Cx(k) + v(k), \tag{4.2}$$

where $\mathrm{y}(k)$ is the measurement vector, C is the measurement matrix and $v(k)$ is the stochastic process of the measurement noise. Based on Kalman filter relation, one of the outputs of each scan is state vector prediction of the next scan, denoted by $\hat{x}(k\,|\,k-1)$ and the prediction error covariance matrix, denoted by $P(k\,/\,k-1)$.

In order to apply one of data association techniques, let there be a gate around the track prediction $\hat{x}(k\,|\,k-1)$, the dimensions of the gate are $K_g \sigma_{ii}, i = 1,...,n$, where K_g is the gate constant, σ_{ii} is the $i-th$ element of the diagonal of the prediction error covariance matrix $P(k\,/\,k-1)$, and n is the dimension space in which the gate is located. Given that the target is moving in a cluttered area, the number of observations inside the gate in each scan may be zero or more, and the probability of detection is less than one $(P_d < 1)$.

For illustration purpose Fig. 4-1 shows track position prediction in three consecutive scans, around which there are gates. The gate size in the figure is identical for the three consecutive scans, but in reality, it is not stationary, depends on the value of the diagonal in the prediction error covariance matrix $P(k\,|\,k-1)$. In scan $k-1$ only one observation is detected in the gate, denoted by O_{k-1}^1, that there are three observations in scan k, and in scan $k+1$ there are two observations inside the gate.
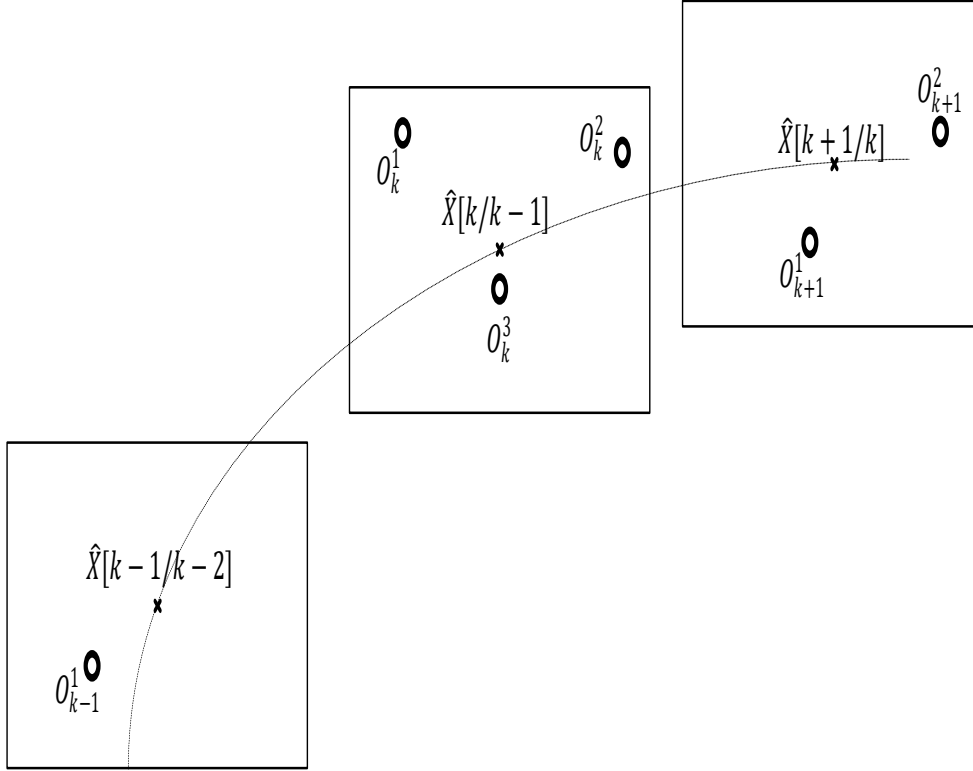
Fig. 4-1: Gate function and observations for three consecutive scans

The following is proposed in order to construct hypotheses whose likelihood can be maximized to estimate the unknown parameters. There are two different cases:

- If the number of incoming observations in the $k-th$ scan is $M_k = 0$, then only one partial hypothesis can be formed:

M_k^0: no target detected, and the number of false alarms is zero.

- If the number of incoming observation within the gate of the $k-th$ scan is $M_k \geq 1$, then two partial hypotheses (M_k^0, M_k^1) can be formed:

M_k^0: no target is detected, and there are (M_k) false alarms

M_k^1: target is detected, and there are $(M_k - 1)$ false alarms.

If the last N scans are considered, by combining the partial hypothesis then the number of formed integral hypotheses is.

$$N_h = 2^{\mathrm{sgn}\, M_{k-N+1}} \times 2^{\mathrm{sgn}\, M_{k-N+2}} \;..\; \times 2^{\mathrm{sgn}\, M_k}, \tag{4.3}$$

where M_k represents the number of observations during the $k-th$ scan, sgn is for signum function, and $2^{\mathrm{sgn}\, M_k}$ represents the number of particular hypotheses generated during the $k-th$ scan.

The total number of hypotheses generated during N consecutive scans is equal to the multiplication of the number of hypotheses generated during that period of scans. It should be noted that contrary to the other MHT approaches, the number of hypotheses in this case is considerably

smaller. The savings can easily be discerned by looking at the $k-th$ scan in Fig. 4-1. Namely in general, four partial hypotheses could be defined for the scenario shown in Fig. 4-1:

(i) The zero hypotheses, with all incoming observations being false alarms.

(ii) The first hypothesis – that observation O_k^1 is originated from the real target and the other two observations (O_k^2 and O_k^3) are originated from false alarms.

(iii) The second hypothesis – that observation O_k^2 is originated from the real target and the other two observations (O_k^1 and O_k^3) are originated from false alarms.

(iv) The third hypothesis – that observation O_k^3 is originated from the real target and the other two observations (O_k^1 and O_k^2) are originated from false alarms. However, since the generalized maximum likelihood (GML) approach will be used to compute the likelihood of each hypothesis individually, it is evident that the first and the second hypotheses are much less likely than the third hypothesis because the statistical distance from the observation O_k^3 to the predicted position is the smallest distance, such that the observations (O_k^1 and O_k^2) will not affect the algorithm. Hence, each partial hypothesis H_k^1 that assumes target detection will also assume that it corresponds to the observation with the least statistical distance from the predicted position.

The classical maximum likelihood method would assume that for each of the integral hypothesis, $H^i, i = 1,...N_h$ the likelihood should be calculated, and the hypothesis which obtained the maximum likelihood is chosen. However, in this case, this is not possible, because the probability of target detection P_d and density of false alarm λ_{fa} are unknown.

For this reason, the new method proposes an approximate GML method, comprised of the following steps:

• Determine an integer variable N that represents the length of the time interval or the number of scans, based on which the unknown probability of target detection P_d and density of false alarm λ_{fa} in the immediate vicinity of its current position will be estimated.

• Symbolically, each integral hypothesis that covers scans from $(k-N+1)^{th}$ to k^{th} can be represented as a series of N binary numbers:

$$H^i = [p_{k-N+1} \quad p_{k-N+2} \quad .... p_k], \tag{4.4}$$

where the variable $p_j = 0$ if all observations in the gate region in the $j-th$ scan are declared as false alarms, and $p_j = 1$, if in the $j-th$ scan the observation statistically closest to the predicted position, and declared as the actual target.

• Form N_h integral hypotheses in the manner described by (4.3) and associate the likelihood function $L(H^i)$, $i = 1,.... N_h$ with each.

• For each integral hypothesis, compute the parameters (P_d^i, λ_{fa}^i), thus maximize the likelihood of the hypothesis $L^{opt}(H^i) = \max_{P_d, \lambda_{fa}} L(H^i)$.

- Select the highest likelihood among all the optimal values of likelihoods $L^{opt}(H^j) = \max_{i=1,...N_h} L^{opt}(H^i)$, and from the chosen hypothesis, determine the optimal estimators (P_d^j, λ_{fa}^j).

The proposed algorithm is required to make a selection among N_h different hypotheses, each of which has two unknown parameters: P_d and λ_{fa}. This type of problem is better known as *multiple composite hypotheses testing* in the literature [65, 66]. The most commonly utilized approach in dealing with unknown parameters refers to replacing them with their maximum likelihood estimates. This is the well-known *generalized likelihood ratio test* (GLRT) [66, p. 200]. In situations where the unknown parameters are not the same for each hypothesis, the GLRT may come up with poor results. As an example, consider the case when the set of unknown parameters for some hypothesis *A* is a subset of unknown parameters for another hypothesis *B*. The maximum achievable likelihood for hypothesis *B* is higher than that for *A* since there are more degrees of freedom to optimize over.

Consequently, the standard GLRT would be "unfairly" biased towards choosing hypothesis *B*. One way to overcome the described problem is to decrease the log-likelihood of each hypothesis by subtracting a term which is proportional to the number of unknown parameters. This approach in the literature is known as the Minimum Description Length (MDL) rule [67]. In approximate terms, it is equivalent to GML rule [65].

However, all hypotheses in the proposed procedure have the same number of unknown parameters, namely probability of detection P_d and density of false alarms λ_{fa}. This makes the MDL rule equivalent to the standard GLRT method [65].

4.2   Computations of the Likelihood

In order to implement such a methodology, it is necessary to define an expression for the likelihood of the integral hypothesis.

The adopted assumptions are quite common in related literature. They are partially grounded in the experience of target tracking engineers but are also motivated by the need to simplify the problem and to make the derivation and justification of theoretical results more tractable. Consequently, the following common assumptions are made:

(1) The prediction of the next state $\hat{x}(k/k-1)$, which is one of the outputs of the Kalman filter, is an unbiased state estimate of $x(k)$. This assumption holds until the target starts maneuvering. Fortunately, these maneuvers usually do not last long, so this assumption is justified most of the time.

(2) The prediction error covariance matrix $S(k/k-1)$, which is also one of the Kalman filter outputs, is an exact measure of prediction uncertainty.

(3) The prediction vector process $\hat{x}(k/k-1)$ is Gaussian, where the mathematical expectation is equal to the true state $X(k)$, with the corresponding error covariance matrix $S(k/k-1)$.

(4) The false alarm frequency is Poisson's stochastic process with a mean value of $\lambda_{fa}V_g$, where λ_{fa} is the density of false alarm and V_g is the volume of the gate. This assumption is justified by the nature of ground clutter, and the electronics (signal detectors, Doppler filters, etc.) used to obtain the measurements. This assumption breaks down in case of targets crossing zero Doppler.

(5) The spatial distribution of false alarms within the gate can be considered uniform due to the volume of the gate is sufficiently small.

(6) The probability of detection P_d can be considered constant because the length of the observation sequence N is sufficiently short. This is quite fragile in the case of new generation aircraft, the

design, and construction materials of which make the detection probability strongly dependent on the incoming angle of the radar's electromagnetic waves.

The sustainability of the assumptions is indeed questionable. However, the proposed method is applicable even if some of the assumptions do not hold. Of course, in such cases, the algorithm's performance will probably not coincide with the derived estimation quality results, but it might still be acceptable.

Therefore, the likelihood of the $i-th$ integral hypothesis can be computed as follows:

$$L(H^i) = \prod_{j=k-N+1}^{k} L(H_j^{p_j}), \ i = 1, ..., N_h \ , \tag{4.5}$$

where $L(H_j^{p_j})$ is the likelihood of the partial hypothesis in the $j-th$ scan, and depends on whether $p_j = 0 \ or \ 1$, it can have values as given in (4.6). The statistical distance in scan j between the predicted position $X[k \ / \ k-1]$ and the closest observation Z_j is $d(j)^2$, and defined as (4.7).

$$L(H_j^{p_j}) = \begin{cases} (1-P_d)\dfrac{(\lambda_{fa}V_g)^{M_j} e^{-\lambda_{fa}V_g}}{M_j!} \cdot \dfrac{1}{(V_g)^{M_j}} & p_j = 0 \\[3em] P_d \dfrac{(\lambda_{fa}V_g)^{M_j-1} e^{-\lambda_{fa}V_g}}{(M_j-1)!} \cdot \dfrac{1}{(V_g)^{M_j-1}} \cdot \dfrac{e^{-\frac{d(j)^2}{2}}}{(2\pi)^{0.5n}|S[j|j-1]|^{0.5}} & p_j = 1 \end{cases} \tag{4.6}$$

$$d(j)^2 = (Z_j - X[j|j-1])^T S^{-1}[j|j-1](Z_j - X[j|j-1]) \ . \tag{4.7}$$

Then, the likelihood of the integral hypothesis H^i can be defined by (4.8).

$$L(H^j) = (1-P_d)^{N-\sum_{j=k-N+1}^{k}(p_j)} P_d^{\sum_{j=k-N+1}^{k}(p_j)} \times$$

$$\dfrac{\lambda_{fa}^{\sum_{j=k-N+1}^{k}(M_j-p_j)} e^{-N\lambda_{fa}V_g}}{\prod_{j=k-N+1}^{k}(M_j-p_j)!} \times \prod_{j=k-N+1}^{k} f_j(Z_j)^{p_j} \ . \tag{4.8}$$

Here, Z_j represents the position of the observation in the $j-th$ scan, which is statistically the nearest observation to the predicted target position, and $f_j(.)$ is the corresponding probability density function (pdf), defined as in (4.9).

$$f_j(Z_j) = \dfrac{1}{(2\pi)^{\frac{n}{2}}|S[j|j-1]|^{0.5}} \times$$

$$e^{-0.5(Z_j - \hat{X}[j|j-1])^T S^{-1}[j|j-1](Z_j - \hat{X}[j|j-1])} \ . \tag{4.9}$$

The following equalities need to be solved in order to maximize the mentioned likelihood (4.8) as a function of unknown parameters by applying (4.10).

$$\frac{\partial L(H^i)}{\partial P_d} = 0 \ , \qquad \frac{\partial L(H^i)}{\partial \lambda_{fa}} = 0 \ . \tag{4.10}$$

Estimation of the probability of detection can be defined by the first derivative of (4.8) with respect to the probability of detection. Let from (4.8) $L(H^j) = (1 - P_d)^Y P_d^Z \times C$.

$$Y = N - \sum_{j=k-N+1}^{k}(p_j) , \tag{4.11}$$

$$Z = \sum_{j=k-N+1}^{k}(p_j) , \tag{4.12}$$

$$C = \frac{\lambda_{fa}^{\sum_{j=k-N+1}^{k}(M_j - p_j)} e^{-N \lambda_{fa} V_g}}{\prod_{j=k-N+1}^{k}(M_j - p_j)!} \times \prod_{j=k-N+1}^{k} f_j(Z_j)^{p_j} , \tag{4.13}$$

$$\frac{\partial L(H^i)}{\partial P_d} = \frac{\partial}{\partial P_d}((1 - P_d)^Y P_d^Z \times C) , \tag{4.14}$$

$$\frac{\partial L(H^i)}{\partial P_d} = C(1 - \hat{P}_d)^Y \times Z \times \hat{P}_d^{Z-1} + (\hat{P}_d^Z \times C \times Y \times (1 - \hat{P}_d)^{Y-1} \times (-1)) , \tag{4.15}$$

$$\frac{\partial L(H^i)}{\partial P_d} = (C(1 - \hat{P}_d)^Y \times Z \times \hat{P}_d^{Z-1}) - (\hat{P}_d^Z \times C \times Y \times (1 - \hat{P}_d)^{Y-1}) , \tag{4.16}$$

$$\frac{\partial L(H^i)}{\partial P_d} = C \times (1 - \hat{P}_d)^{Y-1} \times \hat{P}_d^{Z-1} \times ((1 - \hat{P}_d) \times Z - \hat{P}_d \times Y)) , \tag{4.17}$$

$$\frac{\partial L(H^i)}{\partial P_d} = 0 \Rightarrow \begin{cases} C \times (1 - \hat{P}_d)^{Y-1} \times \hat{P}_d^{Z-1} = 0 \\ (1 - \hat{P}_d) \times Z = \hat{P}_d \times Y \end{cases} , \tag{4.18}$$

$$(1 - \hat{P}_d) \times Z = \hat{P}_d \times Y \Rightarrow \hat{P}_d = \frac{Z}{Y + Z} , \tag{4.19}$$

$$\hat{P}_d = \frac{Z}{Y + Z} = \frac{\sum_{j=k-N+1}^{k}(p_j)}{N - \sum_{j=k-N+1}^{k}(p_j) + \sum_{j=k-N+1}^{k}(p_j)} , \tag{4.20}$$

$$\hat{P}_d = \frac{\sum_{j=k-N+1}^{k}(p_j)}{N} , \tag{4.21}$$

And estimation of the density of false alarm can be defined by the first derivative of (4.8) with respect to the density of false alarm.

Let from (4.8) that $L(H^j) = C1 \times \frac{\lambda_{fa}^{C2} e^{-N \lambda_{fa} V_g}}{C3} \times C4$.

$$C1 = (1 - P_d)^{N - \sum_{j=k-N+1}^{k}(p_j)} P_d^{\sum_{j=k-N+1}^{k}(p_j)} , \tag{4.22}$$

$$C2 = \sum_{j=k-N+1}^{k}(M_j - p_j) , \tag{4.23}$$

$$C3 = \prod_{j=k-N+1}^{k}(M_j - p_j)!, \tag{4.24}$$

$$C4 = \prod_{j=k-N+1}^{k} f_j(Z_j)^{p_j}, \tag{4.25}$$

$$C = \frac{C1 \times C4}{C3}, \tag{4.26}$$

$$L(H^j) = C \times \lambda_{fa}^{C2} \times e^{-N\lambda_{fa}V_g}, \tag{4.27}$$

$$\frac{\partial L(H^i)}{\partial \lambda_{fa}} = \frac{\partial}{\partial \lambda_{fa}}(C \times \lambda_{fa}^{C2} \times e^{-N\lambda_{fa}V_g}), \tag{4.28}$$

$$\frac{\partial L(H^i)}{\partial \lambda_{fa}} = C \times ((\hat{\lambda}_{fa}^{C2} \times e^{-N\lambda_{fa}V_g} \times -NV_g) + (e^{-N\lambda_{fa}V_g} \times C2 \times \hat{\lambda}_{fa}^{C2-1})), \tag{4.29}$$

$$\frac{\partial L(H^i)}{\partial \lambda_{fa}} = (C \times \hat{\lambda}_{fa}^{C2-1} \times e^{-N\lambda_{fa}V_g}) \times (-NV_g \times \hat{\lambda}_{fa} + C2), \tag{4.30}$$

$$\frac{\partial L(H^i)}{\partial \lambda_{fa}} = 0 \Rightarrow \begin{cases} C \times e^{-N\lambda_{fa}V_g} \times \hat{\lambda}_{fa}^{C2-1} = 0 \\ -N \times V_g \times \hat{\lambda}_{fa} + C2 = 0 \end{cases}, \tag{4.31}$$

$$-N \times V_g \times \hat{\lambda}_{fa} + C2 = 0 \Rightarrow \hat{\lambda}_{fa} = \frac{C2}{N \times V_g}, \tag{4.32}$$

$$\hat{\lambda}_{fa} = \frac{\sum_{j=k-N+1}^{k}(M_j - p_j)}{NV_g}. \tag{4.33}$$

The provided estimations are given in (4.34).

$$\hat{P}_d = \frac{\sum_{j=k-N+1}^{k} p_j}{N}, \quad \hat{\lambda}_{fa} = \frac{\sum_{j=k-N+1}^{k}(M_j - p_j)}{NV_g}. \tag{4.34}$$

4.3 Analysis of the proposed estimator features

Properties of the proposed estimation technique are tested by averaging a large number of Monte-Carlo simulations (20000 runs), and the length of the estimation sequence was $N = 12$. Quality of the estimated probability of detection $\hat{P}_d$ is shown in Fig. 4-2. The parameter K_g, which refers to the width of the gate, was varied from 2 to 4 with increment step 0.1 along the horizontal axis. The density of false alarm was constant in all the experiment and amounted to $\lambda_{fa} = 10^{-5}$. The vertical axis shows the average value of the estimated probability of detection $\hat{P}_d$. The obtained graph is very interesting because it leads to the conclusion that the estimated probability of target detection $\hat{P}_d$ is highly dependent on the size of the gate K_g.

The plot in Fig. 4-3 shows the variance of the estimated probability of target detection. The results were largely as expected. Namely, as the probability of target detection is increased, the variance of the estimated probability of target detection is decreased. However, it is interesting that

59

this logic changed somewhat as the gate size decreased. Specifically, as the size of the gate decreased, the probability of an object measurement being outside the gate is increased. This favors the estimation of low probabilities of detection, such as approximately < 0.6.

The very high variance of this estimator was surprising, for example for $P_d \approx 0.5$ and $K_g \approx 4.0$, the standard deviation of estimators was about 0.2, which is high compared to the quantity that is being estimated. However, it is good to know that the standard deviation decreases considerably as the probability of target detection is increased. For instance, where $P_d \approx 0.9$ and $K_g = 4.0$, the standard deviation of estimators was about 0.1, which is acceptable.

Similarly, the estimation of the density of false alarms $\hat{\lambda}_{fa}$ for different values of gate size K_g and different values of the real probability of target detection P_d was analyzed. Fig. 4-4 corroborates the estimator quality, or that the bias of the estimated density of false alarms depends on the size of the gate. What is interesting is that as the size of the gate decreases, the estimates of the density of false alarms is increasing and vice-versa. The reason for this is likely that an estimate of the density of false alarm is the quotient of the estimated number of false alarms in the gate and the volume of the gate. The volume of the gate is increased by cubic of the parameter K_g and the estimated number of false alarms by a slower function of this parameter, resulting in the dependency shown in the figure. It is also important to note that the optimal K_g that ensures unbiased estimation of both parameters P_d and λ_{fa} is dependent on the true and unknown value of the probability of detection P_d.

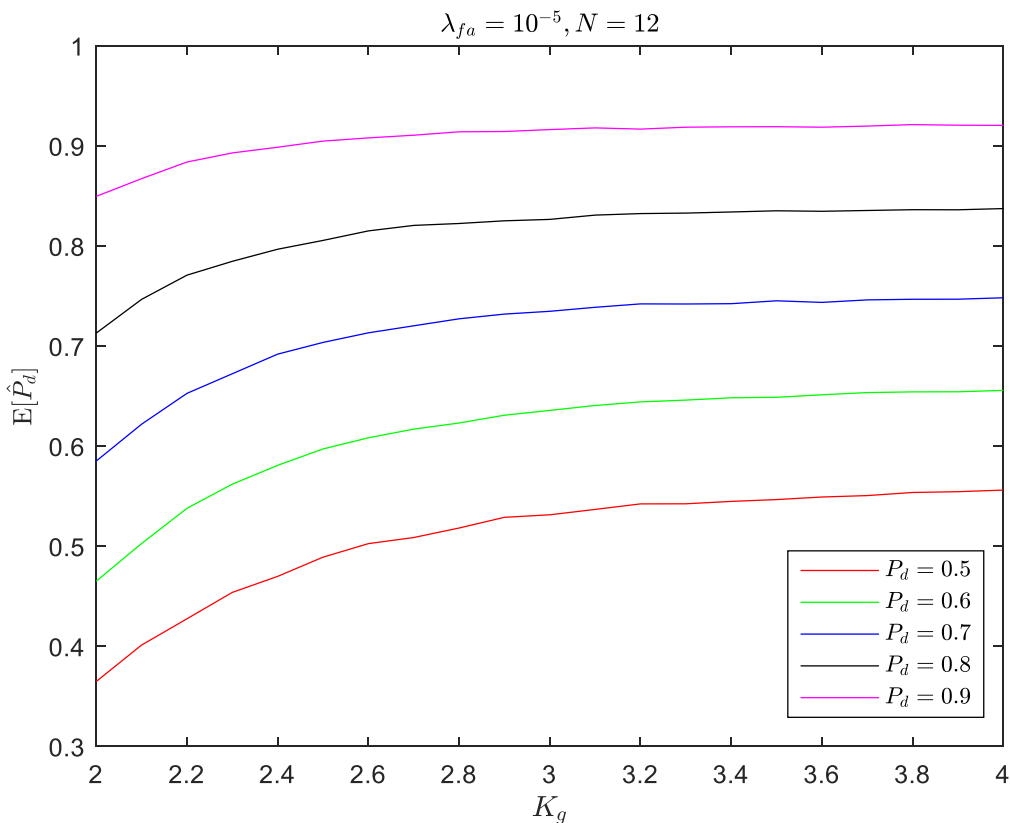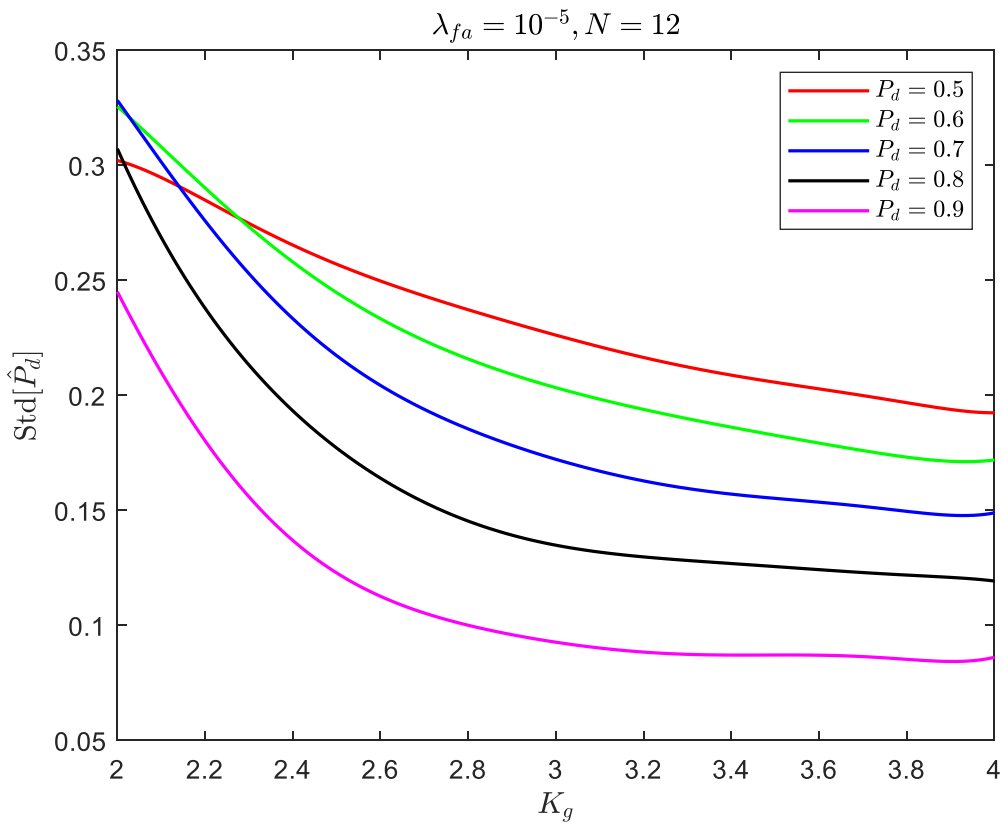Fig. 4-2: Averaged estimation of the probability of detection

$$\lambda_{fa} = 10^{-5}, N = 12$$

Fig. 4-3: Standard deviation of the estimated probability of detection

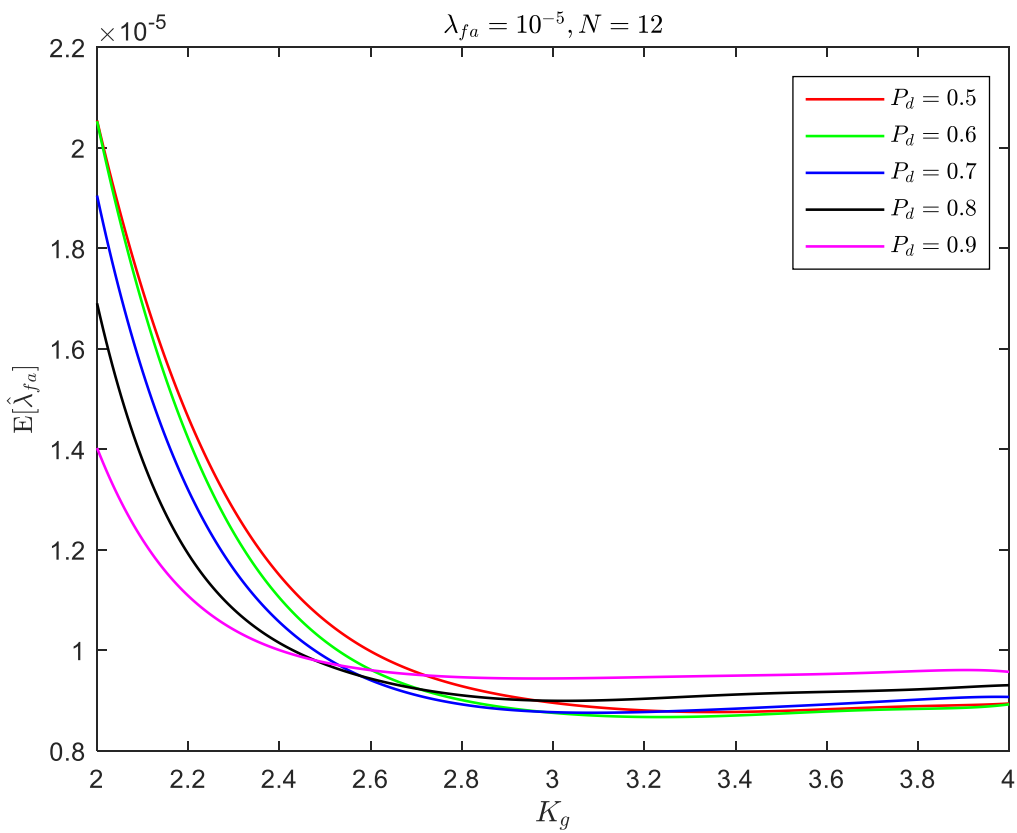$$\lambda_{fa} = 10^{-5}, N = 12$$

Fig. 4-4: Averaged estimation of the density of false alarms

Fig. 4-5 shows the variance of the estimated density of false alarms. It is evident that as the gate size increases, the variance of the estimated density of false alarms is decreased, as expected. On the other hand, it is apparent that the variance is quite large. The standard deviation of the estimated density of false alarms for gate size $K_g = 4.0$ and actual density of false alarms $\lambda_{fa} = 10^{-5}$ is very high and amounts to approximately 4×10^{-6}.
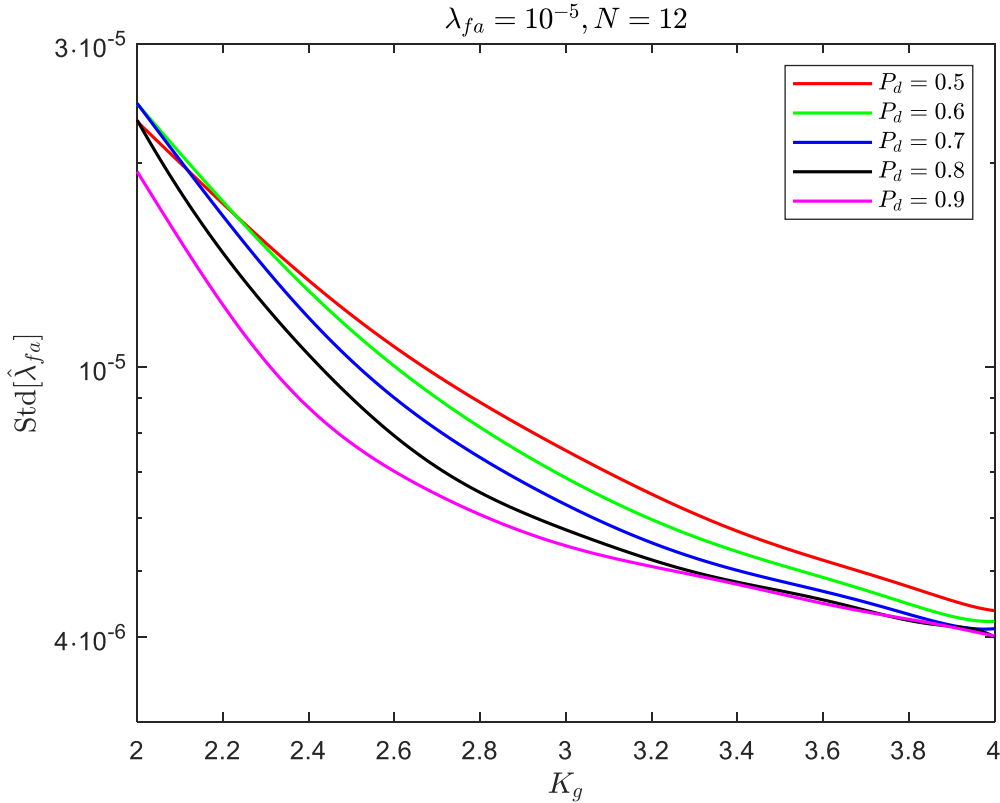
Fig. 4-5: Standard deviation of the estimated density of false alarms

Fig. 4-6 shows how the quality of the estimated probability of detection $\hat{P}_d$ changes as a function of the density of false alarm λ_{fa}. The estimation quality was analyzed for two fixed values of the density of false alarms $\lambda_{fa} = 10^{-5}$ and $\lambda_{fa} = 10^{-6}$. The dashed line was for the density of false alarm $\lambda_{fa} = 10^{-6}$, and the full line was for the density of false alarm $\lambda_{fa} = 10^{-5}$. It is evident at first glance that the bias of the estimated probability of detection is greater when the density of false alarms is high, which is as expected. Moreover, another conclusion is that the difference in the quality of estimation of $\hat{P}_d$ is more apparent at lower probabilities of target detection, or in other words, that at higher probabilities of target detection and density of false alarm λ_{fa} has a slightly smaller effect on its estimation.

Additional Monte-Carlo simulations (20000 scans) were undertaken to minimize the effect of random variables and to obtain a clearer picture of the estimator quality.

In the next simulations, the width of the gate size was fixed $K_g = 2.4$, the actual probability of target detection was $P_d = 0.8$, the actual density of false alarms was fixed $\lambda_{fa} = 10^{-5}$, and the length of sequence N was varied from 6 to 16. Fig. 4-7 shows the estimated probability of detection

$\hat{P}_d$ as a function of the length of sequence N. It is apparent that for a length of sequence N=8, the relative bias of estimated probability of detection was about 2% and that it additionally decreases as N increases.

$$N = 12$$

Fig. 4-6: Quality of Estimation of probability of detection as a function of density of false alarms

$$\lambda_{fa} = 10^{-5}, P_d = 0.8, K_g = 2.4$$
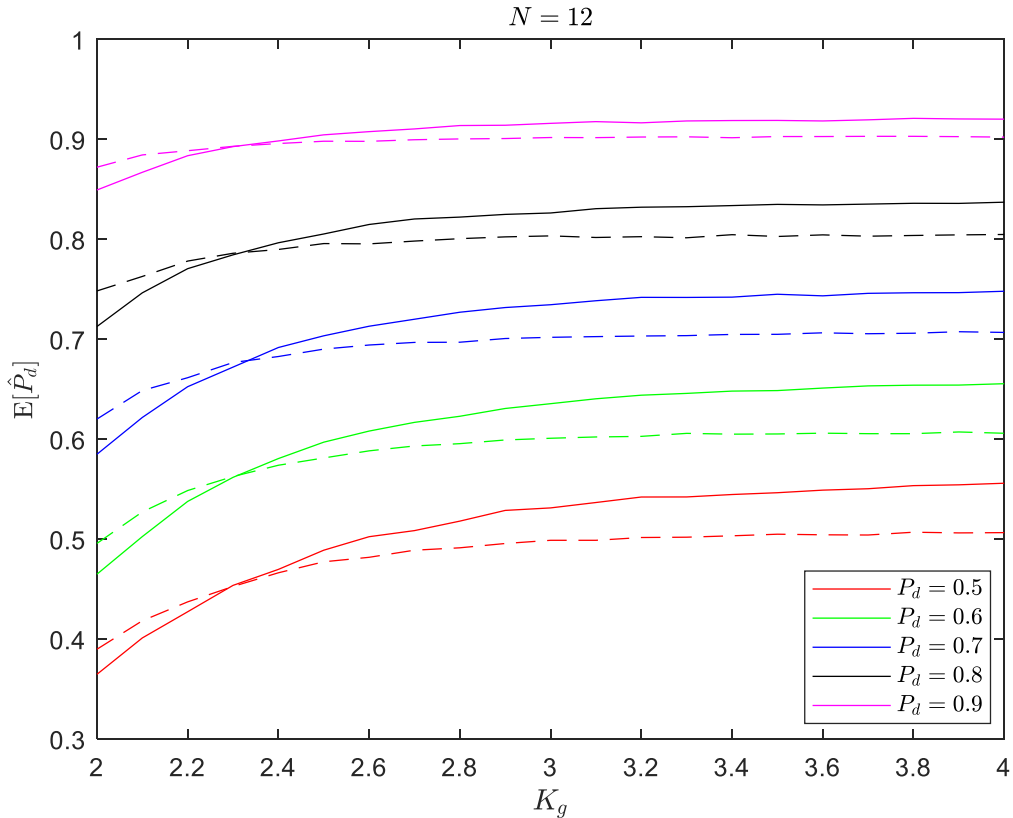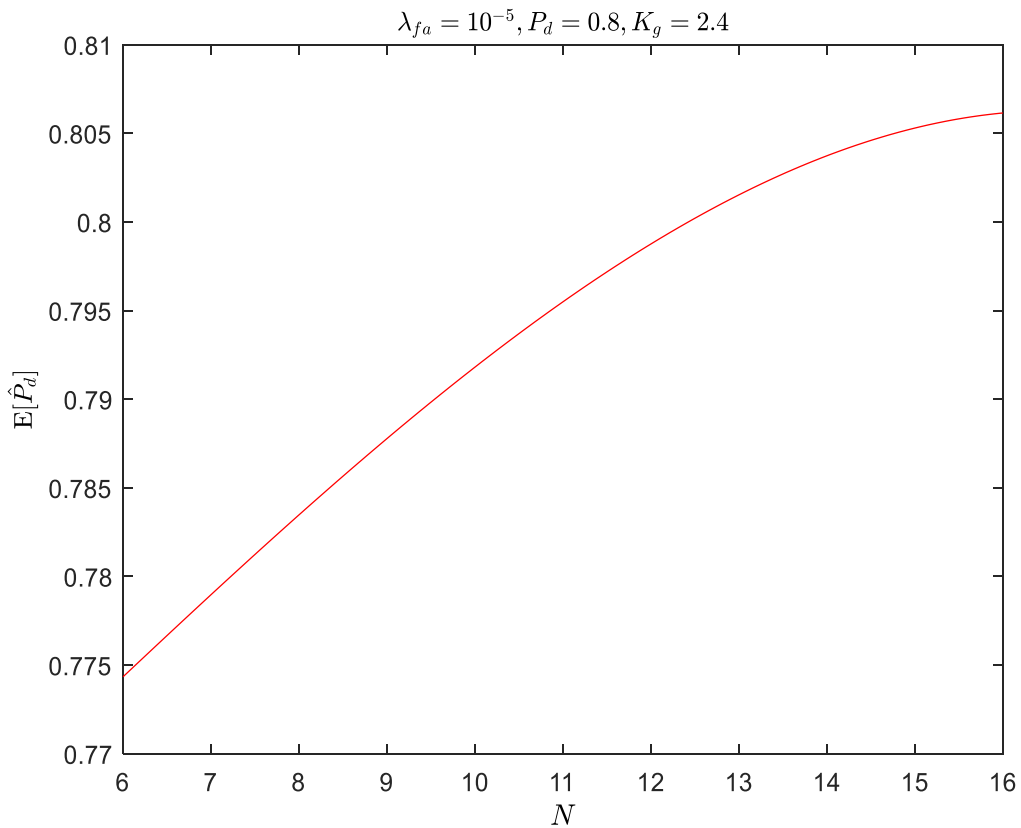

Fig. 4-7: Average estimations of probability of detection as a function of length of sequence N

63

Variation in the variance of the estimated probability of detection is shown in Fig. 4-8. The plot indicates that the quality of estimation of the probability of detection is improving considerably with increases of the parameter N. Standard deviation of this estimation was $Std[\hat{P}_d] = 0.23$ for N=8 and dropped to $Std[\hat{P}_d] = 0.164$ for N=16, which is about 20% of the estimated quantity and not negligible.

$$\lambda_{fa} = 10^{-5}, P_d = 0.8, K_g = 2.4$$
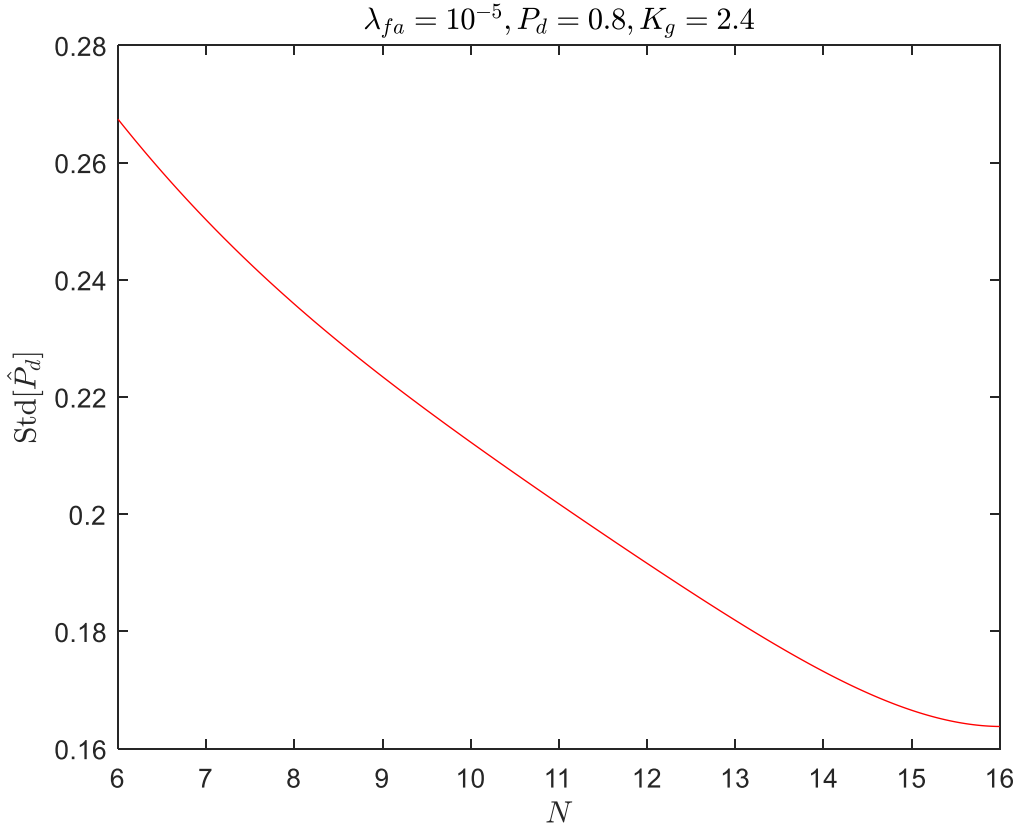
Fig. 4-8: Standard deviation of the estimated probability of detection as a function of length of sequence N

The estimated density of false alarms $E[\hat{\lambda}_{fa}]$ and standard deviation of the estimated density of false alarm $Std[\hat{\lambda}_{fa}]$ as a function of the length of sequence N are shown in the figures (Fig. 4-9 and Fig. 4-10), respectively.

In the Fig. 4-9, the density of false alarm bias is positive at smaller lengths of sequence N, and as the parameter N is increased, the bias of the estimated density of false alarms is decreased. The interesting thing is that the bias in the density of false alarm increases as the density of false alarm decreases. It is difficult to efficiently estimate such a low density of false alarm, especially if estimated locally, and in limited observation space.

Variation in the standard deviation of the estimation of the density of false alarms $Std[\hat{\lambda}_{fa}]$ is shown in Fig. 4-10, which is high relative to the estimated density of false alarm $E[\hat{\lambda}_{fa}]$, especially at smaller lengths of the sequence N, about 1.43×10^{-5} when N=6 and decreases as N is increased to be 0.88×10^{-5} when N=16, still high.

The conclusion is that the standard deviation of the estimation of the density of false alarms is high relative to the absolute value of the parameter being estimated. The result indicates that the variance of the new proposed estimators can be decreased if the number of consecutive scans used for the estimation is chosen correctly. However, this would preclude the possibility of matching the dynamics of unknown parameter estimation.

Fig. 4-9: Average estimations of the density of false alarm as
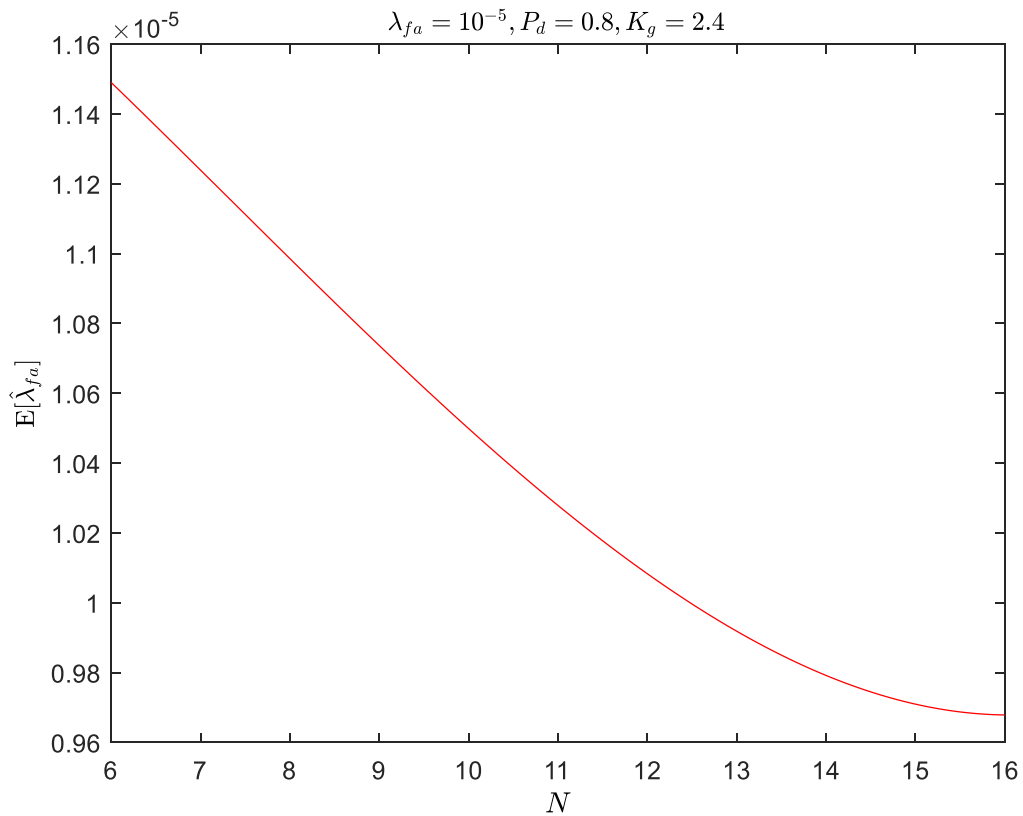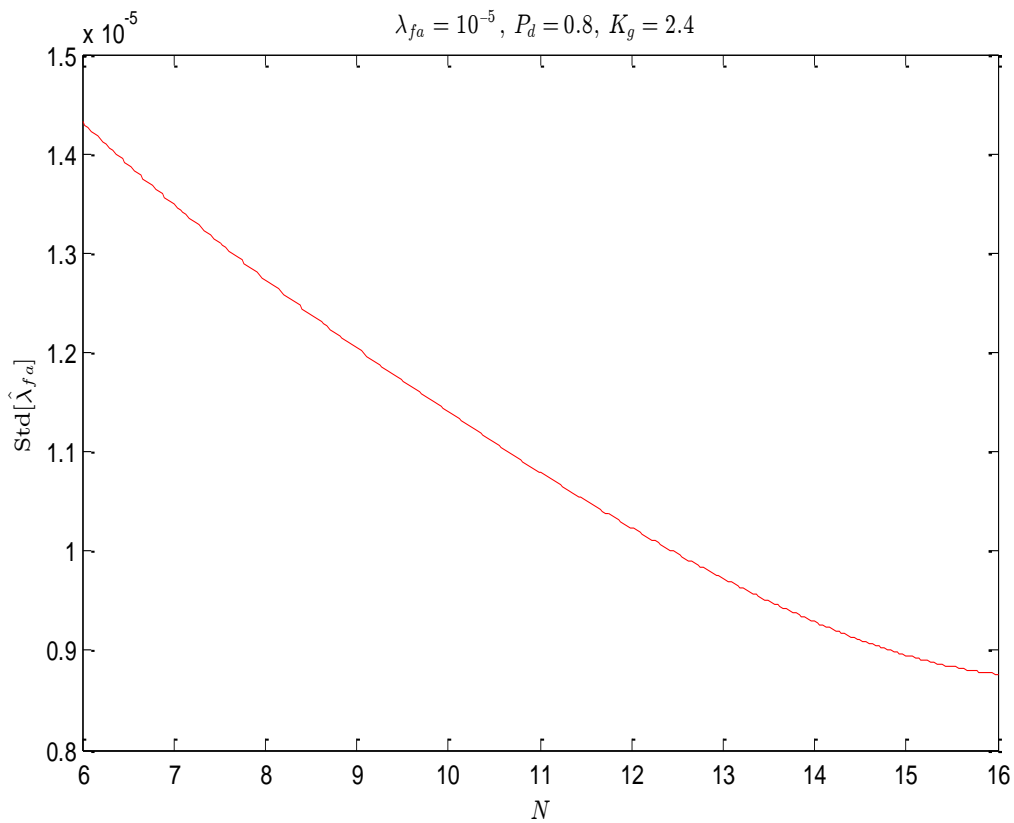a function of length of sequence N

Fig. 4-10: Standard deviation of the estimated density of false alarm
as a function of length of sequence N

To illustrate the influence of gate size K_g and the length of sequence (N) on the average mean of the estimated probability of detection $\hat{P}_d$ and density of false alarms $\hat{\lambda}_{fa}$ when the actual probability of detection was $P_d = 0.8$ and density of false alarms was $\lambda_{fa} = 10^{-5}$, some simulation results are shown in the figures (Fig. 4-11, Fig. 4-12, Fig. 4-13, and Fig. 4-14).

The two elements gate size K_g and the length of a sequence N, both have a considerable influence on the performance of the proposed estimator. So careful choice of these elements is essential and one needs to design another two procedures to reduce the bias and variance.

I will consider, in the next simulations, the influence of the gate size K_g on the quality of the estimated probability of detection $E[\hat{P}_d]$ and density of false alarms $E[\hat{\lambda}_{fa}]$.

The width of gate size was set changeable $K_g \in \{2.4,\ 2.6,\ 2.8\}$, the actual probability of target detection as in the previous simulation example was fixed during the simulation $P_d = 0.8$, the actual density of false alarms also fixed $\lambda_{fa} = 10^{-5}$, and the length of sequence N was varied from 6 to 16.

The estimated probability of detection $E[\hat{P}_d]$ as a function of the length of sequence N for different values of K_g is shown in Fig. 4-11. It is apparent that at N=6, the relative bias of the estimated probability of detection $E[\hat{P}_d]$ was negative, about 3.7% when $K_g = 2.4$ also the bias is negative, about 1.24% when $K_g = 2.6$. Additionally, the bias decreases as N increases and at N=12 the bias was decreased up to negative 0.18% for $K_g = 2.4$, also for $K_g = 2.6$, at N=7 the bias is decreased up to negative 0.26 % and bias continue decreasing until unbiased estimation is obtained, then after that, the bias starts increasing with increasing N again.

For the width of the gate size $K_g = 2.8$ and at N=6 the bias is positive, about 0.88%, and increases as N increase.

One can conclude from these results that, estimation of the probability of detection $E[\hat{P}_d]$ is highly dependent on the width of gate size K_g and length of sequence N.

The mechanism of influence of the parameters K_g and N to the quality of estimator is very complicated. For example, if K_g is small, the probability of correct observation to be out of the gate is high. Consequently, the bias of the P_d estimation will be negative. On the other hand, the length of sequence N increases the accuracy of the estimation. Because better and for some certain value the estimator become unbiased.

A similar explanation may be found for a different combination of K_g, P_d, and λ_{fa}. It is very difficult to design the model for all these influences, but it is obvious that these influences have a deterministic nature and a new idea appeared to model these phenomena in the form of linear regression.

The linear regression model is often used as a statistical tool if we intend to establish a numerical relationship between particular physical quantities. Then we declare one of these quantities dependent and the remaining independent quantities and a linear conditionality are established between them. Clearly, in most cases, this link is not justified by any physical laws. However, in a number of practical examples, assuming relatively small deviations of independent

variables, the linear regression method solves the problems and produces satisfactory results. When higher accuracy is insisted on, non-linear regressions can be used instead of linear ones. However, a priori knowledge of the type of nonlinearity involved in modeling is then necessary. In this doctoral dissertation, a linear regression model was used to establish a relationship between bias in estimating unknown parameters based on the size of the window function, the length of the estimation sequence, and the rough estimates of the target detection probability and the density of false alarms. As will be seen below, such linear regression fully met expectations and produced more than satisfactory results.

Variation in the variance of the estimated probability of detection for different values of gate size K_g is shown in Fig. 4-12.

The figure indicates that the quality of estimation of the probability of detection is improving considerably with increasing the parameters N and the appropriate choice of the width of gate size K_g.

The extracted standard deviation of the probability of detection from the figure can be concluded in Table 4-1.

Table 4-1: Standard deviation of the estimated probability of detection for different values of gate size and the length of sequence N

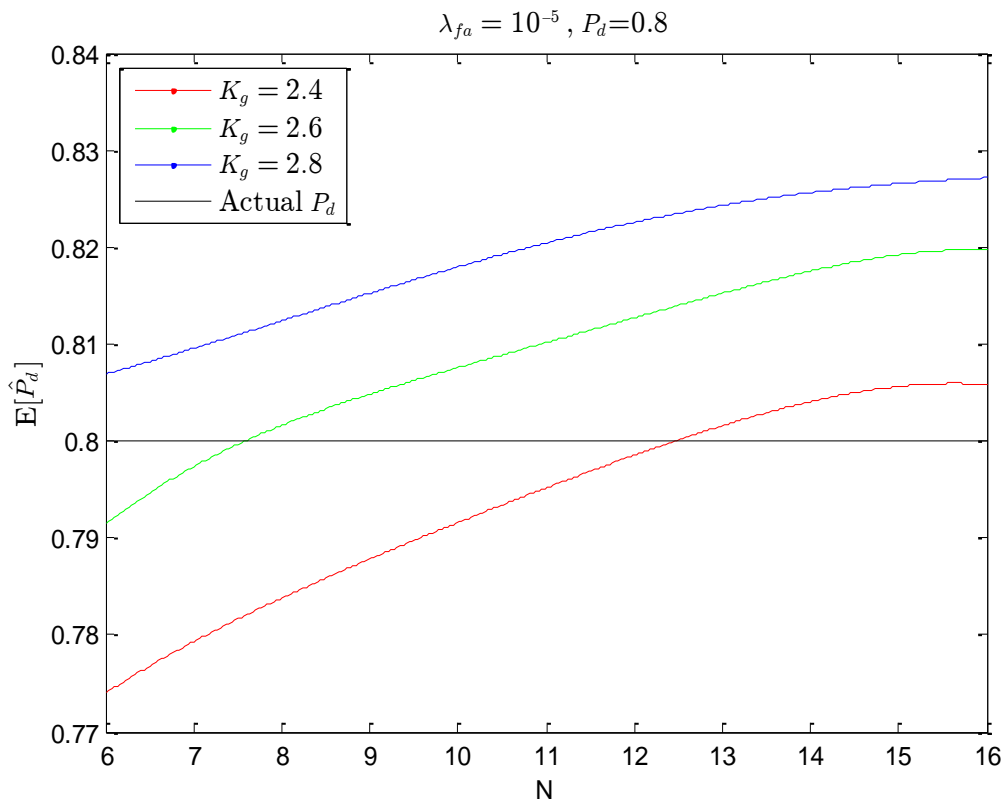| N	$K_g =2.4$	$K_g =2.6$	$K_g =2.8$
	Standard deviation $[\hat{P}_d]$		
6	0.2740	0.2433	0.2198
16	0.1640	0.1330	0.1170

Fig. 4-11: Average of the estimated probability of detection as a function of length of sequence N for different values of gate size K_g

Fig. 4-12: Variance of the estimated probability of detection as a function of length of sequence N for different values of gate size K_g

The estimated density of false alarms $E[\hat{\lambda}_{fa}]$ as a function of the length of sequence N for different values of K_g is shown in Fig. 4-13.

It is clear from the figure at the small lengths of sequence N=6 and $K_g = 2.4$ the estimated density of false alarm was $E[\hat{\lambda}_{fa}] = 1.1529 \times 10^{-5}$ with a positive bias about (1.529×10^{-6}). As the length of sequence (N) is increased, the bias of the estimated density of false alarms is decreased. At N=16 the estimated density of false alarms was (0.9676×10^{-5}) with negative bias about (3.24×10^{-7}).

In the second case, when $K_g = 2.6$, at N=6 the estimated density of false alarms was $E[\hat{\lambda}_{fa}] = 1.0388 \times 10^{-5}$ with positive bias about (3.880×10^{-7}). The bias is decreasing with increasing N until N=8 the obtained bias was (3.890×10^{-8}). After that, the bias starts increasing again, and at N=16, the estimated density of false alarms was (9.0897×10^{-6}) with a negative bias about (9.1030×10^{-7}).

The third case for $K_g = 2.8$, at N=6 the estimated density of false alarms was (0.97536×10^{-5}), the bias is negative, about (2.464×10^{-7}). As the length of sequence N is increased, the bias of the estimated density of false alarms is increased. At N=16, the estimated density of false alarms was (8.9129×10^{-6}) with a negative bias, about (1.0871×10^{-6}).

From the results shown in Fig. 4-13, one can conclude that these results are suffering from a significant bias and the value of bias depends on the gate size K_g and the length of the sequence N.

The estimated density of false alarm is monotonically decreasing as the length of the sequence N is increased. The influence of the parameters K_g and N to the quality of estimation of density of false alarm is very complex. For example, if the gate size K_g is small, then the probability of correct observation to be in the gate is low, the bias, in this case, depends on the length of sequence N as shown in the figure, such as for $K_g = 2.4$ there is a considerable difference in bias when N=6 and N=16. On the other hand, if the size of the gate is big then the probability of miscorrelation will be high. Again the bias in the estimated density of false alarm is significantly dependent on the length of sequence N. For example when $K_g = 2.8$ and N=6 the bias is small and the bias is increasing with increasing N.

Consequently, the estimation of unknown parameters (P_d, λ_{fa}) does not always improve by increasing the length of sequence N because it is also significantly influenced by the gate size K_g.
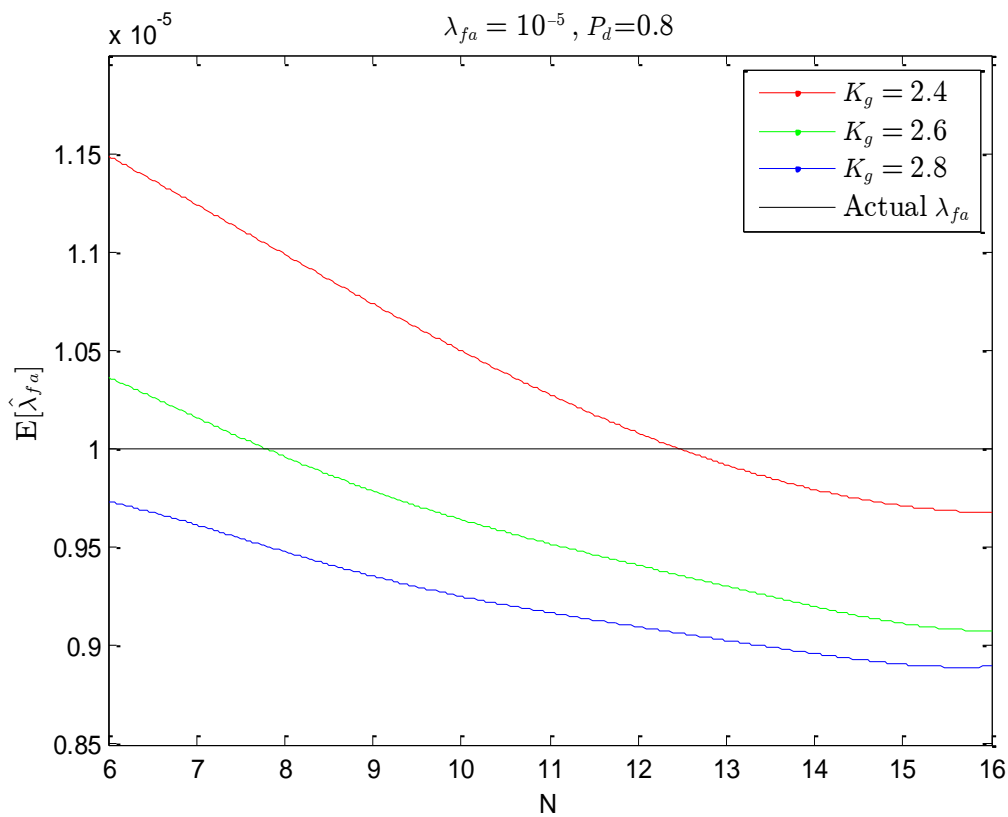
Fig. 4-13:Average of the estimated density of false alarm as a function of
length of sequence N for different values of gate size K_g

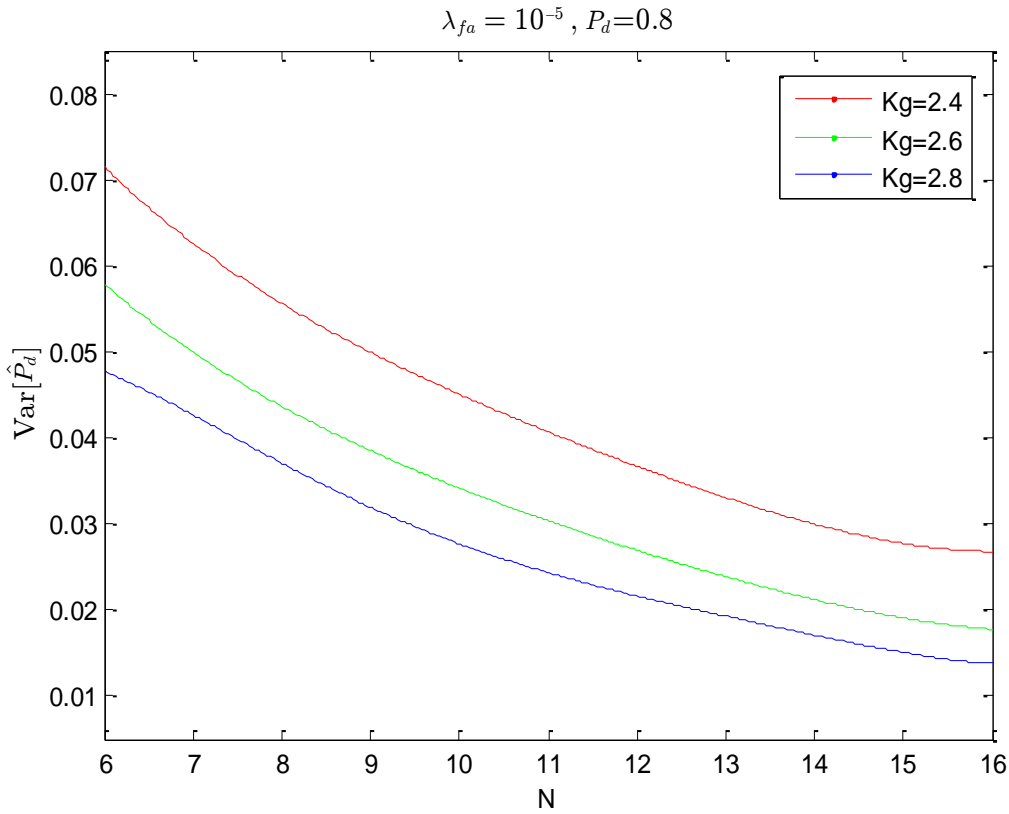Variation in the variance of the estimation of the density of false alarms $Std[\hat{\lambda}_{fa}]$ is shown in Fig. 4-14.

The standard deviation of the density of false alarm estimation is high when $N = 6$ and decreases with increasing the length of sequence N, also decrease with increasing the width of gate size K_g.

The extracted standard deviation values of the estimated density of false from the figure can be concluded in Table 4-2.

Table 4-2: Standard deviation of the estimated density of false alarms for different values of gate size and the length of sequence N

|	$K_g = 2.4$	$K_g = 2.6$	$K_g = 2.8$
N	Standard deviation $[\hat{\lambda}_{fa}]$		
6	1.43×10^{-5}	1.1684×10^{-5}	9.8932×10^{-6}
16	0.88×10^{-5}	6.4051×10^{-6}	5.2939×10^{-6}
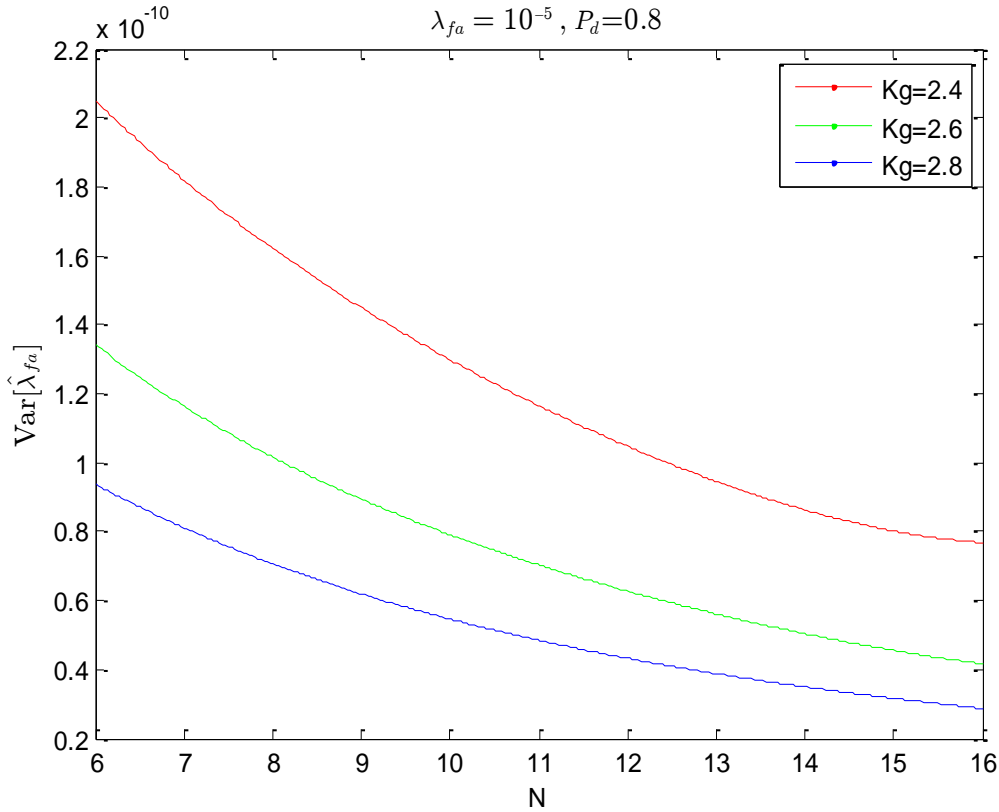
Fig. 4-14: Variance of the estimated density of false alarm as a function of length of sequence N for different values of gate size K_g

The quality of the estimator is shown in the figures (Fig. 4-15 and Fig. 4-16) and illustrated as follow:

More precisely, these figures represent the estimation results of the application of both estimators during 100 consecutive scans, in the case of the probability of detection $P_d = 0.5$ and density of false alarm $\lambda_{fa} = 10^{-5}$, gate constant $K_g = 2.6$, and length of the sequence was N=12. The plots show to what extent the estimators defined by relation (4.34) are not usable, and fluctuations of the obtained estimates are significant.

Namely, a more detailed analysis shows that only 31% of 100 estimates fall within the confidence interval $[0.9P_d, 1.1P_d]$, and around 11% of them are outside this interval $[0.7P_d, 1.3P_d]$. The situation is even worse when it comes to the density of false alarms because 26% of the estimates are in the interval $[0.9\lambda_{fa}, 1.1\lambda_{fa}]$, and 36% are out of that interval $[0.7\lambda_{fa}, 1.3\lambda_{fa}]$. Bearing in mind that all serious data association techniques assume the knowledge of these two parameters, such large estimation errors can impose a significant limitation on the association quality.

Taking into account the conclusion drawn above about the properties of the new proposed estimator, it follows that it has severe shortfalls primarily reflected in a significant bias and significant variance. Two improvement methods are proposed to improve the estimated results.

$$P_d = 0.5, \; \lambda_{fa} = 10^{-5}, \; N=12$$

Fig. 4-15: Estimation of the probability of detection

$$P_d = 0.5, \; \lambda_{fa} = 10^{-5}, \; N=12$$

Fig. 4-16: Estimation of the density of false alarm

71

4.4 Parameters effecting in bias

The bias is a common problem and the undesired effect in system identification utilizing noisy data, where the estimated parameters may contain a considerable error compared with the actual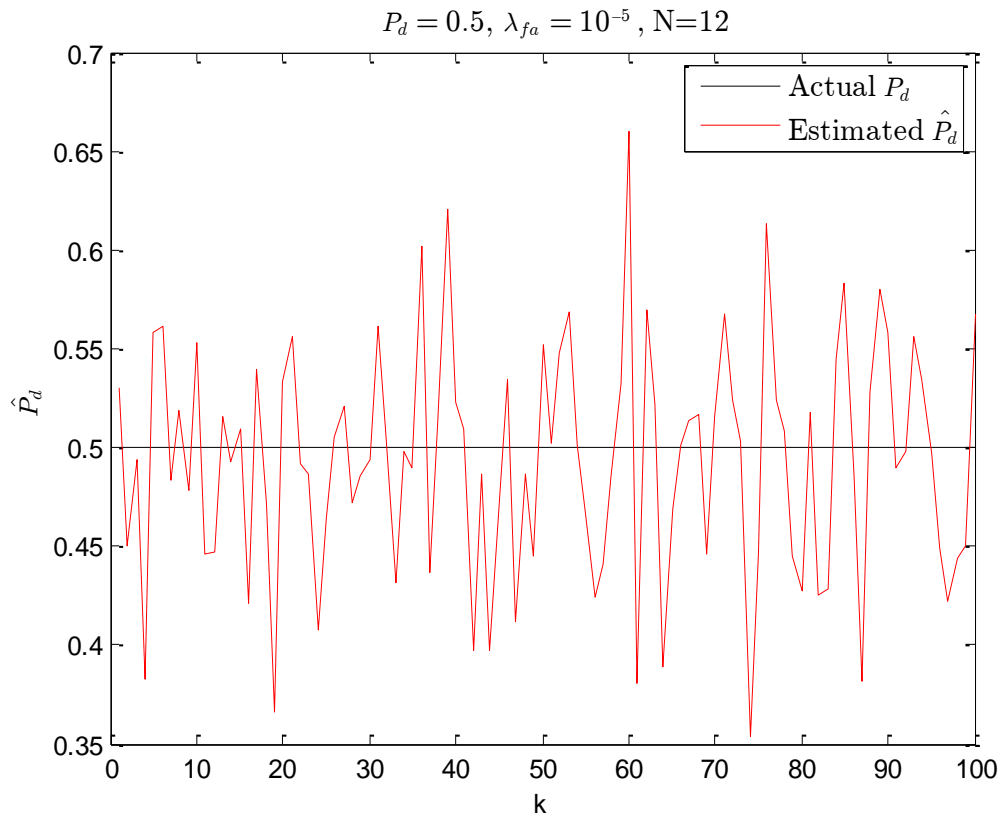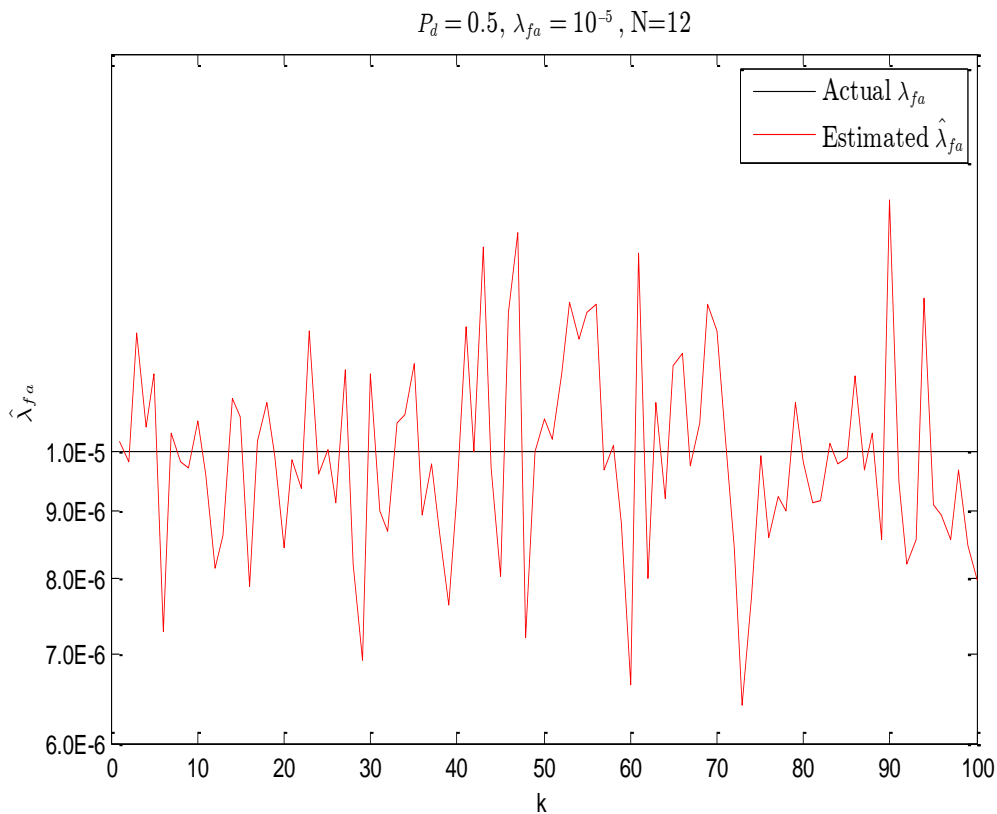 parameters [68]. The model which is identified is valid only for the specified condition. Bias problems occur when there is a random disturbance in the system.

Unfortunately, the exact reason that causes the bias cannot be easily obtained through statistical analysis. However, one can assume that there is an intuitive explanation for the observed phenomenon (bias). Namely, if the density of false alarms λ_{fa} approaches zero and the size of the gate K_g is large, then the estimated probability of target detection $\hat{P}_d$ would be almost equivalent to the problem of estimating the probability of success of Bernoulli random variable. As the length of sequence N increases and approaches infinity, the estimated $\hat{P}_d$ converges to the true value P_d and would improve the quality of estimation. However, increasing the density of false alarms λ_{fa} makes the probability that some of the false alarms are recognized as target reflections, more likely that some false alarms will be mistaken for the real target, thus increasing the perceived number of detections and leads to the artificial increase of the estimated probability of detection $\hat{P}_d$ higher than the true probability of detection P_d.

On the other hand, decreasing the gate size has opposite effects on the estimated probability of detection $\hat{P}_d$, increases the chance of overlooking detected observations belonging to the real target, and increases the possibility of misdetection, which ultimately results in the estimated probability of detection $\hat{P}_d$ lower than the true probability of detection P_d. The struggle between these two phenomena results in the occurrence of a biased estimation, regardless of the observation sequence length N used. As stated in the earlier results such as Fig. 4-2, for each specific value of the probability of detection P_d, the density of false alarms λ_{fa}, and the observation sequence length N, it is possible to find the corresponding value of the gate size K_g that would cancel the bias in the estimation of the probability of target detection $\hat{P}_d$. However, this procedure is not reasonably comprehensible because the probability of detection and the density of false alarms are unknown parameters.

4.5 Further improvements

Two methods are proposed to improve the results of the estimators, one method to reduce the bias, and the other method is to reduce the variance of estimation.

4.5.1 Estimator bias reduction

The first considered step was to introduce bias compensation for both estimators, keeping in mind a nearly deterministic dependency on three parameters: gate size K_g, the estimated probability of target detection $\hat{P}_d$, and estimated density of false alarms $\hat{\lambda}_{fa}$. The proposed improvement is of the form:

$$\hat{P}_d^c = \hat{P}_d + \Delta P_d \ , \ \ \Delta P_d = a_p K_g + b_p \hat{P}_d + c_p \hat{\lambda}_{fa} + d_p \ ,$$
$$\hat{\lambda}_{fa}^c = \hat{\lambda}_{fa} + \Delta \lambda_{fa}, \ \ \Delta \lambda_{fa} = a_\lambda K_g + b_\lambda \hat{P}_d + c_\lambda \hat{\lambda}_{fa} + d_\lambda \ ,$$

(4.35)

where $\hat{P}_d^c$ and $\hat{\lambda}_{fa}^c$ represent the new corrected (unbiased) estimates after reducing the bias, and both the $\hat{P}_d$ and $\hat{\lambda}_{fa}$ are the estimates from the estimators defined by (4.34).

The estimator results are improved by (4.35). The proper selection of the parameters a_p, b_p, c_p, d_p and $a_\lambda, b_\lambda, c_\lambda, d_\lambda$ can improve the estimators' quality considerably. The Generalized Least-Square (GLS) method is used for determining these parameters (4.35). The correction factors can be written in the form of linear regression:

$$Y_i = X^T \varphi_i,\qquad(4.36)$$

where $Y_i \in \{\Delta P_d, \Delta \lambda_{fa}\}$ represents the model output, $X^T = [K_g, \hat{P}_d, \hat{\lambda}_{fa}, 1]$ is the regression vector, and $\varphi_i^T = [a_i\ b_i\ c_i\ d_i]$, $i \in \{P, \lambda\}$ is the vector of unknown parameters. The GLS estimator is.

$$\varphi_i = \left(XX^T\right)^{-1} XY_i.\qquad(4.37)$$

Additional Simulation was performed in order to illustrate the effect of bias reduction. The figures (Fig. 4-17 and Fig. 4-18) present the results of the estimation with and without bias reduction.

The estimated results are obtained by (4.34) and the bias is reduced by (4.35). The bias of the estimated results is evident in the figures, reduced considerably as shown in the figures (Fig. 4-17 and Fig. 4-18), where the mean of the estimated probability of detection was (0.5212) and reduced to (0.4996). For the density of false alarm, the mean was (1.8075×10^{-5}) and reduced to (9.9953×10^{-6}). So the bias reduction procedure improves the results very well as shown in the figure.
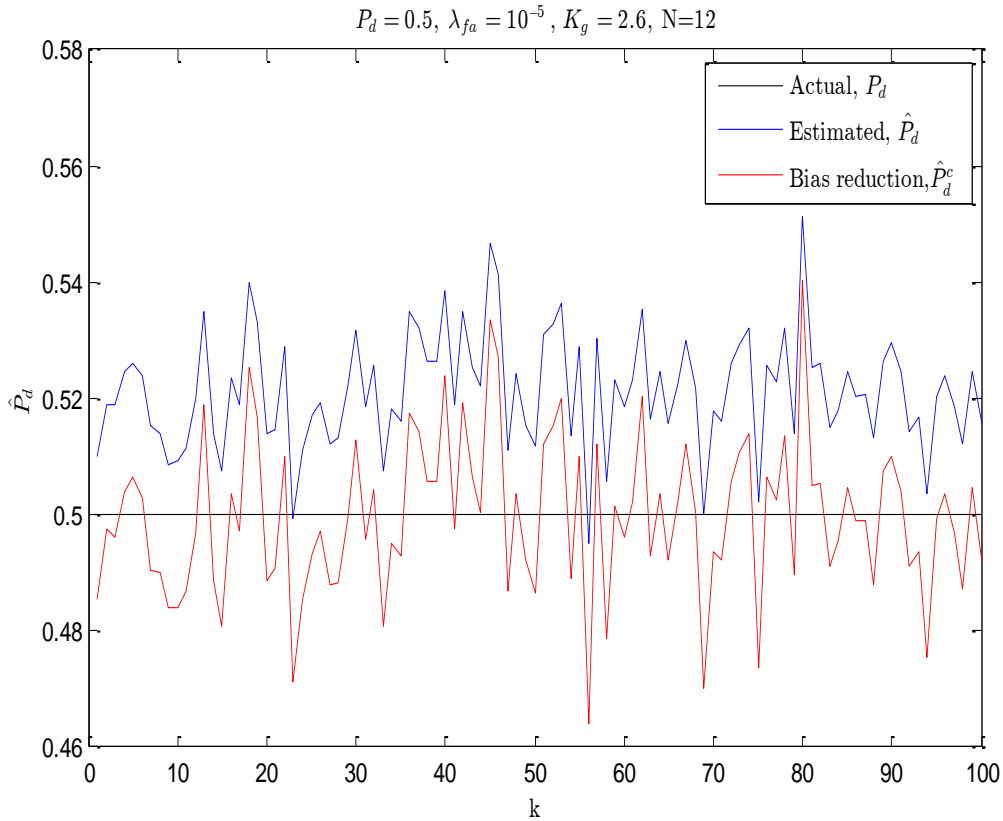

Fig. 4-17: Estimated probability of detection $\hat{P}_d$ and bias reduced $\hat{P}_d^c$

$P_d = 0.5$, $\lambda_{fa} = 10^{-5}$, $K_g = 2.6$, N=12
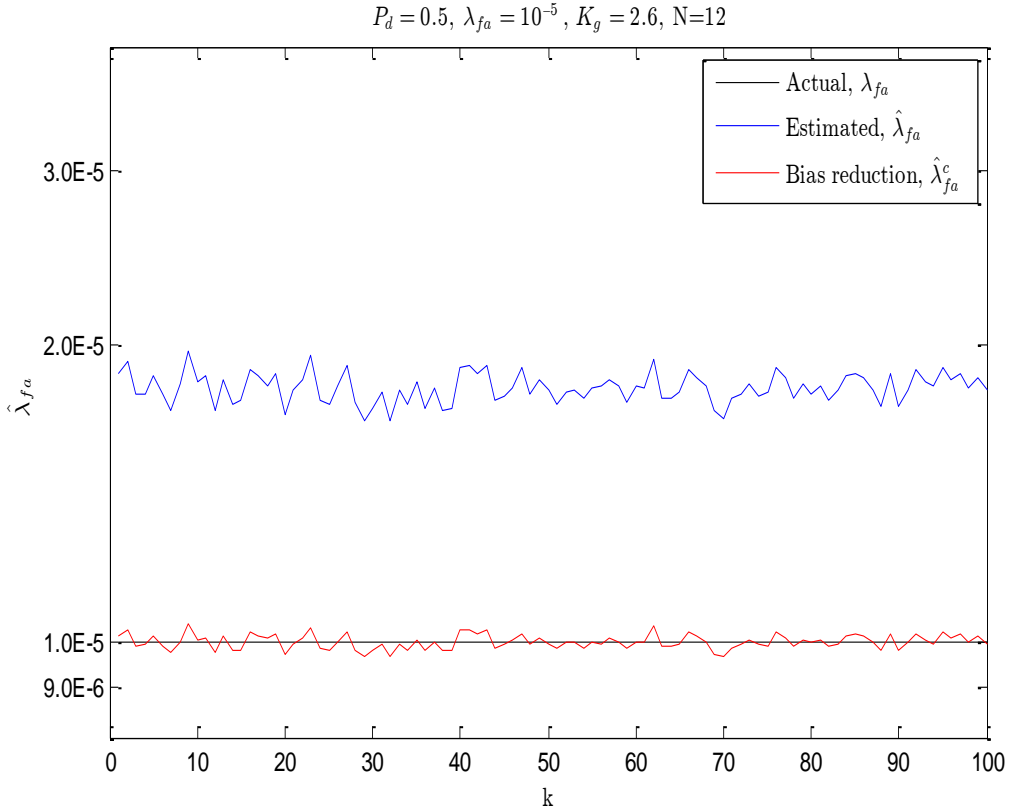
Fig. 4-18: Estimated density of false alarms $\hat{\lambda}_{fa}$ and bias reduced $\hat{\lambda}_{fa}^c$

The reduction procedure was applied with different values of the width of gate size $K_g \in \{2, 2.1, 2.2, ..., 4\}$, the actual density of false alarm $\lambda_{fa} \in \{10^{-7}, 10^{-6}, 10^{-5}\}$, the actual probability of detection $P_d \in \{0.5, 0.6, 0.7, 0.8, 0.9\}$, and the estimated values of the parameters were stored in the lookup table.

Monte-Carlo simulations were performed to illustrate these improvements, and the length of the sequence was fixed $N = 12$. The figures (Fig. 4-19 and Fig. 4-20) show the results of the bias reduction procedure for a fixed probability of detection of $P_d = 0.5$ and fixed density of false alarm $\lambda_{fa} = 10^{-5}$ as a function of the gate size K_g.

Another result of the bias reduction procedure for a fixed probability of detection $P_d = 0.6$ and fixed density of false alarm $\lambda_{fa} = 10^{-5}$ as a function of the gate size K_g is shown in the figures (Fig. 4-21 and Fig. 4-22) respectively.

The choice of these parameters $(P_d \in \{0.5, 0.6\}, \lambda_{fa} \in \{10^{-5}\})$ illustrates the effect of the remedy because the shortfalls of the estimators were the most obvious for this set of parameters (low probability of detection P_d and high density of false alarms λ_{fa}).

A comparison between the estimated probabilities of detection $\hat{P}_d$ and the improved estimation of the probability of detection $\hat{P}_d^c$ is shown in the figures (Fig. 4-19 and Fig. 4-21) for $P_d = 0.5$ and $P_d = 0.6$ respectively. The estimated probability of detection $\hat{P}_d$ of this set of parameters has a considerable bias in high values of the parameter K_g as well, especially at lower values of the actual probability of detection.

The bias in the estimated parameters was considerably reduced by the bias reduction procedure, and significant improvement in results can be seen before and after the remedy in both figures.

It is obvious in Fig. 4-19 the bias is significantly reduced even in the small gate size and did not exceed 2% of the estimated value. While without improvement, the bias in the estimated probability of detection $\hat{P}_d$, when $K_g = 4.0$ was about 11%, and when $K_g = 2.0$ was 26%. Also in Fig. 4-21 the bias is significantly reduced even in the small gate size and did not exceed 1% of the estimated value.

Another comparison between the estimated density of false alarms $\hat{\lambda}_{fa}$ with the improved estimation of the density of false alarms $\hat{\lambda}_{fa}^c$, shown in the figures (Fig. 4-20 and Fig. 4-22) both for actual $\lambda_{fa} = 10^{-5}$ and actual ($P_d = 0.5$ and $P_d = 0.6$), respectively. The estimated density of false alarms $\hat{\lambda}_{fa}$ has a considerable bias in the low values of the parameter K_g. The bias in the estimated parameters was considerably reduced by the bias reduction procedure, and the results are improved significantly, which can be seen in the figures (Fig. 4-20 and Fig. 4-22).

To test the effect of bias reduction procedure on a high probability of detection, another comparison was made between the estimated probability of detection $\hat{P}_d$ and the improved estimation of the probability of detection $\hat{P}_d^c$ when the actual probability of detection is $P_d = 0.8$.

As shown in Fig. 4-23, the estimated probability of detection $\hat{P}_d$ has a considerable bias in the low values of the parameter K_g and high values, as well. The bias in the estimated parameters was considerably reduced by the bias reduction procedure, and significant improvement in the results can be seen after the remedy in Fig. 4-23.

Fig. 4-19: Improvement of the averaged estimated low probability of detection, actual $P_d = 0.5$

$P_d = 0.5, \lambda_{fa} = 10^{-5}$, N=12

Fig. 4-20: Improvement of the averaged estimated density of false alarm
when actual $\lambda_{fa} = 10^{-5}$ and $P_d = 0.5$

P_d=0.6, $\hat{\lambda}_{fa} = 10^{-5}$, N=12

Fig. 4-21: Improvement of the averaged estimated low
probability of detection, actual $P_d = 0.6$
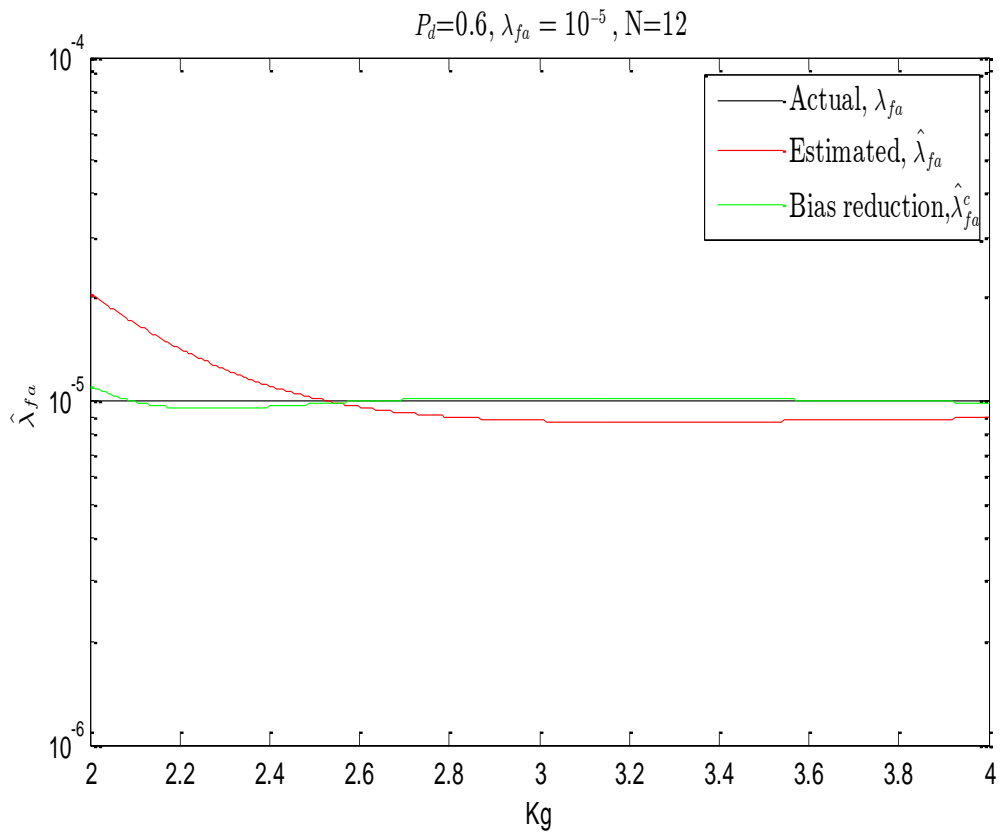
Fig. 4-22: Improvement of the averaged estimated density of false alarm when the actual $\lambda_{fa} = 10^{-5}$ and $P_d = 0.6$
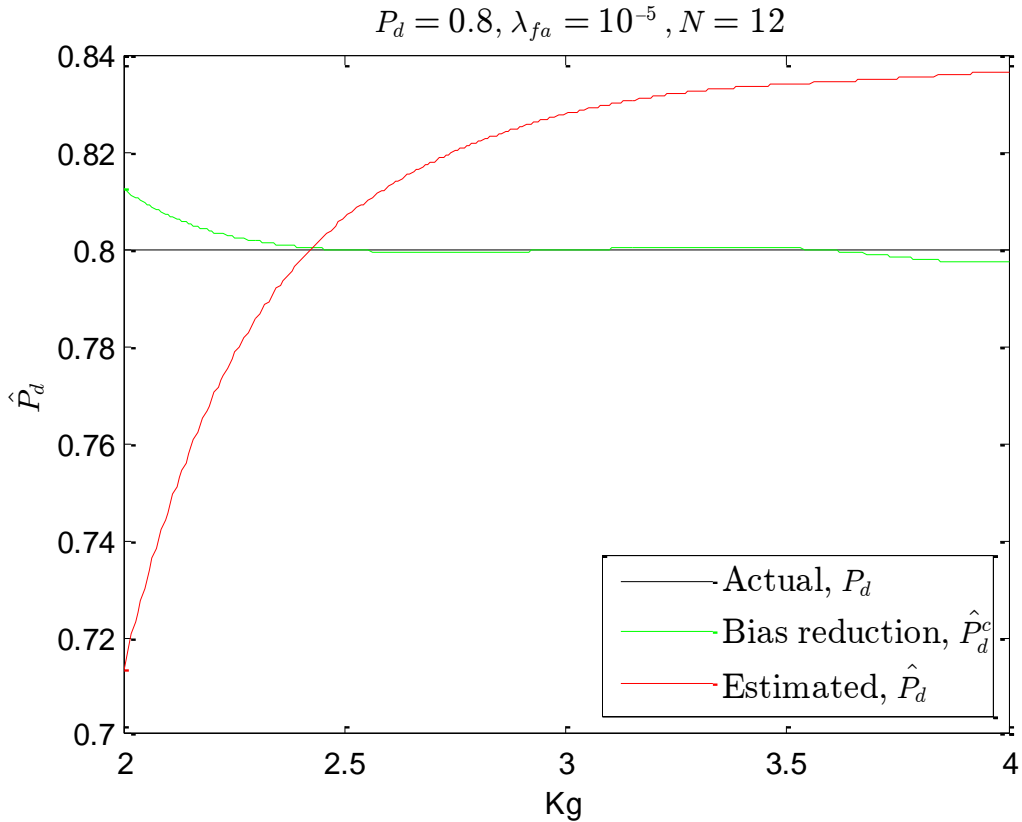
Fig. 4-23: Improvement of the averaged estimated probability of detection, actual $P_d = 0.8$

Fig. 4-24 shows the estimated density of false alarm $\hat{\lambda}_{fa}$ where this parameter has a considerable bias in the low values and high values of the parameter K_g. The bias in the estimated parameters was considerably reduced by the bias reduction procedure, and significant improvement in the results can be seen after the remedy in Fig. 4-24.
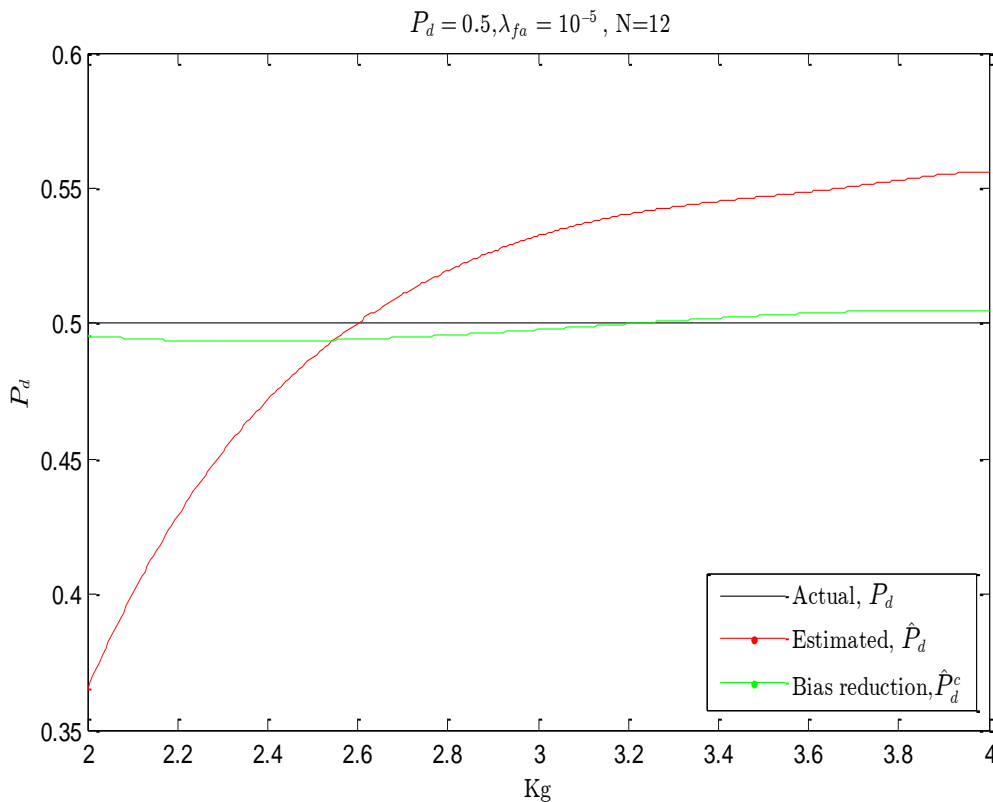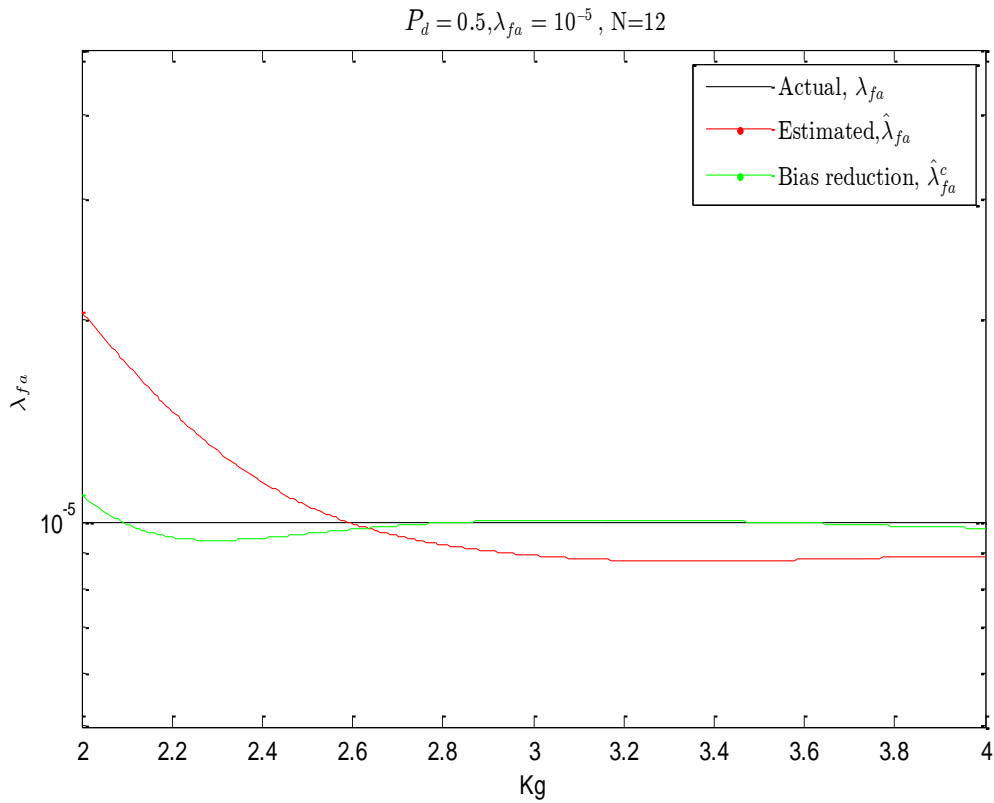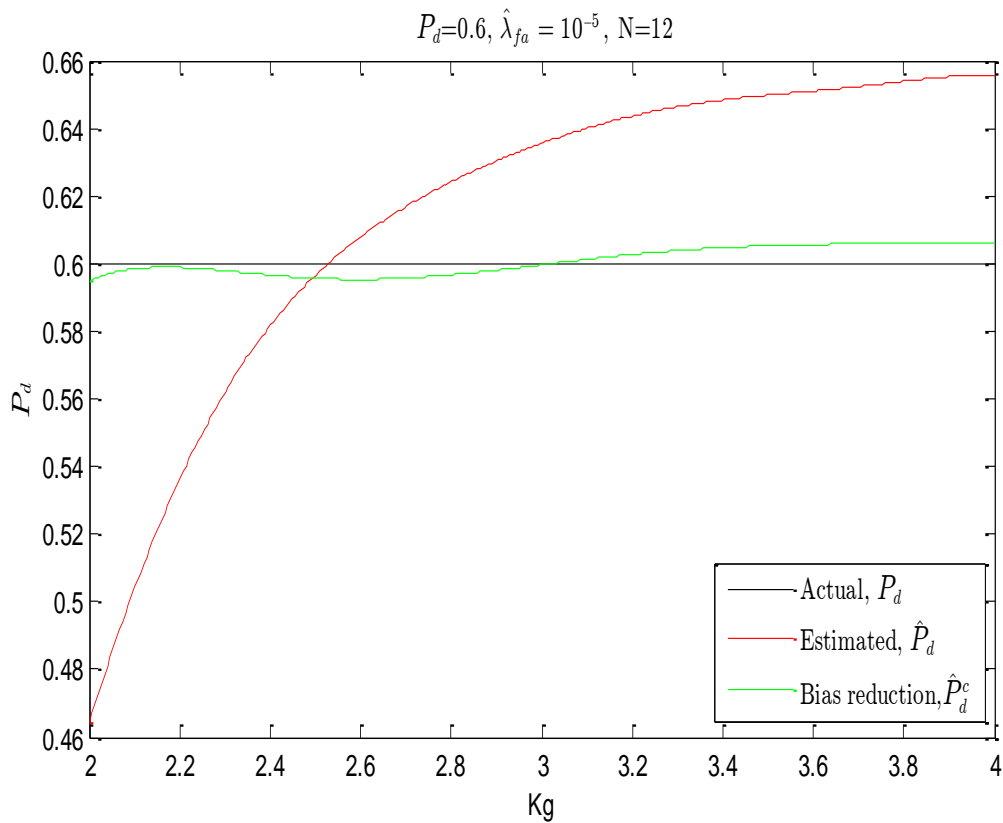
$$P_d = 0.8, \lambda_{fa} = 10^{-5}, N = 12$$
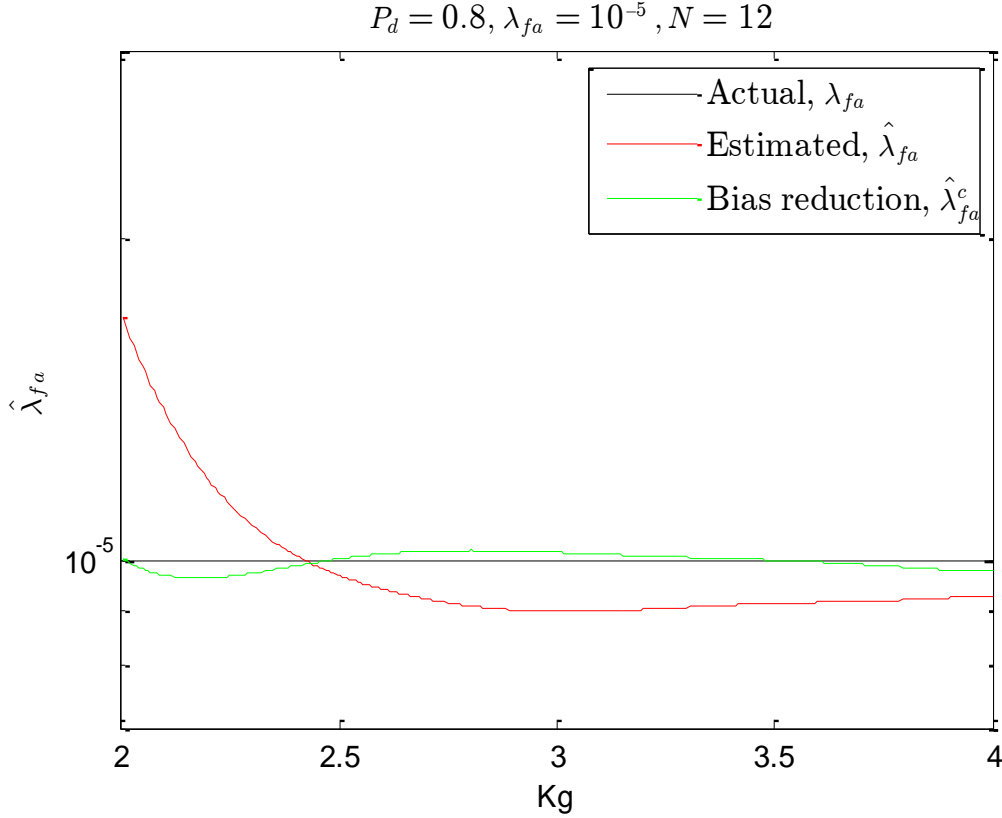
Fig. 4-24 Improvement of the averaged estimated density of false alarm
when the actual $\lambda_{fa} = 10^{-5}$ and $P_d = 0.8$

4.5.2 Estimator variance reduction

The second step in the improvement of the new proposed estimator is variance reduction, through a recursive type of estimator and using a variable forgetting factor.

$$\hat{P}_d^r[k] = \alpha[k]\hat{P}_d^r[k-1] + (1-\alpha[k])\hat{P}_d^c[k],$$
$$\hat{\lambda}_{fa}^r[k] = \alpha[k]\hat{\lambda}_{fa}^r[k-1] + (1-\alpha[k])\hat{\lambda}_{fa}^c[k],$$

(4.38)

where $\hat{P}_d^r$ is the recursive estimate of the probability of detection, $\hat{\lambda}_{fa}^r$ is the recursive estimate of the density of false alarm, α is the variable forgetting factor, the relation can describe its variation (4.39).

$$\alpha[k] = \alpha[\infty] - e^{(-k/\tau)}(\alpha[\infty] - \alpha[0]),$$

(4.39)

where $\alpha[0]$ is the initial forgetting value, $\alpha[\infty]$ is the final forgetting value and τ is a time constant that determines the rate of change of forgetting factor α. The effect of the recursive estimator form was verified experimentally, as in the next figures.

Next figures show the recursive estimator results obtained with rate change of the forgetting factor determined by initial forgetting value $\alpha(0) = 0.92$, final forgetting value $\alpha(\infty) = 0.996$, and $\tau = 20$.

The following comment is warranted at this time: At the beginning of tracking a target, the time profile of the forgetting factor $\alpha[k]$ was selected small (about 0.9) to suppress the effect of erroneous initial conditions $\hat{P}_d^c[0]$ and $\hat{\lambda}_{fa}^c[0]$ as soon as possible. On the other hand, by applying the variance operator on the recursive form of the unbiased estimator given in (4.38).

The ratio of the variance of the recursive estimator and non-recursive estimator after a sufficiently long time interval (i.e., in the steady-state) approaches to $\dfrac{1-\alpha(\infty)}{1+\alpha(\infty)}$ as follow:

$$Var\{X^r\} = \alpha^2[\infty]Var\{X^r\} + (1-\alpha[\infty])^2 Var\{X^c\}, \tag{4.40}$$

$$Var\{X^r\}(1-\alpha^2[\infty]) = (1-\alpha[\infty])^2 Var\{X^c\}, \tag{4.41}$$

$$\frac{Var\{X^r\}}{Var\{X^c\}} = \frac{(1-\alpha[\infty])^2}{1-\alpha^2[\infty]} = \frac{1-\alpha[\infty]}{1+\alpha[\infty]}, \tag{4.42}$$

where: X^r represents $\hat{P}_d^r$ or $\hat{\lambda}_{fa}^r$ and X^c represents $\hat{P}_d^c$ or $\hat{\lambda}_{fa}^c$.

Therefore the stationary value of the final forgetting factor $\alpha[\infty]$ should be high and close to 1, thereby reducing the estimation variance. This analysis is derived with the assumption that there is no correlation between the right-hand side terms of (4.38). The value of the parameter τ needs to be consistent with the length of sequence N, and due to experience based on numerous simulations, the ratio $\dfrac{\tau}{N} \in [1.5, 2]$ should be satisfied.

Additional simulations were performed in order to illustrate the effect of variance reduction. The estimated results are obtained by (4.34), the bias is reduced by (4.35), and the variance is reduced by (4.38). These simulation results are obtained when the density of false alarms was $\lambda_{fa} = 10^{-5}$, probability of detection $P_d \in \{0.5, 0.8\}$, the length of sequence (N=12), and fixed gate size ($K_g = 2.6$).

First, let us analyze the estimation quality at a high probability of target detection $P_d = 0.8$. Fig. 4-25 presents the actual probability of detection P_d, the estimation after the bias reduction $\hat{P}_d^b$ and the estimation after bias and variance reduction $\hat{P}_d^r$.

The influence of the variance reduction procedure is obvious in that figure. Also, Fig. 4-26 illustrates the actual density of false alarms λ_{fa}, the estimation after the bias reduction $\hat{\lambda}_{fa}^b$, and the estimation after the bias and variance reduction $\hat{\lambda}_{fa}^r$. The plot illustrates a significant reduction in the estimation variance.

The standard deviation, for the probability of detection, $Std[\hat{P}_d]$ was about 24%, and for the density of false alarm $Std[\hat{\lambda}_{fa}]$ was 32% in the non-recursive case. After applying the variance reduction procedure, the standard deviation was decreased to below 0.2% for both parameters.

Fig. 4-27 represents the variation of the forgetting factor $\alpha(t)$ obtained by equation (4.39), used in the variance reduction procedure through the recursive type and described by (4.38). Variation of the forgetting factor considerably depends on the time constant τ, initial forgetting value $\alpha[0]$, and final forgetting value $\alpha[\infty]$.

Recursive estimation of the probability of detection $\hat{P}_d^r$ and density of false alarms $\hat{\lambda}_{fa}^r$ for different initial conditions are shown in Fig. 4-28, and Fig. 4-29 respectively.

One can conclude, from the previous results that the variance reduction procedure reduces the variance considerably, and this certainly attests to an improved quality of the estimators.

$$P_d = 0.8, \lambda_{fa} = 10^{-5}, K_g = 2.6, N=12$$

Fig. 4-25: Recursive estimation of probability of detection at fixed actual $P_d = 0.8$ and $\lambda_{fa} = 10^{-5}$

$$P_d = 0.8, \lambda_{fa} = 10^{-5}, N=12$$

Fig. 4-26: Recursive estimation of density of false alarms at fixed actual $P_d = 0.8$ and $\lambda_{fa} = 10^{-5}$

80

$$\alpha(0) = 0.92,\ \alpha(infinite) = 0.996$$

Fig. 4-27: Forgetting factor α

$$P_d = 0.8, \lambda_{fa} = 10^{-5}, K_g = 2.6, N = 12$$

Fig. 4-28: Recursive estimation of probability of detection at fixed actual

$$P_d = 0.8 \ \text{and} \ \lambda_{fa} = 10^{-5} \text{ for different initial conditions}$$

81

$$P_d = 0.8, \lambda_{fa} = 10^{-5}, K_g = 2.6, N = 12$$

Fig. 4-29 Recursive estimation of density of false alarms at fixed

$P_d = 0.8$ and $\lambda_{fa} = 10^{-5}$ for different initial conditions

Second let us analyze the estimation quality at low probability of target detection when the variance is pronounced (i.e., for the actual probability of target detection $P_d = 0.5$, density of false alarms of $\lambda_{fa} = 10^{-5}$), and N=12 with a fixed gate size ($K_g = 2.6$).

Fig. 4-30 represents the actual value of the probability of detection, its estimation after the bias reduction $\hat{P}_d^b$ and its estimation after bias and variance reduction $\hat{P}_d^r$.

The figure Fig. 4-31 illustrates the actual value of the density of false alarms λ_{fa}, its estimation after bias reduction $\hat{\lambda}_{fa}^b$, and its estimation after bias and variance reduction $\hat{\lambda}_{fa}^r$. From the figures, the variance is significantly reduced.

Fig. 4-32 represents the actual value of the probability of detection P_d, its estimation after bias and variance reduction $\hat{P}_d^r$ for different initial conditions. Also, Fig. 4-33 illustrates the actual density of false alarm λ_{fa} and the estimated one after bias and variance reduction $\hat{\lambda}_{fa}^r$ for different initial conditions.

It is obvious from the first glance, that the figures (Fig. 4-30, Fig. 4-31, Fig. 4-32 and Fig. 4-33) indicate a significant reduction in the estimation variance and, consequently, higher quality of the new proposed estimators.
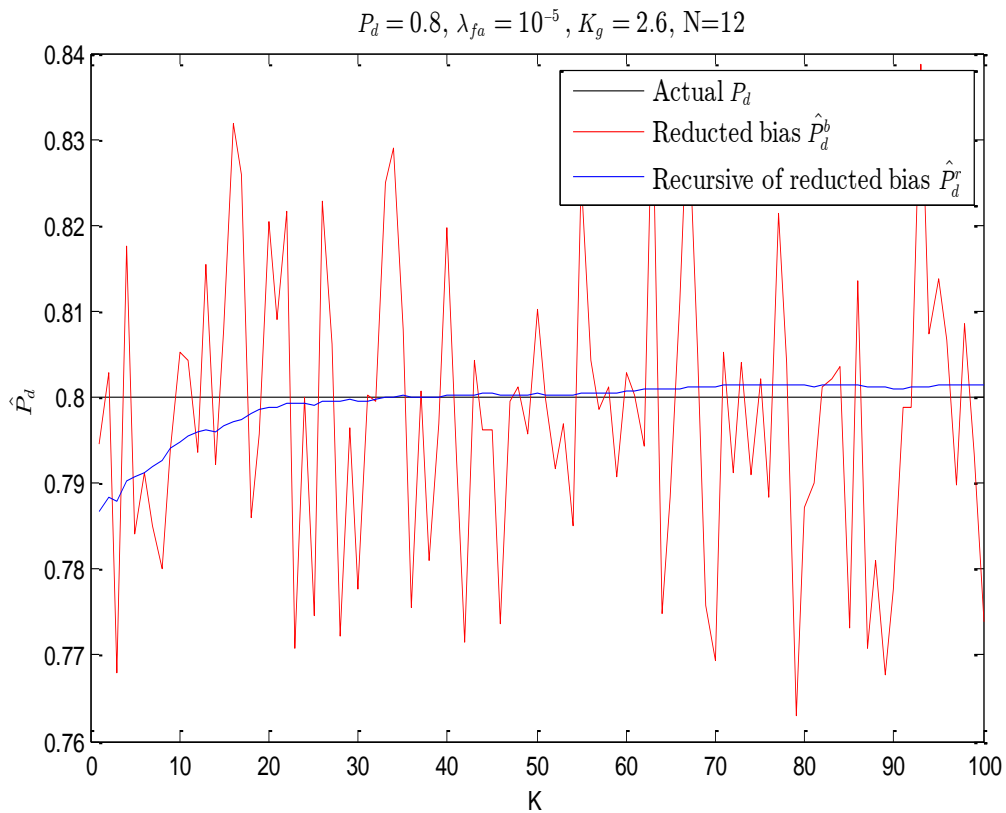
Fig. 4-30: Recursive estimation of probability of detection
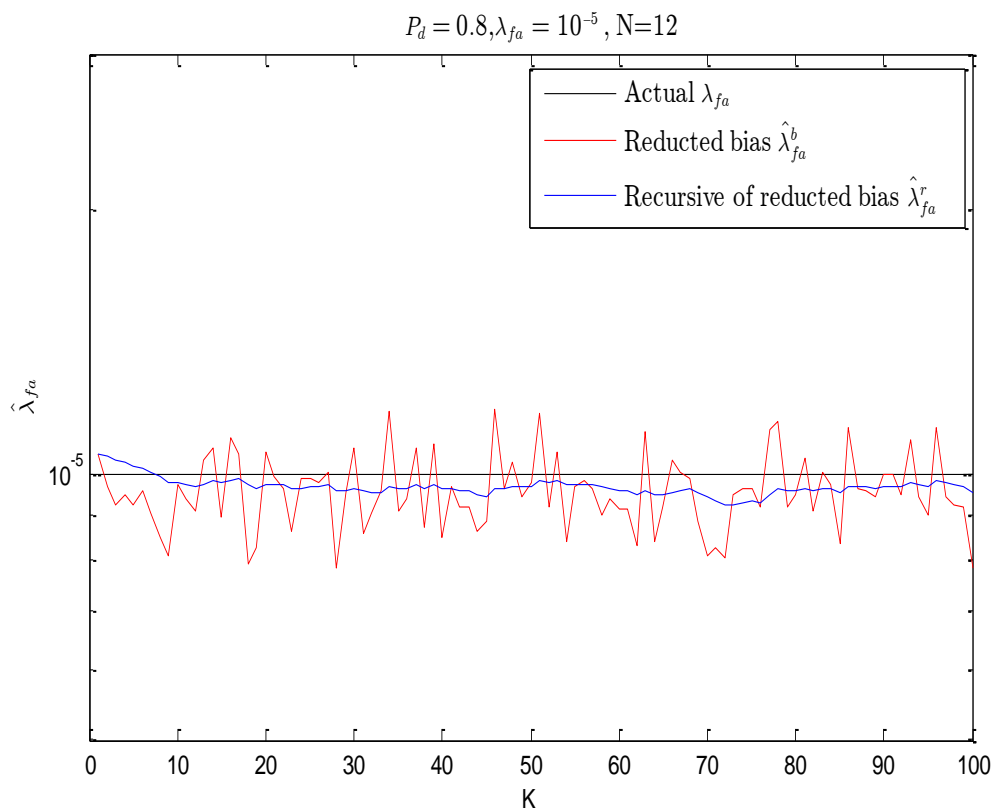at fixed actual $P_d = 0.5$ and $\lambda_{fa} = 10^{-5}$
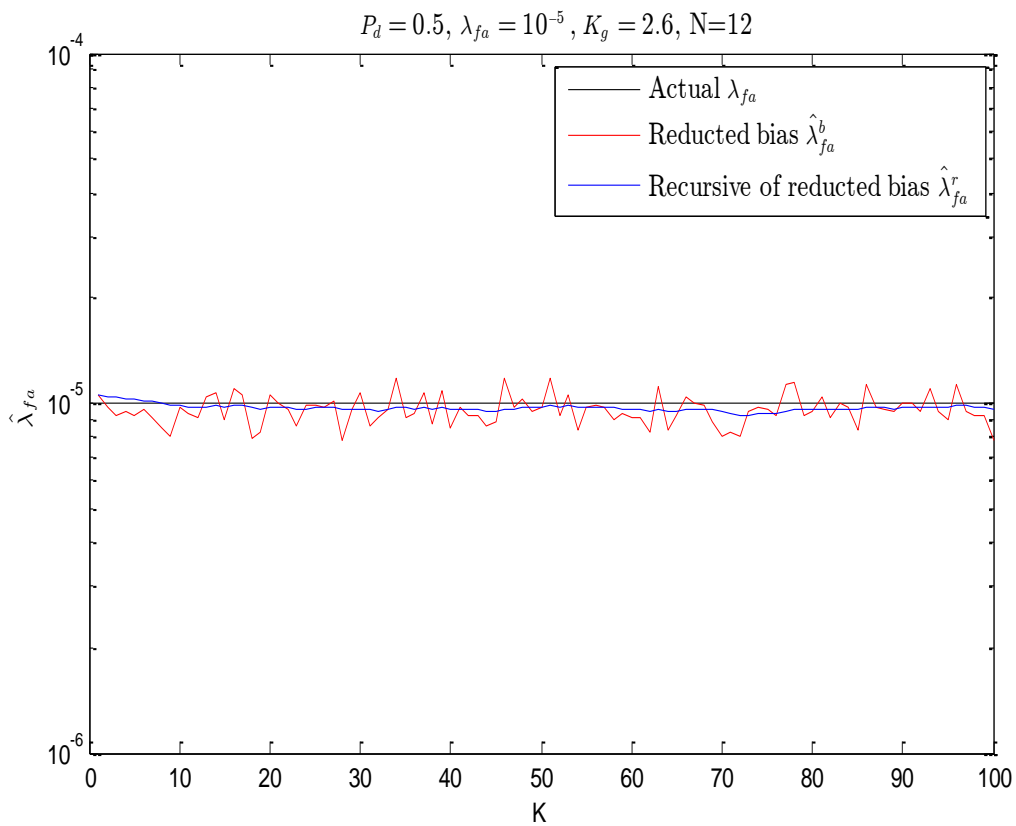
Fig. 4-31: Recursive estimation of density of false alarms at
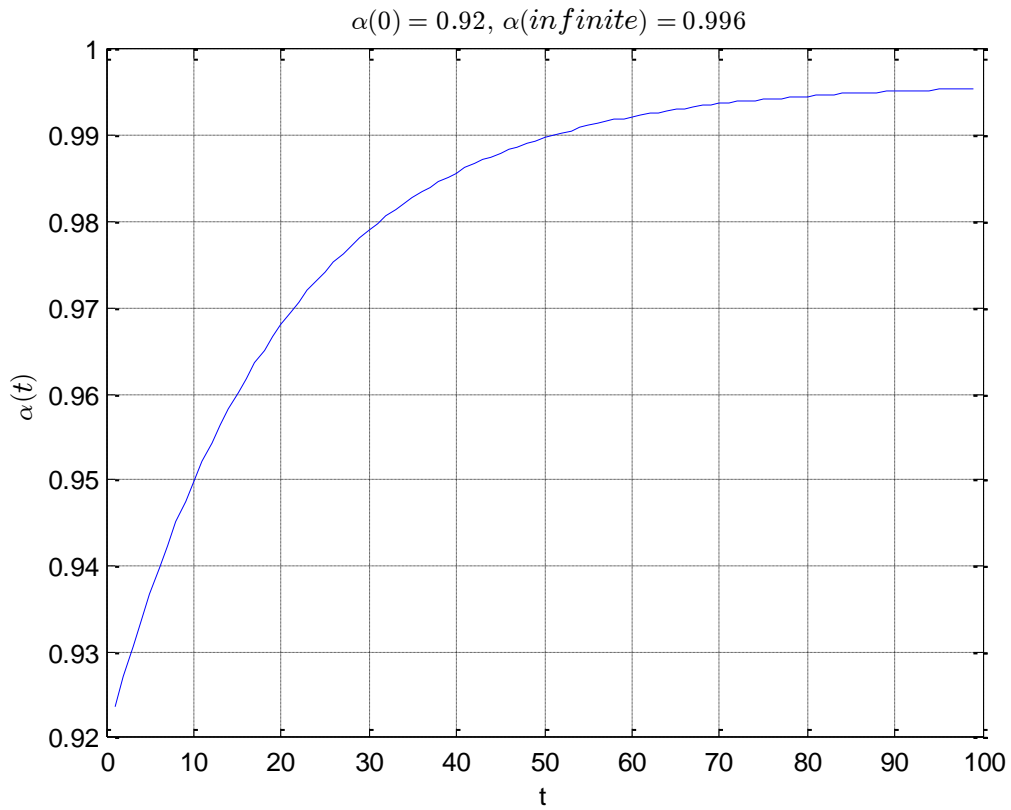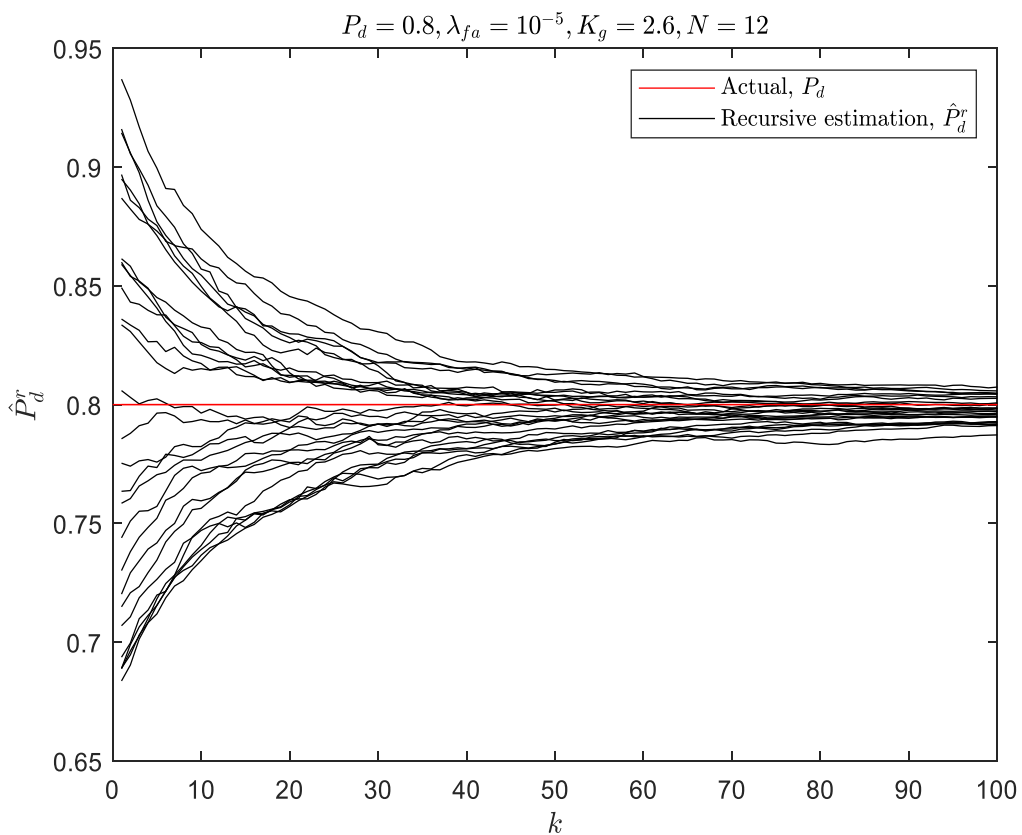fixed actual $P_d = 0.5$ and $\lambda_{fa} = 10^{-5}$
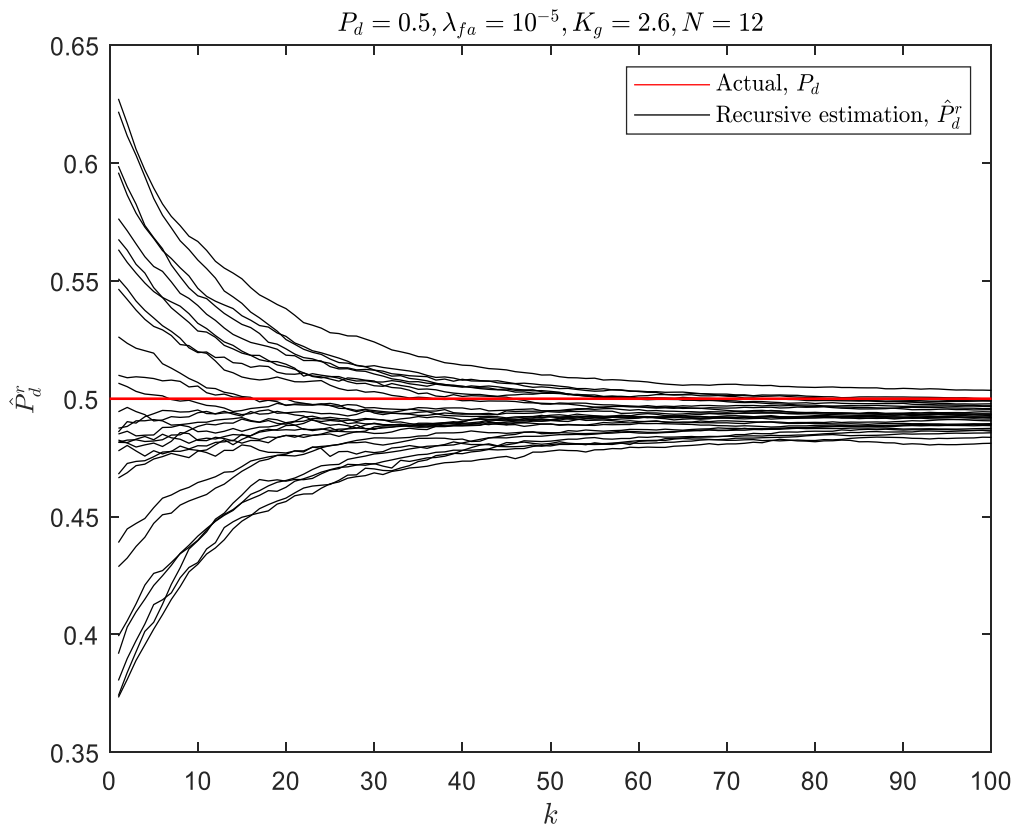
Fig. 4-32: Recursive estimation of probability of detection at fixed actual $P_d = 0.5$ and $\lambda_{fa} = 10^{-5}$ for different initial conditions
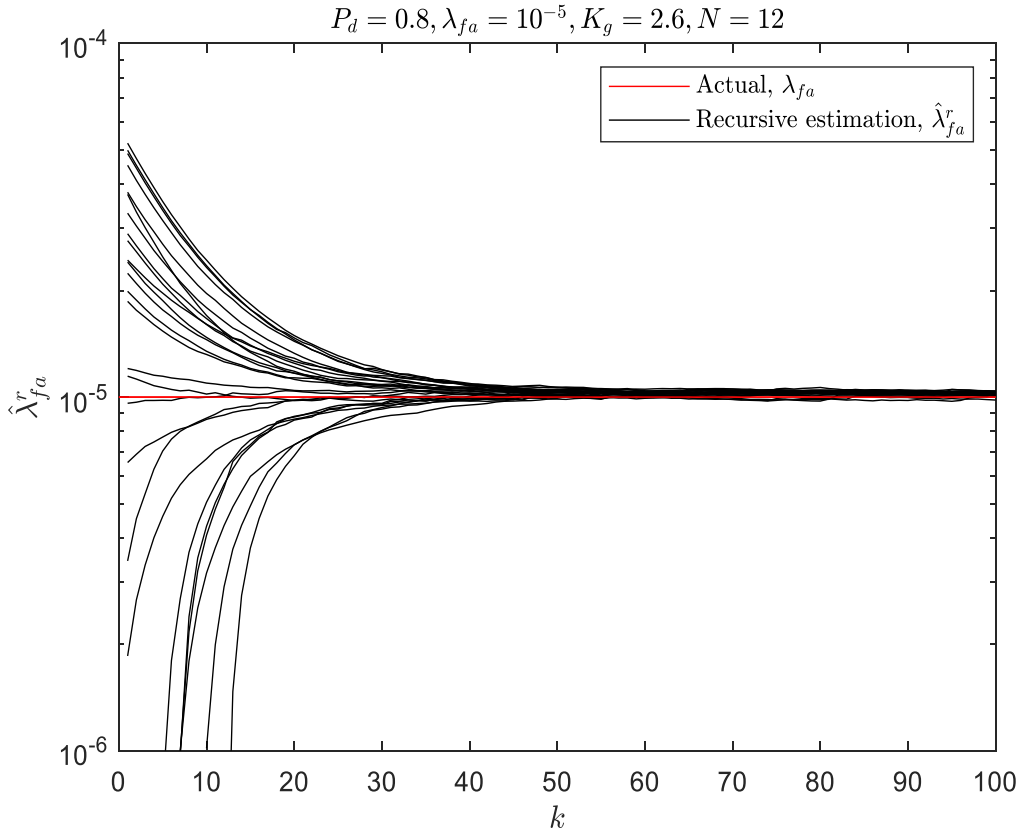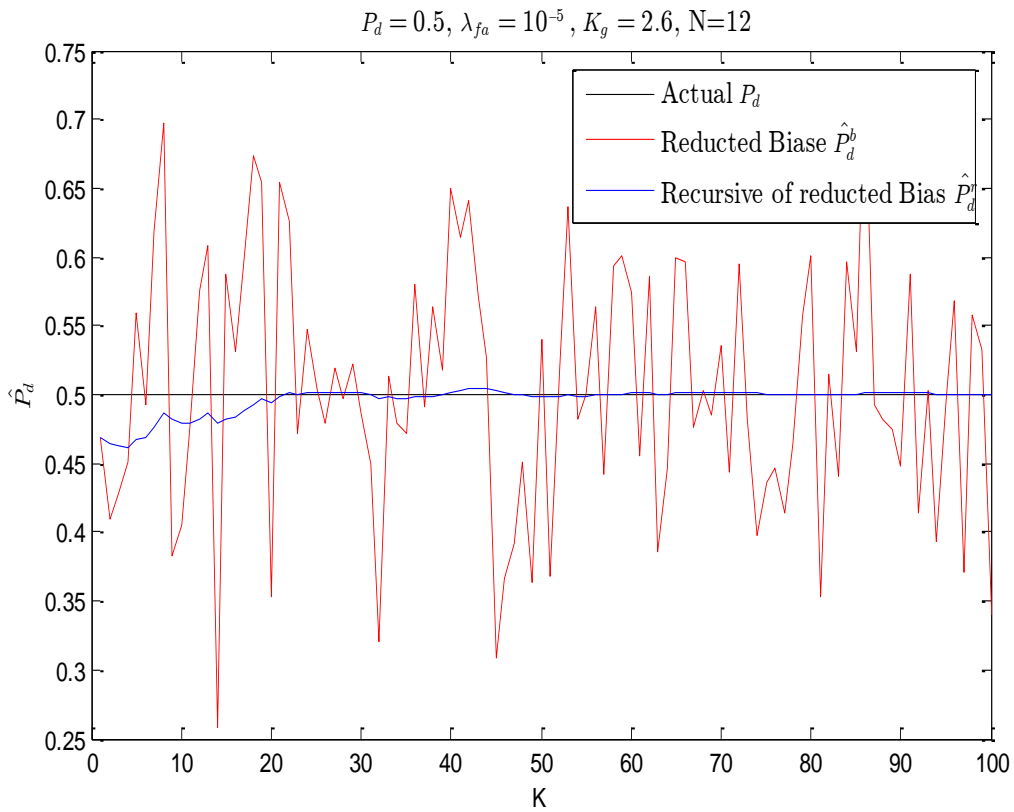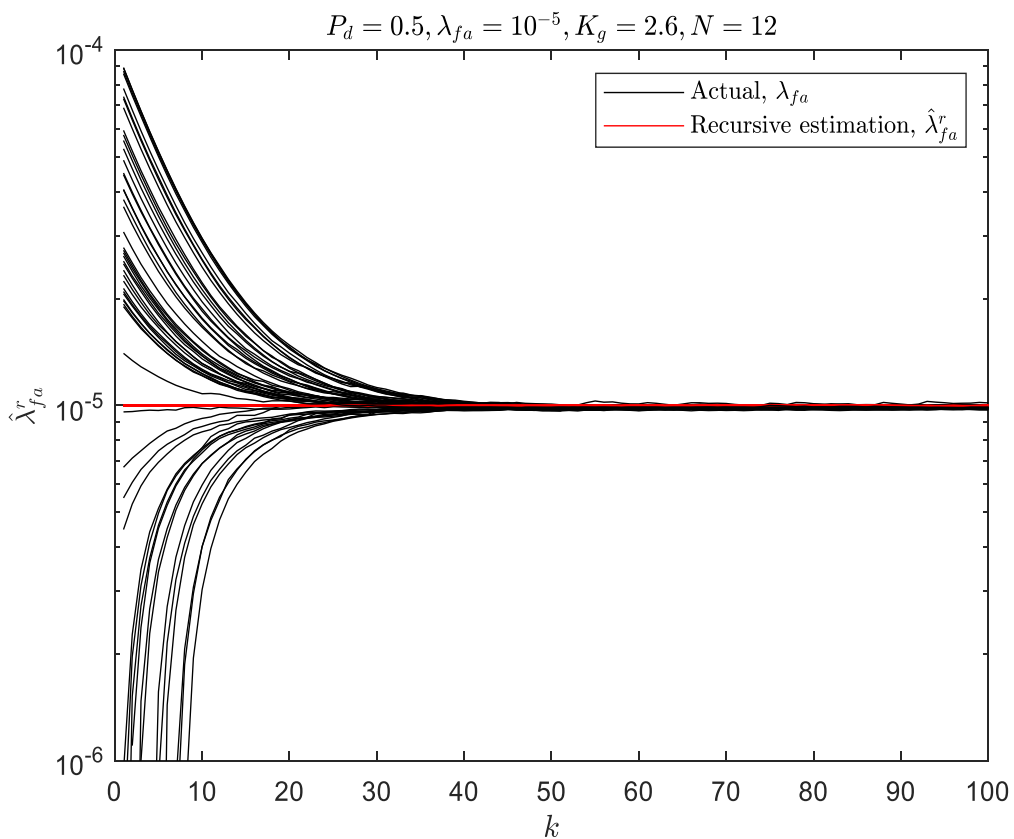

Fig. 4-33: Recursive estimation of density of false alarms at fixed actual $P_d = 0.5$ and $\lambda_{fa} = 10^{-5}$ for different initial conditions

4.6   Statistics of the estimated parameters

In order to confirm the previous analyses, the figures Fig. 4-34 and Fig. 4-35 illustrate the mean value $E[\hat{P}_d^r]$ and the standard deviation $Std[\hat{P}_d^r]$ of the recursive estimated probability of detection for an actual probability of target detection $P_d = 0.5$ and density of false alarms $\lambda_{fa} = 10^{-5}$ during 100 scans. It can be noted that the bias is although present but not significant, this result is consistent with the analysis shown in Fig. 4-19.

In other words, the recursive form did not undermine the improvement achieved by bias reduction in the estimated probability of detection $\hat{P}_d^c$.

Also, both figures Fig. 4-36 and Fig. 4-37 illustrate the mean value $E[\hat{\lambda}_{fa}^r]$ and the standard deviation of the recursive estimated density of false alarm $Std[\hat{\lambda}_{fa}^r]$ for an actual probability of target detection $P_d = 0.5$ and density of false alarms $\lambda_{fa} = 10^{-5}$ during 100 scans. Also note that the bias exists but not significant, this result is consistent with the analysis shown in Fig. 4-20. In other words, the recursive form did not undermine the improvement achieved by bias reduction in the estimated density of false alarms $\hat{\lambda}_{fa}^c$.

On the other hand, the positive effect of the variance reduction procedure is evident in both figures Fig. 4-35 and Fig. 4-37. The standard deviation in the non-recursive estimators for both parameters was about 49% for the probability of detection, as in Fig. 4-3, and around 100% for the density of false alarm, as in Fig. 4-5, now significantly decreased for each of these parameters. This indeed confirms an improved quality of the estimators. In other words, even though the form of the proposed estimator is simple, which is one of its advantages, the main shortfalls can easily be eliminated, as shown in the figures.
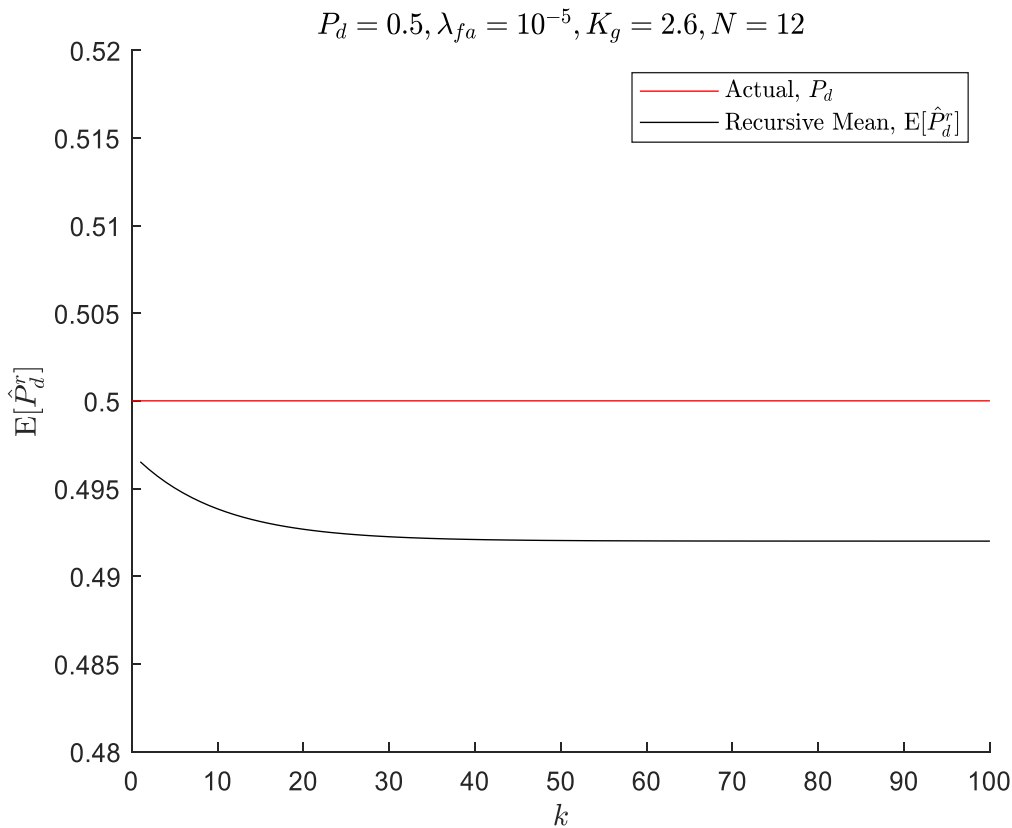
Fig. 4-34: Mean value of recursive estimates of the probability of target detection
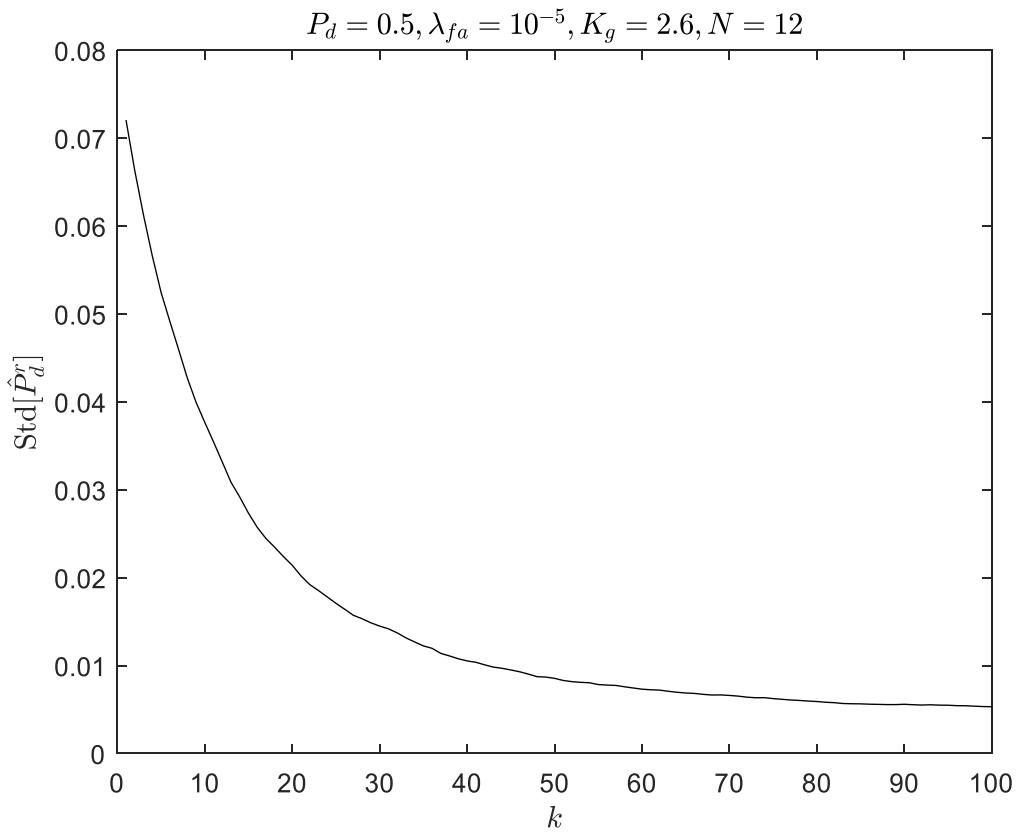
Fig. 4-35: Standard deviation of recursive estimates of the probability of detection.
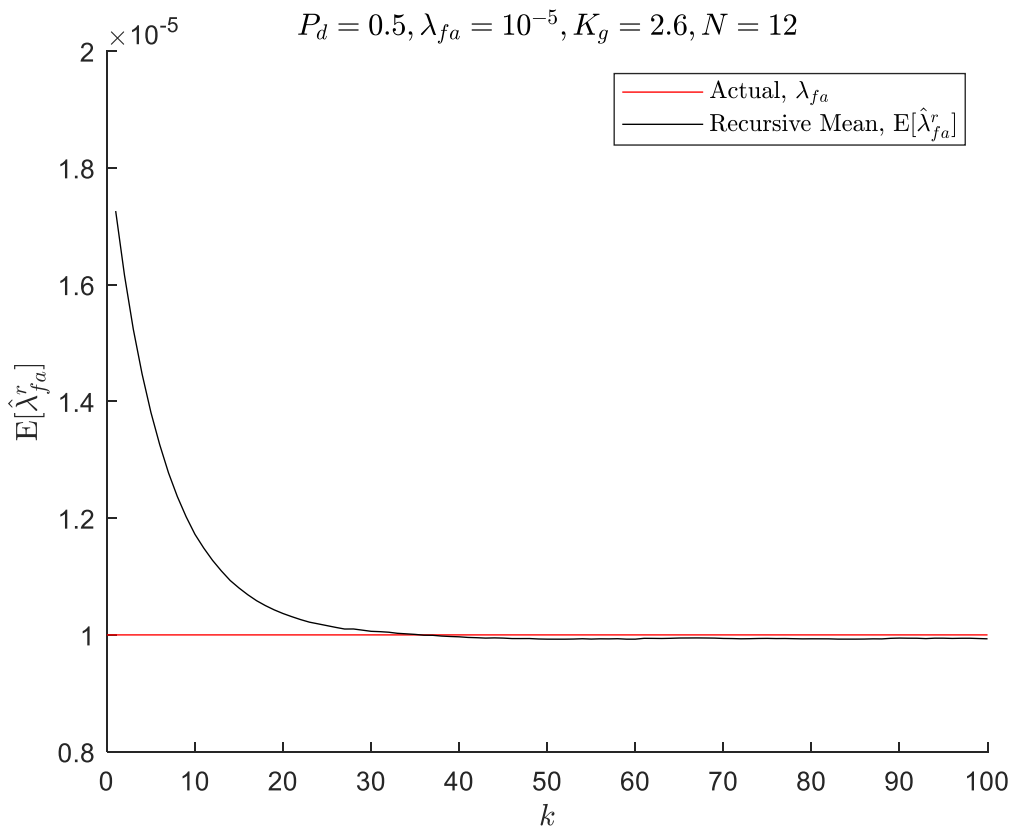
Fig. 4-36: Mean value of recursive estimates
of the density of false alarm.

$$P_d = 0.5, \lambda_{fa} = 10^{-5}, K_g = 2.6, N = 12$$
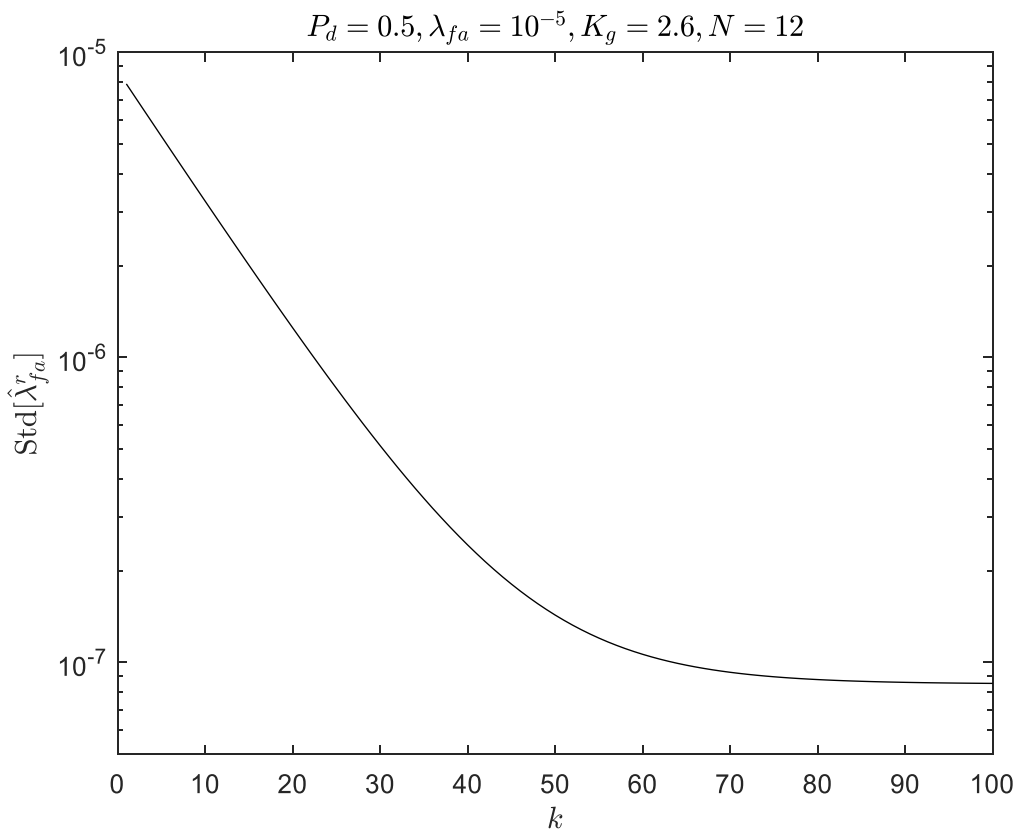
Fig. 4-37: Standard deviation of recursive estimates
of the density of false alarm

4.7   Estimator sensitivity analysis

The technique of estimation of the probability of detection and density of false alarms described in the previous sections of this chapter is highly effective and much simpler than other techniques available in the literature.

Behavior of the new proposed algorithm for different initial conditions and the covariance matrix R is known are displayed in the figures (Fig. 4-28, Fig. 4-29, Fig. 4-32, and Fig. 4-33) for the two values of probability of detection ($P_d = 0.8$ and $P_d = 0.5$) with a fixed density of false alarms ($\lambda_{fa} = 10^{-5}$), gate size ($K_g = 2.6$), length of sequence ($N = 12$), and from these figures it is evident that the estimation is improved and converges to the correct values as the number of scans are increased.

It would be interesting to analyze how the possible error in the prediction covariance matrix influences the performance of the estimation algorithm. These errors are generally caused by unknown or erroneous information about the covariance matrix of measurement noise.

The behavior of the algorithm when the covariance matrix R is unknown is shown in the figures (Fig. 4-38 and Fig. 4-39).

It is evident that it has a significant bias. For this reason, in a case of an unknown measurement noise covariance matrix, it is necessary to adapt the original proposed approach with the estimates of the measurement noise covariance matrix in each scan to enhance the convergence and remove the bias.

87
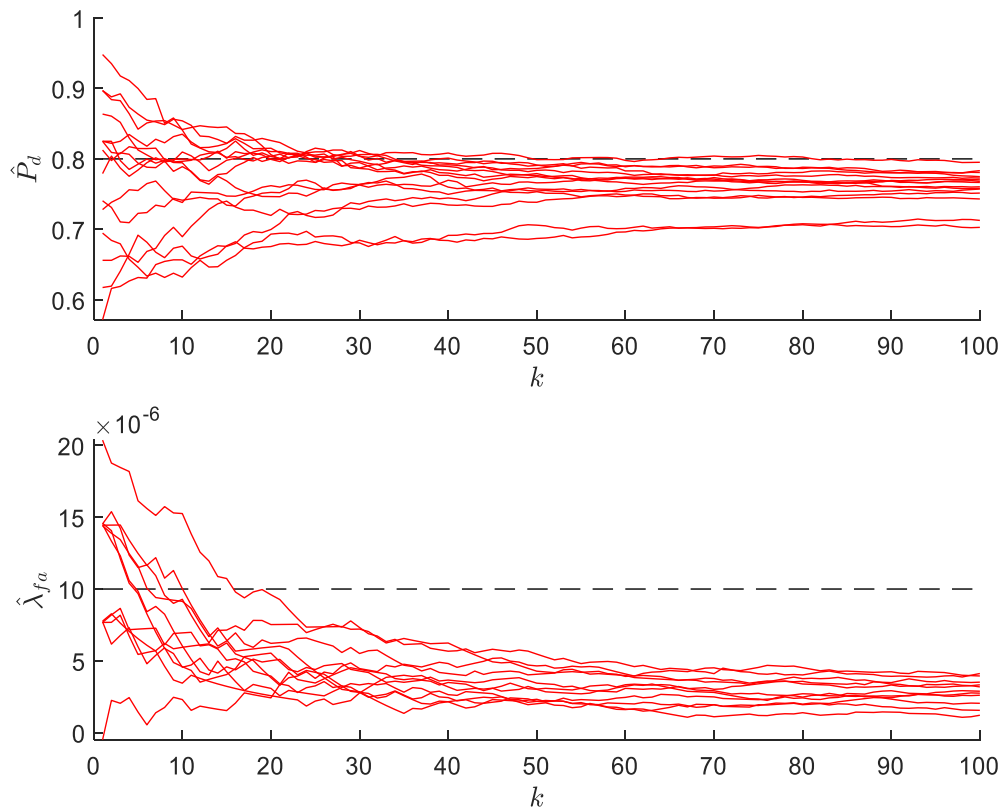
Fig. 4-38: Estimation results for the probability of detection and density of
false alarms when the measurement noise matrix is unknown
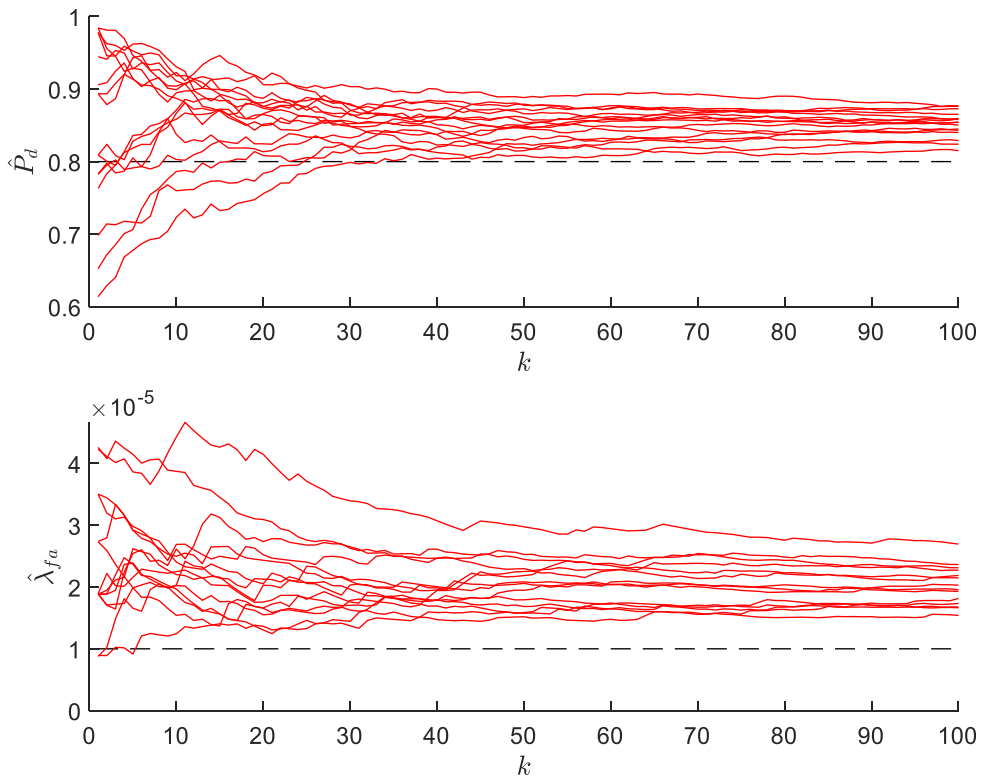
Fig. 4-39: Estimation results for the probability of detection and density of
false alarms when the measurement noise matrix is unknown

4.8 Estimator adaptation

The previous section demonstrates the sensitivity of a two-step GML approach estimator to unknown measurement noise statistics and, therefore, erroneous covariance error prediction matrix of a model described in (4.1) and (4.2). Since the prior knowledge about the measurement noise is not known, the goal is to estimate the measurement noise simultaneously with tracking parameters [69]. The equation (4.2) is used to define the residual as:

$$r(k) = y(k) - H\hat{x}(k \mid k-1), \tag{4.43}$$

$$y(k) = Hx(k) + v(k), \tag{4.44}$$

where $r(k)$ is the residual vector, $y(k)$ is the measurement vector.

The covariance matrix of the residual is

$$E\{r(k)r^T(k)\} = C_r = R + HS(k \mid k-1)H^T. \tag{4.45}$$

The measurement noise covariance matrix can be estimated as:

$$\hat{R} = \hat{C}_r - HS(k \mid k-1)H^T, \tag{4.46}$$

where: $\hat{R}$ is the estimated measurement covariance matrix, $S(k \mid k-1)$ is the covariance matrix of prediction error, $\hat{C}_r$ is the estimated residual covariance matrix, and obtained as follows.

From the two equations (4.43) and (4.44), the residual vector will be as (4.47).

$$r(k) = H x(k) + v(k) - H \hat{x}(k \mid k-1), \tag{4.47}$$

$$r(k) = v(k) - H(x(k) - \hat{x}(k \mid k-1)), \tag{4.48}$$

$$r(k) = v(k) + H\tilde{x}(k \mid k-1), \tag{4.49}$$

$$C_r = Cov(v(k) + H\tilde{x}(k \mid k-1)), \tag{4.50}$$

$$C_r = E\left[[v(k) + H\tilde{x}(k \mid k-1)][v(k) + H\tilde{x}(k \mid k-1)]^T\right], \tag{4.51}$$

$$\text{cov}(r(k)) = E\begin{bmatrix} v(k)v^T(k) + v(k)[H\tilde{x}(k \mid k-1)]^T + \\ H\tilde{x}(k \mid k-1)v^T(k) + H\tilde{x}(k \mid k-1)[H\tilde{x}(k \mid k-1)]^T \end{bmatrix}, \tag{4.52}$$

$$C_r = E\left[v(k)v^T(k)\right] + E\left[v(k)\tilde{x}^T(k \mid k-1)H^T\right] + $$
$$E\left[H\tilde{x}(k \mid k-1)v^T(k)\right] + E\left[H\tilde{x}(k \mid k-1)\tilde{x}^T(k \mid k-1)H^T\right], \tag{4.53}$$

$$C_r = R + \sigma_{v,\tilde{x}}H^T + H\sigma_{\tilde{x},v} + HS(k \mid k-1)H^T, \tag{4.54}$$

$$C_r = R + HS(k \mid k-1)H^T, \tag{4.55}$$

$$\hat{C}_r \approx \frac{1}{N}\sum_{k=K-N+1}^{K} r(k)r^T(k), \tag{4.56}$$

where: C_r is the residual covariance matrix, $\sigma_{v,\tilde{x}}$ is the cross-covariance matrix between ($v(k)$, $\tilde{x}(k \mid k-1)$), R is the covariance matrix of the measurement noise, $S(k \mid k-1)$ is covariance matrix prediction error.

The white measurement noise $v(k)$ is uncorrelated with the prediction error $\tilde{x}(k \mid k-1)$ that is why the correlation coefficient between them is zero.

In order to illustrate the described estimation procedure, the following simulation has been performed.

The assumed model has a vector $x(k)$ of four states, which are the spatial coordinate (x) with its velocity and the spatial coordinate (y) with its velocity. The measurement is updated in each scan, the measurement covariance matrix $(\hat{R})$ is estimated, and after that estimate the two parameters $\hat{P}_d$ and $\hat{\lambda}_{fa}$. By implementing this adaption to the new proposed algorithm, an augmented system is obtained to estimate the measurement noise covariance matrix $(\hat{R})$ simultaneously as well as the probability of detection $\hat{P}_d$ and density of false alarm $\hat{\lambda}_{fa}$ in each scan. The results of the augmented algorithm are shown in Fig. 4-40.

It is clear from Fig. 4-40, that the performance is better than that in the previous case when there was no a priori knowledge about measurement noise covariance matrix.

One can make a comparison in the dynamics of the first case when the measurement noise error covariance matrix is known in advance (R), which shown in both figures (Fig. 4-28 and Fig. 4-29), and the dynamics of the second case which is obtained after estimating the measurement noise covariance matrix $(\hat{R})$ as shown in Fig. 4-40 are as follow :

• The dynamics of convergence in both cases are similar.

The standard deviation in the case of the estimated measurement noise covariance matrix $(\hat{R})$ is somewhat higher than that of the case when the measurement noise covariance matrix is known (R) in advance.

Fig. 4-40: Estimation of the probability of detection and density of false alarms after estimating the measurement noise covariance matrix $(\hat{R})$.
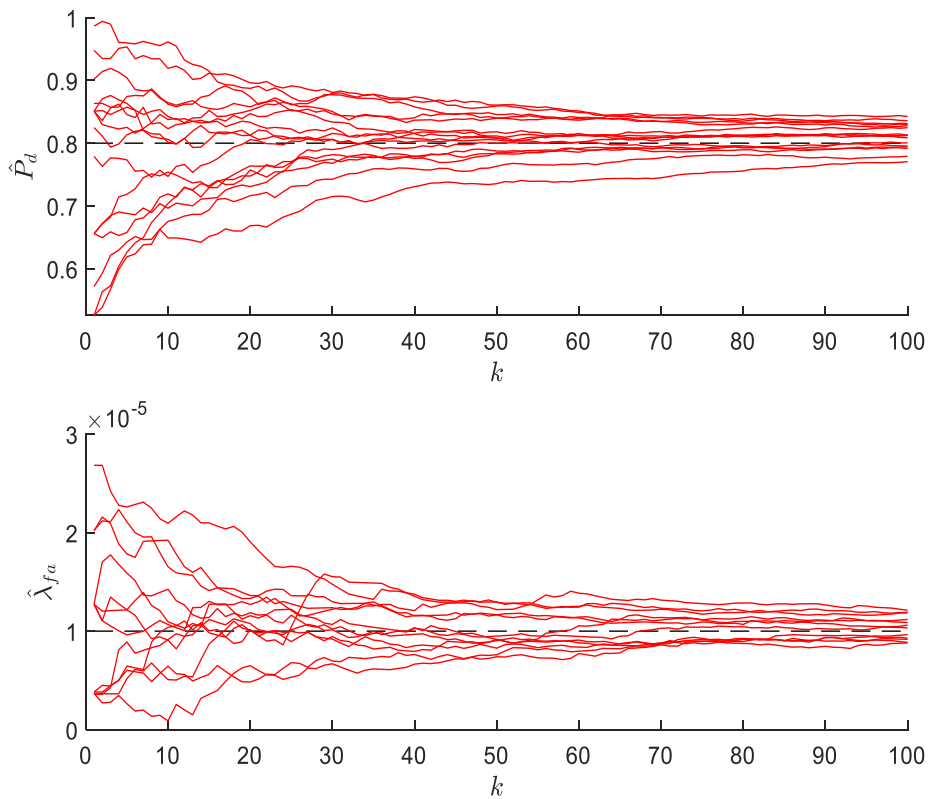
4.9 Estimate of Cramer-Rao Lower Bound

$CRLB$ is a familiar performance evaluation method. In the estimation theory and the statistics, the Cramer Rao Lower Bound ($CRLB$) gives the minimum achievable of variance or standard deviation for an unbiased estimator and provides a useful method for assessing parameter estimation techniques for consistency [70].

For maximum likelihood estimation, one use the logarithm of the measurement density function for a continuous observation or the logarithm of probability mass function for discrete observation to define the log-likelihood function for the unknown parameter.

$$l(\alpha;x) = \begin{cases} \ln fx(x;\alpha) & continous \\ \ln \Pr[X = x;\alpha] & discrete \end{cases}. \tag{4.57}$$

The derivative of the log-likelihood function is used to derive the maximum likelihood estimator, to examine the statistics of the first and the second derivatives of the log-likelihood function, when the data are the random variables that define the observations, specifically the second moment of the first derivative and the first moment of the second derivative.

$$I(\alpha) = E\left[\left(\frac{\partial}{\partial \alpha}l(\alpha;X)\right)^2\right] = -E\left[\frac{\partial^2}{\partial \alpha^2}l(\alpha;X)\right] \tag{4.58}$$

This relationship (4.58) is subject to the condition, that the derivatives and the moments exist. This expectation is called fisher information (*FI*) and important in the study of the estimation theory. In fact, one can show that the mean square error for any unbiased estimator must be greater than or equal to the inverse of fisher information.

$$E[\hat{\alpha}] = \alpha \Rightarrow E\left[(\hat{\alpha} - \alpha)^2\right] \geq \frac{1}{I(\alpha)} \tag{4.59}$$

It is important to keep in mind that $CRLB$ is applied only to unbiased estimation. To apply Cramer-Rao Lower Bound ($CRLB$) for the new proposed estimator, first, compute the *Fisher information matrix* (FIM) that the observations carry about the unknown parameters P_d and λ_{fa}. The FIM is then used to compute the Cramer-Rao Lower Bound on the variance of these two parameters.

Assume for the time being that $N = 1$, i.e., P_d and λ_{fa} are estimated by using only the observations derived from the current scan. Afterward, we will show that the cumulative information contained in a sequence of $N > 1$ scans is approximately just the multiple of the *FI* (*Fisher information*) for one scan. To simplify the notation, λ is introduced to be $\lambda \triangleq \lambda_{fa}V_g$, M is used to denote the random variable defined by the number of observations in the current scan and m to denote the argument of the corresponding probability mass function.

As shown below, it turns out that the FIM for a set of observations received in one scan is completely determined by the cardinality m of this set. This number will be zero if there are no false alarms, and the target is either not detected or found outside the gate. Similarly, there are $m \geq 1$ observations in the following two cases:

1) The target was outside the gate or was not detected at all, and there were m false alarms.

2) The target was inside the gate and was detected, and there were m - 1 false alarm.

The probability of receiving m observations is therefore given by:

$$
p_m(m; P_d, \lambda) =
\begin{cases}
(1 - P_g P_d) e^{-\lambda}. & m = 0 \\[4mm]
\dfrac{(1 - P_g P_d) \lambda^m e^{-\lambda}}{m!} + \dfrac{P_g P_d \lambda^{m-1} e^{-\lambda}}{(m-1)!}. & m \geq 1
\end{cases}
\tag{4.60}
$$

The corresponding log-likelihood is

$$
l(P_d, \lambda) =
\begin{cases}
\ln(1 - P_g P_d) - \lambda, & m = 0 \\[4mm]
\ln(1 - P_g P_d) P_g P_d \\
+ (2m-1) \ln \lambda - 2\lambda - \ln m!(m-1)!, & m \geq 1
\end{cases}
\tag{4.61}
$$

The first and second partial derivatives are

$$
\frac{\partial l(P_d, \lambda)}{\partial P_d} =
\begin{cases}
-\dfrac{P_g}{1 - P_g P_d}, & m = 0 \\[4mm]
-\dfrac{P_g}{1 - P_g P_d} + \dfrac{1}{P_d}, & m \geq 1
\end{cases}
\tag{4.62}
$$

$$
\frac{\partial^2 l(P_d, \lambda)}{\partial P_d^2} =
\begin{cases}
-\dfrac{P_g^2}{(1 - P_g P_d)^2}, & m = 0 \\[4mm]
-\dfrac{P_g^2}{(1 - P_g P_d)^2} - \dfrac{1}{P_d^2}, & m \geq 1
\end{cases}
\tag{4.63}
$$

$$
\frac{\partial l(P_d, \lambda)}{\partial \lambda} =
\begin{cases}
-1 & m = 0 \\[4mm]
\dfrac{2m-1}{\lambda} - 2, & m \geq 1
\end{cases}
\tag{4.64}
$$

$$
\frac{\partial^2 l(P_d, \lambda)}{\partial \lambda^2} =
\begin{cases}
0 & m = 0 \\[4mm]
-\dfrac{2m-1}{\lambda^2}, & m \geq 1
\end{cases}
\tag{4.65}
$$

$$
\frac{\partial^2 l(P_d, \lambda)}{\partial P_d \partial \lambda} = 0.
\tag{4.66}
$$

The Hessian of the log-likelihood is

$$H(m;P_d,\lambda) = \begin{cases} \begin{bmatrix} -\dfrac{P_g^2}{(1-P_gP_d)^2} & 0 \\ 0 & 0 \end{bmatrix}, & m=0 \\[2em] \begin{bmatrix} -\dfrac{P_g^2}{(1-P_gP_d)^2}-\dfrac{1}{P_d^2} & 0 \\ 0 & -\dfrac{2m-1}{\lambda^2} \end{bmatrix}, & m\geq 1 \end{cases}$$ \quad (4.67)

The FIM is the negative expectation of the Hessian:

$$I(P_d,\lambda) = -H(0;P_d,\lambda)p_M(0) - \sum_{m=1}^{\infty} H(m;P_d,\lambda)p_M(m),$$ \quad (4.68)

$$I(P_d,\lambda) = \begin{bmatrix} \dfrac{P_g^2}{(1-p_gP_d)^2} & 0 \\ 0 & 0 \end{bmatrix}(1-P_gP_d)e^{-\lambda} + \sum_{m=1}^{\infty} \begin{bmatrix} \dfrac{P_g^2}{(1-P_gP_d)^2}+\dfrac{1}{P_d^2} & 0 \\ 0 & \dfrac{2m-1}{\lambda^2} \end{bmatrix}$$ (4.69)

$$\times \left(\frac{(1-P_gP_d)\lambda^m e^{-\lambda}}{m!} + \frac{P_gP_d\lambda^{m-1}e^{-\lambda}}{(m-1)!} \right).$$

Next, some intermediate results are derived. Namely, the Poisson probability mass function $\lambda^m e^{-\lambda}/m!$ sums to one, so:

$$\sum_{m=1}^{\infty} \frac{\lambda^m e^{-\lambda}}{m!} = \sum_{m=0}^{\infty} \frac{\lambda^m e^{-\lambda}}{m!} - e^{-\lambda} = 1-e^{-\lambda}.$$ \quad (4.70)

$$\sum_{m=1}^{\infty} \frac{\lambda^{m-1}e^{-\lambda}}{(m-1)!} = \sum_{m=0}^{\infty} \frac{\lambda^m e^{-\lambda}}{m!} = 1 .$$ \quad (4.71)

The mean of the Poisson distribution is λ, which yields:

$$\sum_{m=1}^{\infty} m\frac{\lambda^m e^{-\lambda}}{m!} = \sum_{m=0}^{\infty} m\frac{\lambda^m e^{-\lambda}}{m!} = \lambda,$$ \quad (4.72)

$$\sum_{m=1}^{\infty} m\frac{\lambda^{m-1}e^{-\lambda}}{(m-1)!} = \sum_{m=0}^{\infty} (m+1)\frac{\lambda^m e^{-\lambda}}{m!} = \lambda+1.$$ \quad (4.73)

Using the above results, we have:

$$\sum_{m=1}^{\infty} \left(\frac{(1-P_gP_d)\lambda^m e^{-\lambda}}{m!} + \frac{P_gP_d\lambda^{m-1}e^{-\lambda}}{(m-1)!} \right) = (1-P_gP_d)(1-e^{-\lambda})+P_gP_d,$$ \quad (4.74)

$$\sum_{m=1}^{\infty} m \left(\frac{(1-P_g P_d)\lambda^m e^{-\lambda}}{m!} + \frac{P_g P_d \lambda^{m-1} e^{-\lambda}}{(m-1)!} \right) = (1-P_g P_d)\lambda + P_g P_d (\lambda+1). \tag{4.75}$$

$$\sum_{m=1}^{\infty} m \left(\frac{(1-P_g P_d)\lambda^m e^{-\lambda}}{m!} + \frac{P_g P_d \lambda^{m-1} e^{-\lambda}}{(m-1)!} \right) = \lambda + P_g P_d. \tag{4.76}$$

Substituting into (4.69) gives the following expressions for the entries of the Fisher information matrix:

$$l_{11}(P_d,\lambda) = \frac{P_g^2 e^{-\lambda}}{1-P_g P_d} + \left(\frac{P_g^2}{(1-P_g P_d)^2} + \frac{1}{P_d^2} \right) \tag{4.77}$$

$$\times ((1-P_g P_d)(1-e^{-\lambda}) + P_g P_d),$$

$$l_{22}(P_d,\lambda) = \frac{1}{\lambda^2}(2\lambda + P_g P_d - (1-P_g P_d)(1-e^{-\lambda})), \tag{4.78}$$

$$l_{12}(P_d,\lambda) = l_{21}(P_d,\lambda) = 0. \tag{4.79}$$

Up to now, we have considered only the information contained in the cardinality m of the set of received observations and have disregarded the concrete values $z_1,...,z_m$ of these observations. Now we want to show that these values carry no additional information about P_d and λ_{fa}. Let $f(z)$ denote the predictive Gaussian probability density function, as before. The probability that the i-th observation z_i belongs to the actual target is provided by

$$P_g P_d \frac{\lambda^{m-1} e^{-\lambda}}{(m-1)!} \frac{1}{V_g^{m-1}} f(x_i). \tag{4.80}$$

While the probability that all observations are caused by false alarms is expressed through

$$(1-P_g P_d) \frac{\lambda^m e^{-\lambda}}{m!} \frac{1}{V_g^m}. \tag{4.81}$$

The total probability of observing $z_1,...,z_m$ for $m \geq 1$ is

$$p(z_1,..,z_m; P_d,\lambda) = (1-P_g P_d) \frac{\lambda^m e^{-\lambda}}{m!} \frac{1}{V_g^m}$$

$$+ P_g P_d \frac{\lambda^{m-1} e^{-\lambda}}{(m-1)!} \frac{1}{V_g^{m-1}} \sum_{i=1}^{m} f(z_i). \tag{4.82}$$

Obviously, the log-likelihood is (up to an additive constant) the same as in (4.61). Therefore, the derived FIM retains the same values even if the positions of the observations are not considered.

Next, we consider the case when data from $N > 1$ scans are used to estimate the probability of detection P_d and density of false alarms λ_{fa}. Assuming that the probability of gating $P_g = 1$ and that exactly one target is present (but not necessarily observed) in each scan, the joint probability of the sets of observations from each scan is simply the product of the probabilities of individual observation sets since target detections and false alarms are independent events across scans. Consequently, the cumulative FIM is just the FIM for one individual scan multiplied by N, at least,

under the stated assumptions. In reality, we have $P_g < 1$ and possibly more than one target. Consequently, the derived result holds only approximately.

The CRLB of an unbiased estimator is given by the inverse of the derived FIM. However, the CRLB depends on the actual bias in the case of a biased estimator. The proposed estimator is comprised of a two-step maximization algorithm: firstly, the likelihood of each hypothesis is maximized with respect to the probability of detection P_d and density of false alarms λ_{fa}, and the hypothesis with the largest maximized likelihood is selected. Consequently, the derivation of the expression for estimation bias is complicated and will not be considered in further discussion. Finally, the CRLB is roughly approximated as $I^{-1}(P_d, \lambda)$. As shown in the plot below Fig. 4-41, the estimator variance is somewhat higher than the approximate CRLB, even with the proposed variance reduction techniques.
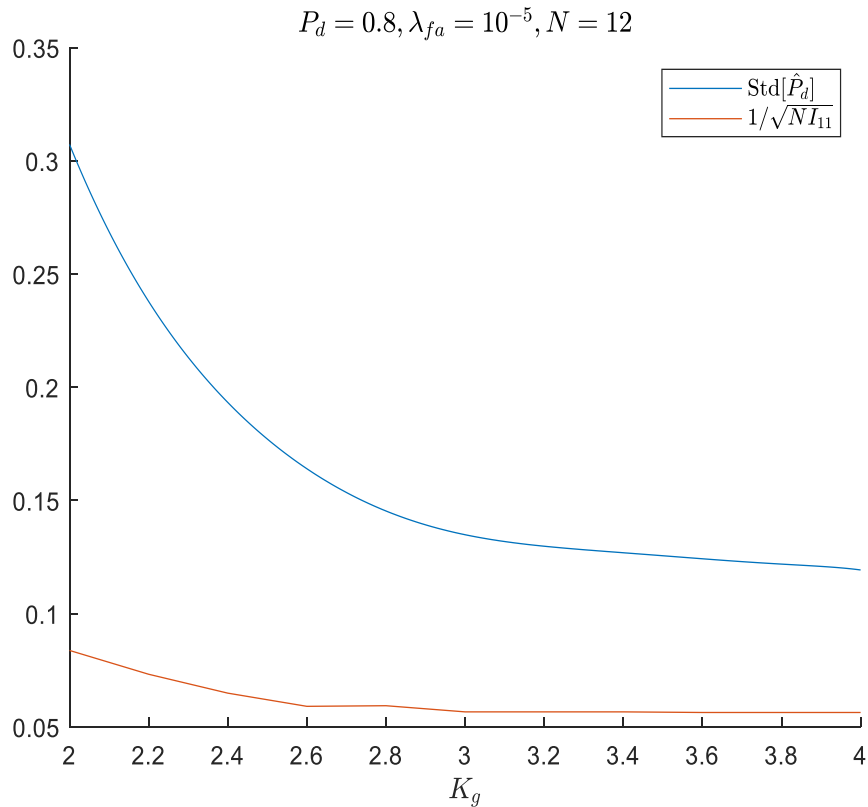
Fig. 4-41: Comparison of Cramer-Rao lower bound and experimentally determined standard deviation of $\hat{P}_d$

4.10 On the efficiency of the proposed approach

Two criteria are utilized to assess the efficiency of the target tracking system that utilizes the estimated parameters from the proposed algorithm. The first criterion is the mean square error, which is defined as the distance between the position of the moving target and the predicted target position. The second criterion is the processing time, which is the time needed by the tracking system to complete the execution of the observed data in one scan.

Efficiency of the new proposed algorithm using the first criterion was illustrated by conducting two simulations. The first simulation assumes that the two parameters P_d and λ_{fa} are constants, and known in advance with some uncertainty (algorithm A1), while the second simulation utilizes the estimated parameters $\hat{P}_d^c$ and $\hat{\lambda}_{fa}^c$ from the new proposed algorithm

95

(algorithm A2). Both simulations use the JPDA data association and the standard Kalman filter for tracking purpose. The performance of the tracking system is analyzed by the mean of the accumulative RMSE (root-mean-square error), given by (4.83).

$$J(k) = \sqrt{\frac{1}{k} \sum_{i=1}^{k} d^2(i)} \ , \qquad (4.83)$$

where $d^2(i)$ represents the Euclidian distance between the position of the moving target and its estimation in the $i-th$ scan.

The simulation scenario has been divided into three portions, and each portion is composed of 100 scans with its specific probability of detection P_d. During the first portion, the probability of detection was $P_d = 0.9$, in the second portion was $P_d = 0.6$, and in the last portion was $P_d = 0.8$. Algorithm A1 utilizes a constant probability of detection $P_d = 0.8$. The plot is very interesting due to three striking effects. The first gives an impression of the extent to which the tracking performance is degraded by the reduction in the probability of target detection. In this sense, probably the most informative period is after the first portion when the probability of detection falls from 0.9 to 0.6. The second effect shows that the proposed algorithm A2 has its own dynamics and, subsequently, some time is needed to detect the change in the estimated parameter. This dynamic can be changed by changing the τ parameter, but this affects the estimation variance, as already mentioned. Finally, perhaps the most important visible effect is the benefit obtained by applying the proposed estimation technique. As expected, the benefit is more noticeable if the difference between the true and the assumed value of the parameter is greater.
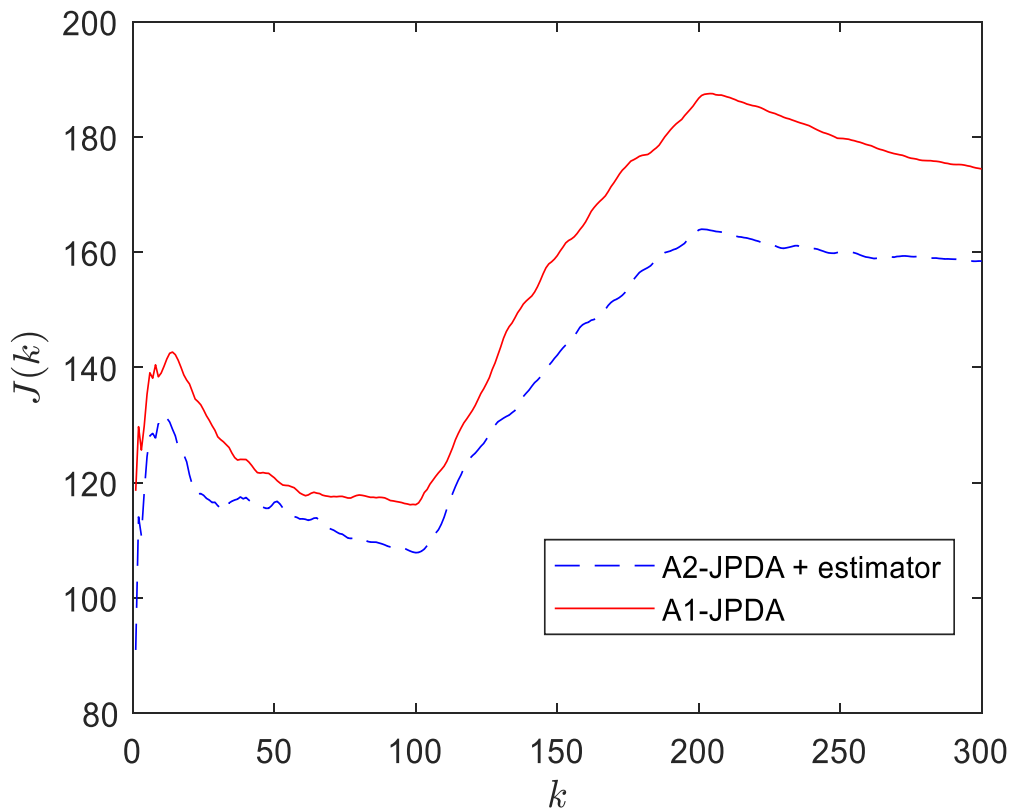

Fig. 4-42: Cumulative RMSE measure for algorithms A1 (with constant parameters) and A2 (with adaptive parameters)

The second criterion used to assess the tracking algorithm is the numerical complexity. Processing time is used as a measure of numerical complexity, with algorithms being implemented on the same computer platform under identical conditions.

Comparative analysis to illustrate the computational complexity of the existing algorithm (CPHD filter) [4, 9, 10], which has become quite popular in the recent years and the new proposed algorithm for estimating the unknown parameters, where JPDA approach [55,9] is used for data association. As expected, the obtained results show that the computational complexity of the algorithm depends to a great extent on the probability of detection as well as the density of false alarms.

Fig. 4-43 shows the processing time of both algorithms depending on the probability of detection P_d, the constant density of false alarms λ_{fa}, and Fig. 4-44 shows the processing time of both algorithms depending on the density of false alarm λ_{fa} with a constant probability of detection.

The simulation has included in its scope five moving targets in a maneuver during 100 scans, where each simulation is repeated 100 times to obtain the average processing time for an individual realization. Fig. 4-43 shows the processing time of both algorithms when the density of false alarm is constant ($\lambda_{fa} = 2.5 \times 10^{-6}$), and the probability of target detection is varying ($P_d \epsilon \{0.5, 0.55, 0.6, ..., 0.9\}$). On the other hand, Fig. 4-44 displays the average processing time of both algorithms when the probability of target detection is constant ($P_d = 0.8$), and the density of false alarms is varying ($\lambda_{fa} \epsilon \{0.1 \times 10^{-5}, \ 0.5 \times 10^{-5}, \ 10^{-5}\}$).

The overall conclusion of this analysis is that the newly proposed method with the JPDA data association has lower numerical complexity than the CPHD filter. The interesting feature can be seen in Fig. 4-43, which refers to the fact that with the increase of the probability of target detection, the numerical complexity of the new proposed algorithm is increased, while CPHD filter numerical complexity is decreased. The reason for this phenomenon is that the CPHD filtering process is simplified with the increase of the probability of target detection, whereas in the number of hypotheses that the new proposed filter takes into account increases. Fig. 4-44 also shows that the CPHD filter is susceptible to an increase in the density of false alarm due to an increase in the cardinality of the random finite set. On the other hand, the new proposed algorithm is much less susceptible to the increase of this parameter due to all false observations, regardless to the number of observation within the gate, because it takes in to account only the nearest observation to the predicted target position, neglect the rest false observations and slightly increase in numerical processing time as shown in Fig. 4-44 due to increase in complexity of JPDA data association procedure.

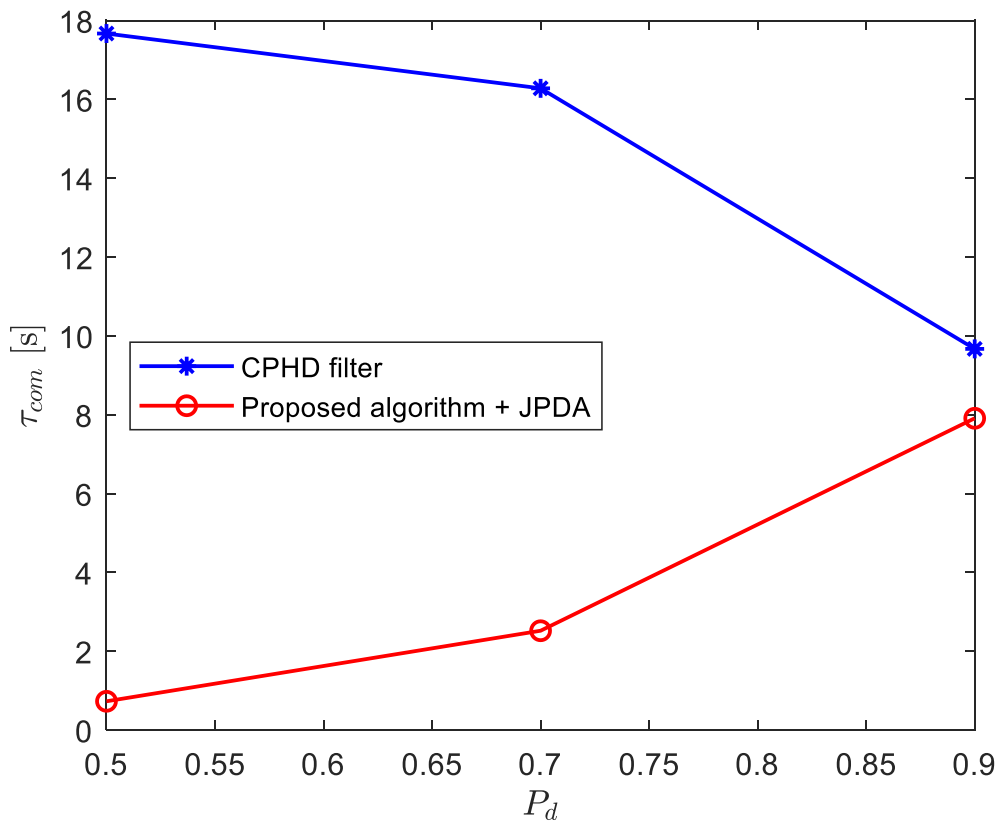Fig. 4-43: Processing time of the algorithms depending on the probability of detection with a constant density of false alarms ($\lambda_{fa} = 2.5 \times 10^{-6}$)
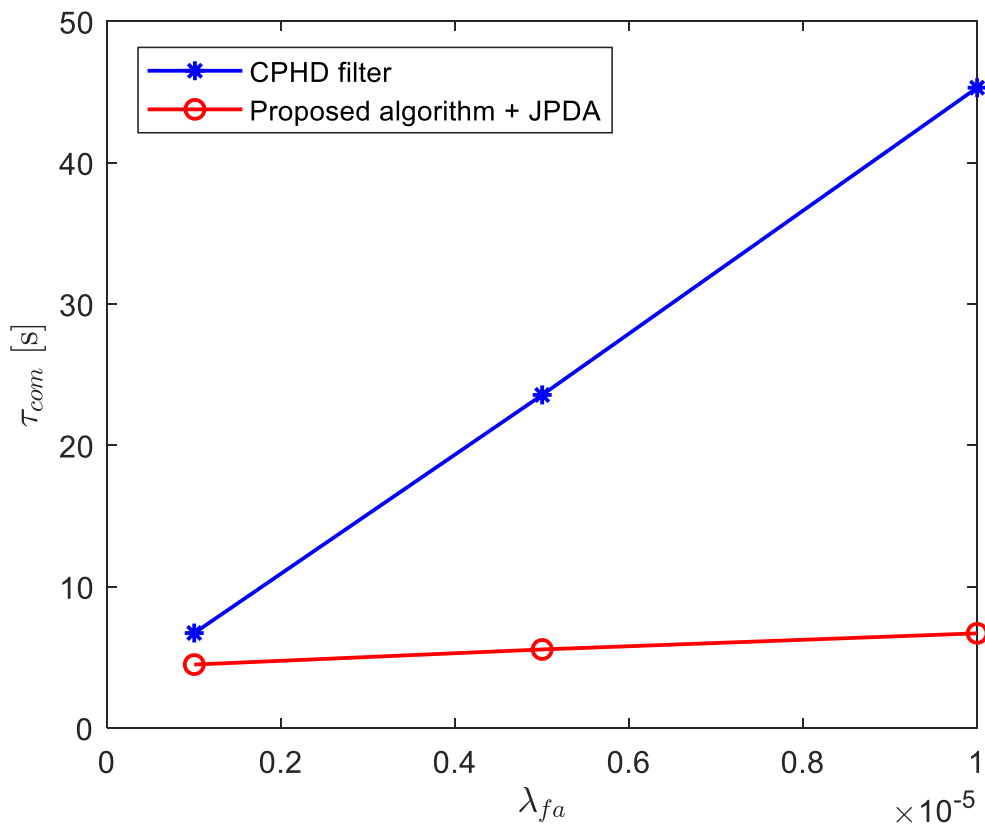

Fig. 4-44: Processing time of the algorithms depending on the density of false alarms with a constant probability of detection ($P_d = 0.8$)

4.11 Constraints of the new proposed algorithm

The increase of density of false alarm λ_{fa} degrades the performance of all the existing techniques for data association and the estimation of the probability of target detection. For very high clutter densities, the only reasonable approach might be to assume that P_d is known and to estimate only λ_{fa}.

I aimed to derive an upper limit of density of false alarm λ_{fa} above which the proposed estimation procedure "breaks down". One felt that such a measure would establish an interesting criterion for the comparison of various existing techniques. Also one can offer the following (perhaps unconventional) comment: there seems to be quite a lot of competition among manufacturers of guided missiles in terms of the lowest permissible flight altitudes since such extreme conditions require careful optimization of both hardware and software resources in order to attenuate the effects of disturbances.

While analyzing the proposed algorithm, one can notice that the zero integral hypotheses exhibited the highest likelihood by far, such that the estimated probability of target detection is equal to zero. It is difficult to find the threshold value of λ_{fa} at which this occurs, but it is reasonable to assume that it occurs when the likelihood H_j^0 and H_j^1 converge:

$$\frac{\lambda_{fa}^{M_j}}{M_j!} \approx \frac{\lambda_{fa}^{M_j-1} e^{-\lambda_{fa} V_g}}{(M_j-1)!} \frac{1}{\sqrt{(2\pi)^n \det(S[j \,|\, j-1])}} . \tag{4.84}$$

After simplifications, the equation (4.84) is reduced to the next equation (4.85).

$$\lambda_{fa} \approx \frac{1}{\sqrt{(2\pi)^n \det(S[j \,|\, j-1])}} , \tag{4.85}$$

where the best case $d = 0$ was used for the statistical distance of the nearest detected target from the prediction and detection probability $P_d = 0.5$.

The last expression is not informative because the critical density of false alarms on the number of false alarms within the gate and determinant of the covariance matrix. If (4.85) is simplified further, and the average value $\lambda_{fa} V_g$ is used instead of the number of detections M_j, and volume of the rectangular gate is $V_g = (2K_g\sigma_1)(2K_g\sigma_2)...(2K_g\sigma_n)$, where σ_i, $i = 1,...,n$ are the diagonal elements of the covariance matrix $S[j \,/\, j-1]$, the result proposes that the critical time for applying this method is related to the size of the gate K_g.

$$K_g \approx (\frac{\pi}{2})^{0.5} . \tag{4.86}$$

However, this condition is derived from a series of approximations. Moreover, one could not arrive to a general condition for the applicability of the proposed method.

Chapter Five

Conclusion

Moving target tracking became a particular topic of interest and grew over the past decades. At first, the motivation for developing these algorithms has been solely for military purposes, but later their applicability has significantly increased to civilian areas. Many literature sources describe different structures of target tracking systems, various solutions for target state estimation filters, and several algorithms for the measurement-to-track associations. All these concepts, however, share one characteristic, that their efficiency is mainly dependent on the knowledge of the probability of target detection and density of false alarms. This can be quite a drawback due to the fact that these statistical parameters are usually unknown and it is difficult to estimate them. Because these parameters are unknown and non-stationary in both time and space. The importance of this problem has been described in many literatures, where they stated that the exact knowledge of the probability of detection and density of false alarm is crucial for good behavior of the modern target tracking filters. There have been many attempts to estimate these parameters, and many valuable results in this regard are reported by many researchers as mentioned in the previous chapters. However, these results suffer from a set of defects such as it is sensitivity to an initial value of the filter, estimation in wide surveillance region, some approaches did not estimate the probability of detection, even that probability is not estimated for a particular target, most of the proposed algorithms depend on specific data association approach, and the numerical complexity of the algorithms are very high.

Finally, available estimators are highly demanding, because of the number of needed mathematical operations in real-time or the complexity of expressions that have to be computed.

This research proposes an approach for estimating the probability of detection of a single target as it moves in a cluttered environment, along with the estimation of the density of false alarms in its immediate vicinity.

The new proposed algorithm is based on a generalized maximum likelihood principle (GML). Apart from computing the likelihood of each of the generated hypotheses, their number of generated hypotheses was decreased (no more than two particular hypotheses in each scan) in order to drive down the numerical complexity of the approach. The form of the proposed estimator is much simpler than in other available techniques. The main advantage of this approach is that the estimation of density of false alarm is not based on a set of measurements from a wide region in which the target moves, but on the measurements from a gate located around the predicted target position, and contrary to other methods reported in the previous literature, which mostly estimate the clutter density in a wide surveillance areas. Another advantage is that the new proposed approach does not require a specific form of data association. So that it can be used in parallel with any moving target tracking algorithm or a general estimator of the detection profile and clutter environment.

It was shown that the simplicity of the estimators was on account of considerable bias, which is inherent in nearly all similar techniques reported in the literature, but also a relatively large estimator variance.

This research proposed and experimentally verified ways of overcoming these shortfalls. Namely, estimator bias compensation was proposed to reduce the bias, which is a linear function of the gate size, the estimated probability of target detection and the estimated density of false alarm, where all the regression model parameters are determined by applying the least square method. This modification resulted in the nearly total elimination of bias relative to the original. The other proposed estimator modification is related to estimator variance reduction accomplished by introducing recursive estimation of the probability of detection and density of false alarm. Special attention was devoted to the time profile of the forgetting factors. This remedy improved the proposed estimators considerably, resulting in a substantial variance reduction, which is especially important when the probability of detection is low.

Tracking performance is analyzed by means of the cumulative RMSE measure of the moving target position and its estimation. Two simulations were conducted. The first simulation assumes a priori knowledge of these two parameters, while the second simulation utilizes the parameters estimated from the new algorithm. The obtained results are as expected, where the RMSE of the second simulation is less than that of the first simulation.

By comparing the CPHD filter and the new proposed algorithm in the computational complexity, the obtained results are as expected, shows that the numerical complexity of the algorithm depends on a great extent on the probability of target detection as well as the density of false alarms

A comparison in the computational complexity between the CPHD filter and the new proposed algorithm for estimating the unknown parameters was performed. Processing time is used as a measure of numerical complexity, with algorithms being implemented on the same computer platform under identical conditions.

As expected, the result shows that the numerical complexity of the algorithm depends on a great extent on the probability of target detection as well as the density of false alarms. However, the interesting result refers to the fact that with the increase of probability of target detection the CPHD filter numerical complexity decreases because the process of the filter is simplified with the increase of the probability of detection. On the other hand, the numerical complexity of the new proposed algorithm increases because the number of hypotheses is increasing with increasing the probability of detection. Also, this comparison shows that the CPHD filter is very sensitive to an increase in the density of false alarm due to an increase in the cardinality of the random finite set. On the other hand, the new proposed algorithm is less sensitive to the increase in the density of false alarms because the algorithm takes into account only the false observation which has the smallest statistical distance from the predicted position of the tracked target.

The overall conclusion of this analysis is that the new proposed method has lower numerical complexity than the CPHD filter.

The new proposed algorithm has satisfactory performance when a prior knowledge about the measurement noise covariance matrix is available, but it has a significant bias when that knowledge is incorrect. For this reason, an adaptation to the new proposed algorithm was proposed which estimates the measurement noise covariance matrix in each scan.

The performance of all the existing techniques for data association and the estimation of the probability of target detection is degraded when the density of false alarm is very high. The only reasonable approach might be to assume that the probability of target detection is known and to estimate only the density of false alarm. So one of the constraints of the proposed estimator is that it performs poorly when the density of false alarms is very high, that is detected in such cases the zero integral hypothesis exhibited the highest likelihood by far, such that the target detection estimate was equal to zero. It is not easy to find the threshold value of density of false alarm at which this occurs which opens the possibilities for future research.

My opinion for future research is that the presented results open the possibilities with the aim of improving the quality and applicability of the algorithm and conducting further analyses. The new proposed approach can be expanded and used in a multiple target scenario, in which case the significant problem is tracking the closely spaced targets, where their gates are partly overlapped. In such cases, the new proposed approach can and should be modified. The basic idea on which the algorithm is based would remain the same, but the number of integral hypotheses would increase, the expression for their likelihood would be altered, and the regression form for estimator bias elimination would be changed. In other words, expansion is possible but not trivial, requires an in-depth analysis.

Another proposal for future research is that it would be interesting to investigate the case in which the knowledge about a model noise is unavailable as well. This case is somewhat more

complicated and will probably require a more complex noise statistics estimator structure. Also, the existing augmentation of the algorithm can be further improved by introducing an adaptive estimation of the measurement noise covariance matrix.

References

[1] S. Blackman and R. Popoli, Design and Analysis of Modern Tracking Systems, Norwood - USA: Artech House Radar Library, 1999.

[2] A. Elhasaeri, A. Marjanovic, S. Vujnović, G. Kvascev and Ž. Đurović, "Probability of Detection and False Alarm Density Estimation in Target Tracking Systems With Unknown Measurement Noise Statistics," in *Int. Conf. on Elec., and Comp. Engineering IcETRAN*, Srebrno jezero- Serbia, 2019.

[3] A. Al-Hasaeri, A. Marjanović, S. Vujnović, P. Tadić and Ž. Đurović, "On False Alarms Density and Detection Profile Estimation in Target Tracking systems," in *XIV International SAUM Conference on Systems, Automatic Control, and Measurements*, Niš- Serbia, 2018.

[4] I. Schlangen, V. Bharti, E. Delande and D. E. Clark, "Joint multi-object and clutter rate estimation with the single-cluster PHD filter," *IEEE 14th International Symposium on Biomedical Imaging (ISBI),* p. 1087–1091, 19 June 2017.

[5] B. Benfold and I. Reid, "Stable multi-target tracking in real-time surveillance video," *IEEE Conf. on Computer Vision and Pattern Recognition (CVPR),* 22 August 2011.

[6] G. Pulford, "Taxonomy of multiple target tracking methods," *IEE Proceedings - Radar, Sonar and Navigation,* vol. 152, no. 5, pp. 291-304, 17 October 2005.

[7] A. Gad, F. Majdi, and M. Farooq, "A comparison of data association techniques for target tracking in clutter (IEEE Cat.No.02EX5997)," in *Fifth Int. Conf. on Information Fusion*, Annapolis, MD, USA, 2002.

[8] D. Mušicki, R. Evans and B. La Scala, "Integrated track splitting filter - Efficient multi-scan single target tracking in clutter," *IEEE Transactions on Aerospace and Electronic Systems,* vol. 43, no. 4, pp. 1409 - 1425, November 2007.

[9] S. He, H.-S. Shin and A. Tsourdos, "Joint Probabilistic Data Association Filter with Unknown Detection Probability and Clutter Rate," *Sensors,* vol. 18, no.1, pp. 269-283, 16 Jan. 2018.

[10] R. Mahler, B.-T. Vo and B.-N. Vo, "CPHD filtering with unknown clutter rate and detection profile," *IEEE Trans. on signal processing,* vol. 59, no.8, pp. 3497-3513, Aug. 2011.

[11] S. S. Blackman, Multiple-target tracking with radar applications, Dedham-England: Artech House, 1986.

[12] D. Reid, "An algorithm for tracking multiple targets," *IEEE Trans. on Automatic Control,* vol. 24, no. 6, pp. 843 - 854, June. 1979.

[13] N. Wax, "Signal to noise Improvement and Statistics of Tracking Populations," *Applied Physics,* vol. 26, no. 5, pp. 586-595, 1955.

[14] R. W. Sittler, "An Optimal Data Association Problem in Surveillance Theory," *IEEE Transactions on Military Electronics,* pp. 125 - 139, 2 April 1964.

[15] Y. Bar-Shalom and E. Tse, "Tracking in a cluttered environment with probabilistic data association," *Automatica,* vol. 11, pp. 451-460, September 1975.

[16] R. A. Singer and J. J. Stein, "An optimal tracking filter for processing sensor data of imprecisely determined origin in surveillance systems," *IEEE Conference on Decision and Control,* pp. 171-175, Dec. 1971.

[17] S. A. and H., Radar system design and analysis, Dedham-England: Artech House, 1984.

[18] A. Al-Hhasaeri, P. Tadić, A. Marjanović and Ž. Đurović, "Analysis of a method for mitigating miscorrelation in target tracking algorithm," in *4-th International Conference on Electrical, Electronic and Computing Engineering (IcETRAN)*, Kladovo- Serbia, 2017.

[19] A. Al-Hasaeri, P. Tadić, A. Marjanović and Ž. Đurović, "On the Robustness of Target Tracking With Respect to Errors in Parameter Values," in *5-th International Conference on Electrical, Electronic and Computing Engineering (IcETRAN)*, palić- Serbia, 2018.

[20] P. Konstantinova, A. Udvarev and T. Semerdjiev, "A Study of a Target Tracking Algorithm Using Global Nearest NeighborApproach," in *International Conference on Computer Systems and Technologies - CompSysTech*, Sofia-Bulgarian, 2003.

[21] T. Benedict and G. Bordner, "Synthesis of an optimal set of radar track-while-scan smoothing equations," *IRE Transactions on Automatic Control,* pp. 27-32, 4 July 1962.

[22] S. and H. R, "Performance measure and optimization conditions for a third-order sampled data tracker," *IEEE Transactions on Automatic Control, Ac-8,* pp. 182-183, April 1983.

[23] P. R. Kalata, "The Tracking Index: A Generalized Parameter for α-β and α-β-γ Target Trackers," *IEEE Transactions on Aerospace and Electronic Systems* vol. AES-20, no. 2, pp. 174-182, 2 March 1984.

[24] K. and A. J., "Transient response of tracking filters with randomly interrupted data," *IEEE Transactions on aerospace and electronic systems,* vol. AES-6, pp. 313-323, May 1970.

[25] K. Rameshbabu, J. Swarnadurga, G. Archana and K. Men, "Target tracking system using Kalman filter," *International Journal of Advanced Engineering Research and Studies,* pp. 90-94, Dec. 2012.

[26] A. Gelb, J. F. Kasper, R. A. Nash, C. F. Price and A. A. Sutherland, Applied optimal estimate, Cambridge: MIT Press, 1974.

[27] G. Welch and G. Bishop, "An Introduction to the Kalman Filter, Los Angeles: SIGGRAPH,2001.

[28] J. A. J. and Y. Bar-shalom, "On Optimal Tracking in Multiple Target Environments," *Proceeding of the third symposium on Non-linear estimation theory and its application,* pp. 457-462, 11-13 Dec. 1972.

[29] H. N. Nguyen and F. Guillemin, "On process noise covariance estimation," in *Mediterranean Conference on Control and Automation (MED)*, Valletta, Malta, 2017.

[30] R. Mehra, "Approaches to adaptive filtering," *IEEE Transactions on automatic control,* vol. 17, no. 5, p. 693–698, 1972.

[31] R. Kashyap, "Maximum likelihood identification of stochastic linear systems," *IEEE Transactions on Automatic Control,* vol. 15, no. 1, pp. 25-34, 1970.

[32] K. Myers and B. Tapley, "Adaptive sequential estimation with unknown noise statistics," *IEEE Transactions on Automatic Control,* vol. 21, no. 4, pp. 520-523, 1976.

[33] Samuel S. Blackman, "Multiple Hypothesis Tracking for multiple target tracking," *IEEE Aerospace and electronic system magazine,* vol. 1, pp. 5-18, 27 April 2003.

[34] Y. Bar-shalom, Multitarget-Multisensor: Applications and Advances, Norwood, MA: Artech House, 1996.

[35] K. Chang and Y. Barshalom, "Joint Probabilistic Data Association for Multitarget Tracking with Possibly unresolved Measurements and Maneuvers," *IEEE Trans. On Automatic Control,* vol. 29, no. 7*,* July 1984.

[36] M. and G. Katta, Linear and combinatorial programming, New York: John Wiley and Sons, 1976.

[37] Y. Barshalom, "Tracking Methods in a Multi-target Environment," *IEEE Trans. On automatic Control,* vol. 23, no. 4, July 1978.

[38] F. Bourgeois and J. C. Lassalle, "Algorithm for the assignment problem," *Communications of the ACM,* vol. 14, no. 12, pp. 805-806, December 1971.

[39] H. Leung, H. Zhijan and M. Blanchette, "Evaluation of multiple radar target trackers in stressful environments," *IEEE Trans. On Aerospace and Electronic Systems.* vol. 25, pp. 663-674, April 2003.

[40] C. Kim, F. Li, A. Ciptadi and J. M. Rehg, "Multiple Hypothesis Tracking Revisited," *IEEE International Conference on Computer Vision,* 7-13 December 2015.

[41] R. Singer, R. Sea and K. Housewright, "Derivation and evaluation of improved tracking filter for use in dense multitarget environments," *IEEE Transactions on Information Theory,* vol. 20, pp. 423-432, 4 July 1974.

[42] T. E. Fortmann, Yaakov Bar-shalom and Molly Scheffe, "Sonar Tracking of Multiple Targets Using Joint Probabilistic Data Association," *IEEE Journal of Oceanic Engineering,* vol. OE-8, no. 3, pp. 173-184, July 1983.

[43] Y. Chen, "A New Data Association Algorithm for Multi-target Tracking in a Cluttered Environment," in *Information Fusion, 2003. Proceedings of the Sixth International Conference of,* vol. 1, 2003.

[44] F. Yang, W. Tang and Y. Liang, "A novel track initialization algorithm based on random sample consensus in dense clutter," *International journal of advanced robotic systems,* vol. 11, October 2018.

[45] H. Liu, T. Li, X. Dan, H. Wang, and S. Zhou, "Fast track initiation followed by confirmation based on amplitude information," *IEEE Radar Conference,* 27 Oct 2015.

[46] H. Leung, Z. Hu and M. Blanchette, "Evaluation of multiple target track initiation techniques in real radar tracking environments," *IEE Proceedings - Radar, Sonar and Navigation,* vol. 143, pp. 246-254, 21 Aug. 1996.

[47] H. Y, X. J and G. X, Track initiation in multi-target tracking, New York: John Wiley & Sons Singapore Pte. Ltd, 2016.

[48] R. O. Duda and P. E. Hart, "Use of the Hough transformation to detect lines and curves in pictures," *Communications of the ACM,* vol. 15, no. 1, pp. 11-15, Jan 1972.

[49] B. and W., "False alarm control in automated radar surveillance system," *IEE International radar conference,* pp. 71-75, 18 Oct. 1982.

[50] M. and Y. A., "Critical Probabilities for optimum tracking system," *international radar conference, Arlington, VA,* New York, April 1980.

[51] S. Wang, Q. Bao and Z. Chen, "Refined PHD Filter for Multi-Target Tracking under Low Detection Probability," *Sensors (Basel),* vol.19, no. 13, 26 June 2019.

[52] D. L. Alspach, "A gaussian sum approach to the multitarget identification-tracking problem," *Automatica,* vol. 11, no. 3, pp. 285-296, May 1975.

[53] R. and D. B., "A multiple hypothesis filter for tracking multiple targets in a cluttered environment," LEIBNIZ information center for science and technology university library, Sunnyvale, California, 1977.

[54] Z. Wang, J. Sun1, Q. Li and G. D, "A New Multiple Hypothesis Tracker Integrated with detection Processing," *Sensors,* vol. 19, no. 23, November 2019.

[55] X. Chen, R. Tharmarasa, T. Kirubarajan and M. McDonald, "Online clutter estimation using a Gaussian kernel density estimator for multitarget tracking," *IET Radar, Sonar and Navigation,* vol. 9, no. 1, pp. 1-9, 26 February 2015.

[56] W. C. Kim and T. L. Song, "Interactive clutter measurement density estimator for multitarget data association," *IET Radar, Sonar & Navigation,* vol. 11, no. 1, pp. 125-132, January 2017.

[57] A. Al-Hasaeri, A. Marjanović, P. Tadić, S. Vujnović and Ž. Đurović, "Probability of Detection and Clutter Rate Estimation in Target Tracking Systems: Generalized Maximum Likelihood Approach," *IET Radar, Sonar and Navigation,* 1 June 2019.

[58] S. Yildirim, L. Jiang, S. S. Singh and T. A. Dean, "Calibrating the Gaussian multi-target tracking model," *Springer, Statistics and Computing,* vol. 25, no. 3, Feb. 2014.

[59] X. Chen, R. Tharmarasa, M Pelletier and T. Kirubarajan, "Integrated Clutter Estimation and Target Tracking Using Poisson Point Process," *IEEE Tran. On Aerospace and Elec. Systems,* vol. 48, no. 2, pp. 1210-1235, April 2012.

[60] Y. Bar-Shalom and X.-R. Li, Multitarget-multisensor tracking: principles and techniques, New York: IEEE AES Systems Magazine, 1996.

[61] D. J. Daley and D. Vere-Jones, An introduction to the theory of point processes, vol. II, New York, NY: Springer, 2003.

[62] D. Musicki and R. Evans, "Joint integrated probabilistic data association:," *IEEE Trans. Aerosp. Electron. Syst.,* pp. 1093-1099, 27 September 2004.

[63] D. Musicki, S. Suvorova, M. Morelande and B. Mora, "Clutter map and target tracking," in *Proc. Int. Conf. on Information Fusion*, Philadelphia, PA, USA, 2005.

[64] K. and H. Lachlan, "Clutter-based test statistics for automatic track," *Acta Automatica Sinica,* vol. 34, no. 3, p. 266–273, March 2008.

[65] S. M. Kay, Fundamentals of statistical signal processing, vol. II: Detection theory, Upper Saddle River, NJ: Prentice-Hall PTR, 1998.

[66] M. Basseville and I. V. Nikiforov, Detection of Abrupt Changes: Theory and Application, Englewood Cliffs, New Jersey: PTR Prentice-Hall, Inc., 1993.

[67] J. Rissanen, "Modeling By Shortest Data Description," *Automatica,* vol. 14, no. 15, pp. 465-471, September 1978.

[68] L. X. LE and W. J. Wilson, "Bias Reduction in Parameter Estimation," *Automatica,* vol. 24. no. 6, pp. 825-828, 1988.

[69] Ž. M. Đurović and B. D. Kovacević, "Robust estimation with unknown," *IEEE Transactions on Automatic Control,* vol. 44, no. 6, p. 1292–1296, 1999.

[70] A. Kizilkaya, "Computation of the exact Cramer–Rao lower bound for the parameters of a nonsymmetric half-plane 2-D ARMA model," *Elsevier science,* vol. 18, no. 5, 2008.

Author biography

Asem Issa Alhasaeri was born on 06.08.1966 in Zwara Libya. He finished elementary school in Tripoli in 1978 and the High School in 1984 also in Tripoli.

He enrolled in the Faculty of Nuclear and Electronic Engineering at the University of Tripoli in 1984, where he graduated in 1991 with a Bachelor's degree in electronics. The diploma thesis entitled "Simulation of queuing systems" was done under the mentorship of dr Faraj Hamad. Asem Issa Alhasaeri enrolled in the Master of Studies in 2001, in the Department for systems and signals at the School of Electrical Engineering, University of Belgrade, and graduated in 2003 with an average grade of 9.0. He defended his Master's thesis entitled "Pattern recognition support to the algorithms of missiles guidance" under the mentorship of Prof. dr Željko Đurović. Later Mr. Alhasaeri enrolled in doctoral studies at the School of Electrical Engineering, Belgrade University, majoring in Control, in 2014-2015, where he was granted a doctoral dissertation entitled "Adaptive techniques in target tracking systems".

From 1991 to 2001 and from 2004 to 2014 he worked at "Electronic Research Center" in Tripoli as an engineer for the development of software used in the unmanned vehicle. Also, he worked as an assistant in high institutes and universities, such as "Injila high institute" in Janzour-Libya, "Nasser University" in Tarhouna, and "Faculty of engineering" in Zwara.

He has co-authored one paper in international scientific journals and five papers at international scientific conferences.

List of publications

[1] Sanja Vujnović, Asem Al-Hasaeri, Predrag Tadić, Goran Kvaščev, "Acoustic Noise Detection for State Estimation**,"** in *3-rd International Conference on Electrical, Electronic and Computing Engineering (IcETRAN), Zlatibor* Serbia, 2016.

[2] Asem Al-Hasaeri, Predrag Tadić, Aleksandra Marjanović and Željko Đurović, "Analysis of a method for mitigating miscorrelation in target tracking algorithm," in *4-th International Conference on Electrical, Electronic and Computing Engineering (IcETRAN)*, Kladovo Serbia, 2017.

[3] A. Al-Hasaeri, A. Marjanović, S. Vujnović, P. Tadić, Ž. Đurović, "On False Alarms Density and Detection Profile Estimation in Target Tracking systems," in *XIV International SAUM Conference on Systems, Automatic Control, and Measurements*, Niš Serbia, 2018.

[4] Asem Al-Hasaeri, Predrag Tadić, Aleksandra Marjanović, and Željko, "On the Robustness of Target Tracking With Respect to Errors in Parameter Values," in the *5-th International Conference on Electrical, Electronic and Computing Engineering (IcETRAN)*, palić Serbia, 2018.

[5] Asem Elhasaeri, Aleksandra Marjanovic, Sanja Vujnović, Goran Kvaščev, and Željko Đurović, "Probability of Detection and False Alarm Density Estimation in Target Tracking Systems With Unknown Measurement Noise Statistics," in *Int. Conf. on Elec., and Comp. Engineering IcETRAN*, Srebrno jezero Serbia, 2019.

[6] Asem. Al-Hasaeri, Aleksandra Marjanović, Predrag Tadić, Sanja Vujnović, Željko Đurović, "Probability of Detection and Clutter Rate Estimation in Target Tracking Systems: Generalized Maximum Likelihood Approach," *IET Radar, Sonar and Navigation,* 1 July 2019.

образац изјаве о ауторству

Изјава о ауторству

Име и презиме аутора _Asem Issa Al-Hasaeri_

Број индекса _2014/5054_

Изјављујем

да је докторска дисертација под насловом

Адаптивне технике у системима за праћење покретних циљева

- резултат сопственог истраживачког рада;
- да дисертација у целини ни у деловима није била предложена за стицање друге дипломе према студијским програмима других високошколских установа;
- да су резултати коректно наведени и
- да нисам кршио/ла ауторска права и користио/ла интелектуалну својину других лица.

Потпис аутора

У Београду, _10. 02. 2020._

образац изјаве о истоветности штампане и електронске верзије докторског рада

Изјава о истоветности штампане и електронске верзије докторског рада

Име и презиме аутора *Asem Issa Al-Hasaeri*

Број индекса *2014/5054*

Студијски програм *Управљање системима и обрада сигнала*

Наслов рада *Адаптивне технике у системима за праћење покретних циљева*

Ментор *Проф. Жељко Ђуровић*

Изјављујем да је штампана верзија мог докторског рада истоветна електронској верзији коју сам предао/ла ради похрањивања у **Дигиталном репозиторијуму Универзитета у Београду.**

Дозвољавам да се објаве моји лични подаци везани за добијање академског назива доктора наука, као што су име и презиме, година и место рођења и датум одбране рада.

Ови лични подаци могу се објавити на мрежним страницама дигиталне библиотеке, у електронском каталогу и у публикацијама Универзитета у Београду.

Потпис аутора

У Београду, *10. 02. 2020*.

образац изјаве о коришћењу
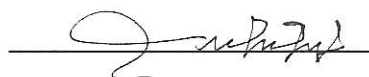
Изјава о коришћењу

Овлашћујем Универзитетску библиотеку „Светозар Марковић" да у Дигитални репозиторијум Универзитета у Београду унесе моју докторску дисертацију под насловом:

Адаптивне технике у системима за праћење покретних циљева

која је моје ауторско дело.

Дисертацију са свим прилозима предао/ла сам у електронском формату погодном за трајно архивирање.

Моју докторску дисертацију похрањену у Дигиталном репозиторијуму Универзитета у Београду и доступну у отвореном приступу могу да користе сви који поштују одредбе садржане у одабраном типу лиценце Креативне заједнице (Creative Commons) за коју сам се одлучио/ла.

1. Ауторство (CC BY)

2. Ауторство – некомерцијално (CC BY-NC)

3. Ауторство – некомерцијално – без прерада (CC BY-NC-ND)

4. Ауторство – некомерцијално – делити под истим условима (CC BY-NC-SA)

5. Ауторство – без прерада (CC BY-ND)

6. Ауторство – делити под истим условима (CC BY-SA)

(Молимо да заокружите само једну од шест понуђених лиценци.
Кратак опис лиценци је саставни део ове изјаве).

Потпис аутора

У Београду, 10.02.2020.